Part 1- Spectroscopic Studies Of Coal Solvent Interaction

Part 2 - Solvation Studies

Thesis submitted for the degree of
Doctor Of Philosophy
at the University Of Leicester

by

Benjamin William Taylor BSc(Leicester)
Department Of Chemistry
University Of Leicester

April 1992

ProQuest LLC
789 East Eisenhower Parkway
P.O. Box 1346
Ann Arbor, MI 48106-1346

Part 1- Spectroscopic Studies Of Coal Solvent Interaction

Part 2 - Solvation Studies

Abstract of thesis submitted for the degree of Doctor Of Philosophy at the University Of Leicester

by
Benjamin William Taylor BSc(Leicester)
Department Of Chemistry
University Of Leicester

An overview of coal from a geological context and a review of the use of ESR in coal research is presented. A series of ESR experiments conducted with a selection of coals are described. These include attempts to identify the environments in which iron (III), manganese (II) and vanadyl ions are bound within coal. It is concluded that the principle vanadyl environment is a porphyrin-like structure and that for iron (III) is clay. No specific environment is proposed for manganese(II) but, a mineral environment is most likely. Extraction by organic solvents yields an extract apparently enriched in iron(III). Possible interpretations of this result are discussed.

IR spectroscopy is used to study carbonyl groups carried by a range of organic solvents introduced into coals. It is concluded that the solvents are hydrogen-bonding to trapped water and carboxylic acid functional groups at the coal surface. Weaknesses in the experimental techniques used are discussed and proposals for future experiments in the area are made.

The NMR chemical shifts of probe species in binary solvent systems are used in an investigation of the Covington model of preferential solvation. It is concluded that, while a useful treatment, the model is flawed in any system where solvent molecules outside the primary solvation shell exert an influence on solute chemical shift.

The IR spectra of the CN stretch of MeCN in methanol shows a transition from discrete bands to a merged band with increasing temperature. The lifetime of the bonded dimer is calculated from curve fitting data. The calculated lifetime, ca. 1 ps, agrees with values reported from molecular dynamics modelling.

Data from molecular dynamics simulations of the TIP4P model for water is used to analyse hydrogen bonding using geometric bonding criteria. Populations of free OH groups and lone pairs are presented for various geometric criteria. It is concluded that molecular dynamics simulations of water are not at variance with Symons' model for the structure of water.

Acknowledgements

This thesis represents the culmination of two decades of education (September 1969-September 1989). During that time a great number of people have influenced my development both personally and intellectually. Chief amongst those who influenced the direction of my studies are Allan Snaith (Essex County Council Child Guidance Clinic), Peter Chester (Colchester Royal Grammar School), Derek Andrews (Department Of Computing Studies, University Of Leicester) and, at the end, my PhD supervisor Martyn Symons (Department Of Chemistry, University Of Leicester).

During the period since 1986, when the work presented in this thesis began, I have had the privilege of working with some very special people; Jane Wyatt, Geoff Archer, Graham Eaton, Ian Podmore and Andy Stevens. Beyond the laboratory my thanks are due to Paul Manning for providing, at different times, everything from a roof over my head to programming advice, with an ever present generous spirit, and to my colleagues at Westland System Assessment Ltd for providing encouragement during the period since I left Leicester in 1989.

Lastly I would like to thank my parents for their everlasting support and also the other special people who have shown me affection over the years. This is for you, I will think of you always.

This thesis was prepared by the author using Microsoft's Word For Windows wordprocessing software and printed on a Hewlett-Packard Deskjet 500 printer. I am indebted to Mr. D.J. Wright, General Manager of Westland System Assessment Ltd, for permission to use company photocopying facilities and to British Gas for funding this work through a CASE award.

CONTENTS

Part 1- Spectroscopic Studies of Coal-Solvent Interaction

Part 2- Solvation Studies

Part 1

Spectroscopic Studies of Coal–Solvent Interaction

1. INTRODUCTION TO COAL STUDIES

1.1. Introduction

Recent years have seen an increased interest in coal chemistry. The principle reason behind this is that coal is now viewed as something more than a source of thermal energy. Coal contains the degraded remains of a plethora of living organisms that have been exposed to high pressure and temperature during an often lengthy geological history. In this respect coal is similar to crude oil, the world's major energy source. With dwindling reserves and rising unit production costs of oil, coal may yet have to be a major chemical feedstock.

Unfortunately coal is not as convenient to use as oil. It is a solid, and so harder to transport and store, it contains inorganic contaminants and its organic components have not been degraded to the same degree as oil. None of these problems are insurmountable. For example powdered coal mixed with air can be pumped like a fluid[1] and the organic components can be broken down to produce synthetic oil by pressure treatments. Only by further research into the properties of coal can the groundwork be laid for the coal utilisation technology of the future.

1.2. The Nature Of Coal

Coal is a very complicated mixture of organic and inorganic components. Coals are described as having a specific 'rank'. The rank of a coal is tied to the degree of alteration from the

precursors. It is normal to think of rank as a function of the carbon content of a coal (higher rank coals have higher content). Carbon content runs from around 70% in lignites up to the mid 90s with anthracites. With increasing rank coal becomes more aromatic and loses volatiles (CO_2, H_2O, CH_4, H_2S). A general sequence of coal types, in increasing rank, is shown below.

- Peat
- Lignite (Brown Coal)
- Sub Bituminous Coal
- High Volatile Bituminous Coal (HVB)
- Medium Volatile Bituminous Coal (MVB)
- Low Volatile Bituminous Coal (LVB)
- Semi-Anthracite
- Anthracite
- Meta-Anthracite

With increasing rank coals become harder and more brittle. The energy released on combustion reaches a maximum between LVB coals and anthracites[2]. Beyond this point there is too much aromatic stabilisation (cf. specific latent heat of benzene vs. cyclohexane) for the energy yield to increase.

With its highly heterogeneous nature it is not possible to think of coal as having a specific molecular structure. It is probably a retrograde step to attempt to do so as it is necessary to always bear in mind that the results obtained in any investigation are

indicative merely of trends and averages. Only in a few cases are any results attributable to easily defined atomic arrangements.

Coals are heterogeneous in the macroscopic regime. Examining lumps of coal from the same seam some will be seen to be dull and powdery, others shinier with vitreous lustre. These differences reflect the different macerals that make up coal. Macerals are the organic geochemical equivalent of minerals; inorganic rocks are composed of minerals where coals are composed of macerals. The macerals that make up coals can be separated by density techniques. Research into them indicates different possible origins i.e. bark, leaves, wood, spores, driftwood, burnt wood etc. The chemical differences between them are generally minimal, their composition and nature being a function of their subsequent geological history rather than of their botanical precursors. Distinctions between macerals will not be considered further in this work, all samples used being crushed coals.

Most properties of coals are related to the structure of coals[3]. The structure of coals changes with rank. X-ray diffraction studies identify structural trends[4,5].

Low Rank	An open structure of randomly oriented and cross-linked aromatic regions.

Medium Rank	A structure with fewer cross-links and reduced porosity. A moderate degree of ring orientation is evident between the larger aromatic areas.
High Rank	Larger aromatic layers with still greater orientation. The pore systems become directional.

The high rank structure might be viewed as 'contaminated graphite', the low rank one as a condensed biochemical macro-molecule. This view is furthered when it is remembered that plants are the precursor of coals. As coal rank increases the hetero atoms are ejected as volatiles by functional group elimination. Methane is also lost (cf. methane danger in mines) so that a high rank coal is a hydrocarbon that is becoming more hydrogen deficient under considerable directed pressure. An ultimate conversion to graphite is quite reasonable to postulate.

1.3. Coal Geology

Conclusions drawn from chemical studies of coal cannot be made in isolation, such work must be interpreted within the framework of coal geology and the particular geological history of the coal(s) under study. It is, therefore, worth looking at coal in its geological context.

When looking at geological history it becomes necessary to alter the perception of time. Of all geological processes only volcanic

eruptions and earthquakes occur fast enough to be visible to the human eye. In geology the standard time unit tends to be one million years (1 My). The scale of events that can be looked at from this new time frame include the splitting apart of continents, the building of mountain ranges from sea-floor sediments and the solid phase recrystallisation of millions of cubic metres of rock. In terms of the geological record the present day erosion of England by the sea represents an 'instantaneous' marine transgression[6].

With the exception of the Bovey Tracey lignite deposit in Devon all British coals date from the same geological period, the Carboniferous[7]. Their average age is around 300 My (or 9.4 X 10^{15}s).

1.3.1. The British Carboniferous

The Carboniferous system is the time period lasting from approximately 345 My to 280 My. It falls between the earlier Devonian and the later Permian. Both of these systems saw arid desert conditions in the British Isles and this is reflected in the distinctive sediments deposited at the time. These include desert sandstones and evaporite deposits (such as the Cheshire salt deposits). The Carboniferous represents the 65 My gap in between during which the climate was more humid and different sediments were deposited as the British Isles crossed the equator. These sediments include marine limestones, deltaic sandstones and the coal measures.

It should not be thought that coal forming conditions have only become established once in the Earth's history. All stratigraphic periods from the Devonian onwards show the development of coals in some part of the world[7]. Earlier coals are not found simply because there were no advanced plants on land to become coal. It would likewise be in error to assume that coal formation is commonplace. Excepting, once again, the Bovey Tracey lignite, coal forming conditions have only once been established in the area now known as the British Isles. What is remarkable about the British coalfields is that they form part of a chain that developed at the same time running from Poland to the Great Lakes. To understand how this coalfield developed it is necessary to examine the paleogeography of the Westphalian (315 My-290 My), the part of the Carboniferous that saw most coal development.

1.3.1.1. Westphalian Paleogeography

In simple terms when the Earth's tectonic plates collide mountain chains are formed along the margins. The classic example today is the Alpine-Himalayan chain. In this process the ocean that separated the continents is lost and the sediments on the shelf seas bordering the ocean are often subjected to severe deformation in an event called an orogeny.

One instance of this process came to a completion in the Late Silurian (430 My to 395 My) in Britain[8]. The mountains formed by the closing of the Iapetus ocean (There is no surviving remnant of the Iapetus ocean. Its existence can only be inferred from the

rocks of the continents that bordered it.) are known as the Caledonides. They stretch from Norway through Scotland, Newfoundland, Nova Scotia and continue as part of the Appalacian mountains of the USA. At this time there was no Atlantic ocean, southern Greenland, Newfoundland and south-west Ireland lay within a few hundred miles of each other. To the south of this continent lay the Rheic ocean. The margins of the Rheic ocean lay through central Germany, France, Spain and the Atlantic seaboard of the USA. This paleogeography is illustrated in Figure 1.1.

By Westphalian times the deformation of this continental margin was well underway in the early stages of what would become the

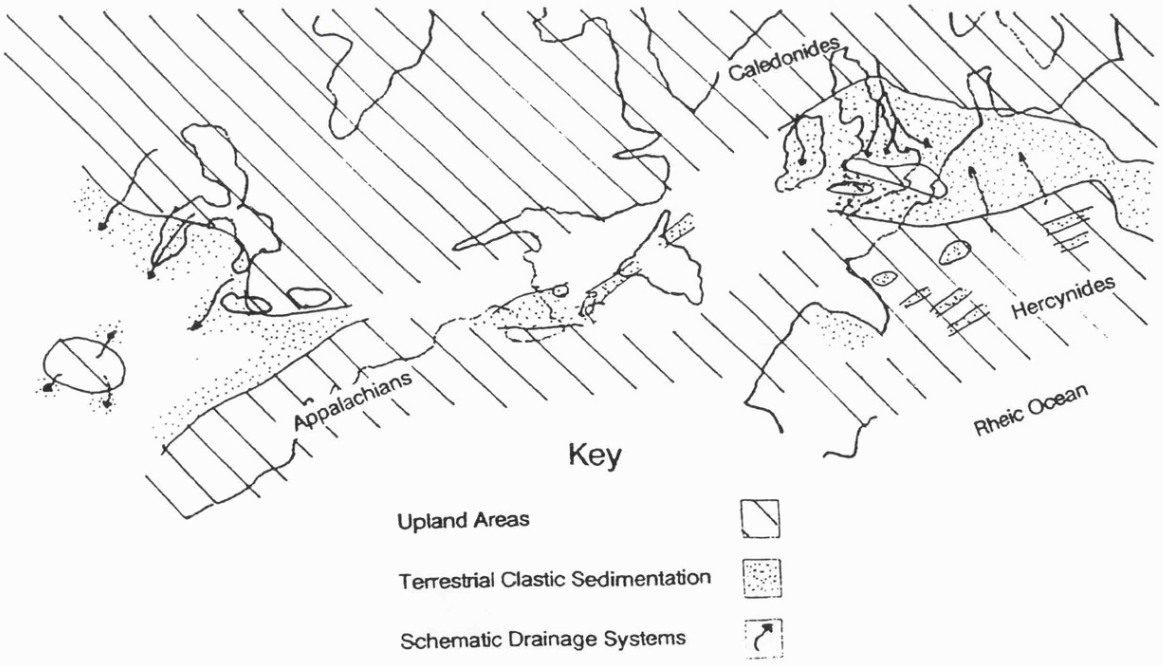

Figure 1.1 Westphalian Paleogeography of NW Europe and NE America[9]

Hercynian orogeny. Island arcs probably lay to the south of Britain in France and Germany. The area between the Caledonides in the north and the developing Hercynides in the south was mostly covered by shallow seas. A few 'positive' areas would have been emergent. St. Georges Land, an island running from Wales through the London region into Belgium, is the most important example. Rivers carrying sediment eroded from the Caledonides flowed into this region. The Namurian (the period before the Westphalian) had seen the development of huge sandy deltas into the sea, seen today as the grits of the Pennines

1.3.1.2. Coal Measures Sedimentation

During the Westphalian the rate of sediment supply was lower and a different kind of sedimentation set in. For about 20 My during the Westphalian a balance between the sediment supply and the sea was maintained. Most of the region seems to have been either shallow sea or low-lying delta. Each phase of delta sinking (or sea rising) would be matched by renewed delta development. The sediments developed appear to form cycles, with the depositional environment getting shallower, from marine muds to fossil soils and coals, within the cycle.

Each cycle represents the pushing out of a delta into the sea. Some cycles are never completed, others can be seen to have been partially eroded before starting again. The study of the coal measures cyclic sedimentation and its interpretation are enormous topics[10].

The coals themselves represent the stage of delta development that correspond to the development of vegetation on the delta. Development of a plant cover does not lead directly to coal. The plant material must be buried beyond the reach of oxygen before it can decompose too far. This implies that the coals represent the plants growing in (or washed into) anaerobic swamps. Once plants died and sank into the debris beneath the water level no further oxidation could take place. To produce a worthwhile seam tens of metres of vegetation would have to accumulate, the degree of compaction from plant material to coal being 80%-90%. This required thickness is why the stability of the deltas is so important. If the deltas were not subsiding then they would silt up and become an oxygenated flood plain. If they were transgressed by the sea too often then the plant debris would be destroyed before enough could accumulate. The accumulation of plant material was clearly aided by the paleoclimate. The climate was hot and humid as the coal swamps developed in the equatorial rain belt. The evidence for this comes from the lack of seasonal growth rings in fossil plant cross-sections. Continental drift theories require the British Isles to have crossed the equator during the Carboniferous as the region was in the southern desert belt during the Devonian and the northern desert belt during the Permian.

The total volume of sediment deposited on the deltas is enormous. In the Lancashire coalfield the total thickness of the coal measures is 3 km. This is after compaction has taken place.

1.3.2. Coalification

Coalification is the process by which compacted plant debris is transformed into coal. In chemical terms it is an example of a reaction being driven by pressure. The equation in question is given below.

Low Grade Material = Volatiles + High Grade Material

The volatiles in question include water, carbon dioxide, hydrogen and methane. The lowest grade of material is unaltered plant debris, the highest is graphite. This picture is over simplistic as the chemical pathways from wood to graphite are not one continuous reaction. The geological evidence is for a two phase conversion with two controlling forces.

The first phase of coalification is driven by compression of the sediment. It represents the changes from peat to lignite (brown coal). The drop in volatile proportion is from about 80% to around 50%. The volume undergoes an 80% reduction. The pressure from additional sedimentary cover is sufficient to drive this change[11].

The second phase of the conversion process takes the volatile component down to around 10%. There is much less reduction in volume associated with this change. During this change extensive chemical restructuring takes place. Functional groups are eliminated and the degree of aromaticity (expressed as the

percentage of carbons shown by ^{13}C NMR to be aromatic) increases from less than 20% to over 90%[12].

Not surprisingly this transformation is heat driven. There are two principle sources of heat in the geological environment. Firstly there is the heat conducted up from the mantle and lower crust. Although dependent on the underlying geology the geothermal gradient averages 3-5 °C per 100m in depth. This would have produced possible temperatures of 200 °C in the British coalfields, assuming that at least 3 km of overlying sediment was present.

The second source of heat is that given off from magmas intruded within the crust. When magmas rise through the crust they will either reach the surface, resulting in a volcano, or they will solidify as an intrusion. Intrusions can vary in size between the Cornubian granite batholith (all the granites from the Scilly Isles to Dartmoor link up underground) and dykes only inches across that follow joints in the host rock.

During the late Carboniferous and Early Permian there was considerable intrusive activity in the British Isles. One example is the Whin Sill in the north of England. The Whin Sill is a sheet of Dolerite (dolerite is an intrusive igneous rock, chemically related to basalt) that today forms the crags that Hadrian's Wall is built on to the east of Carlisle and which underlies much of the Northumbrian coal field. The cooling sill will have released a lot of heat into the overlying coal measures.

This may be a partial explanation as to why the Northumbrian coals are of higher grades than those in Yorkshire and further south.

Another example of an intrusion changing the grade of coal comes from Pennsylvania where a coal seam changes from Bituminous coal to Anthracite and even graphite before being cut by a Basalt dyke. Beyond the dyke the same changes are seen in reverse. This is an example of contact metamorphism, where a rock is metamorphosed by contact with a hot intrusion. Regional metamorphism is the term used for metamorphosis on a large scale where pressure and/or heat are applied to a large area. Medium and high grade regional metamorphism represent environments too extreme for coals to survive. Some graphite bands in schists (a kind of metamorphic rock produced by recrystallisation under elevated temperature and severe directed stress) have been interpreted as being the remains of coal deposits.

1.3.2.1. Geological Evidence

The evidence for this picture of coal development is geological. The first phase (loss of volatiles) represents a purely pressure effect. In parts of the Moscow area there are lignites dating from the Lower Carboniferous (i.e. older than British coals). They were put under pressure by more sediments deposited on top (now removed) but have never been deeply buried because the area has a very stable basement. Neither have they ever been exposed to any igneous or metamorphic episodes, again because of the stable basement. As a result they have experienced sufficient pressure

to remove the excess volatiles and produce lignites, but have never been in an environment where elimination of functionality and aromatisation could take place.

British coals have been exposed to higher thermal gradients as they were deposited in areas with underlying instabilities (the British Carboniferous contains a fair quantity of volcanic rocks). At some stage in their history there has been sufficient heat to activate the reactions necessary to convert lignites to coals.

It has been argued that coalification is a very long term process. The evidence cited for this view is the lack of any true coals in Europe younger than 100 My, all younger deposits being lignites. However, these sediments have not been exposed to the conditions necessary to produce true coals from lignites. In Mexico and Venezuela there are true coals (admittedly of low grade) younger than 30 My.

In geological terms the coalification process is fast. The evidence for this comes from South Wales. Here the coal measures are succeeded by the Pennant Group sandstones. They are coarse grained sandstones interpreted as having been deposited by rivers. Fragments of bituminous coal have been discovered in the Pennant group. These can only have come from the coal measures, immediately beneath the sandstones, which must have already been buried, turned to coal, uplifted and eroded by the close of the Carboniferous.

A coal exposed to specific conditions for a prolonged period of time is likely to show an increasing coal rank with the continued exposure. A limiting rank likely to be attained under any given conditions must be envisaged. This would seem reasonable if the nature of the chemical changes required to enhance coal rank is considered. The reactions will involve carbon-carbon bond cleavage and aromatic ring formation in the solid phase. Such reactions will have sizable potential barriers that must be overcome with the ambient heat the only source of energy.

1.3.3. Conclusion

The worlds greatest coalfield, stretching from Poland to the American mid-west is a legacy of the Hercynian orogeny. Crustal tensions behind the active continental margin caused a weakening and partial collapse of the earth's crust. Sediment flow into the resultant basin was from both the developing Hercynides (to the south) and the older Caledonides (to the north). The sediment flow during the Westphalian just about balanced the rate of collapse and the area was covered with deltas supporting a lush tropical floral cover.

During the later phases of the orogeny tension turned to pressure and the sedimentary basins were buried by material eroded from the newly uplifted mountains. These pressures, in conjunction with the heat of the magmas intruded at the same time, were sufficient to convert the compacted plant debris to bituminous coals and anthracites by very late Carboniferous or earliest Permian times.

1.4. Coal Solvent Interactions

Considerable evidence exists to support the view that coals are three dimensional, porous, cross linked structures with an appreciable amount of low weight material (under 1000 amu) also present[13,14]. It is thought that these smaller fragments will be chemically similar to the bulk. They are not part of the framework but are trapped by cross-links prohibiting escape and/or bound by hydrogen bonds or other weak methods of binding.

One of the principle forms of evidence for this picture comes from solvent absorption studies. Coals show a considerable propensity for swelling on the adsorbtion of certain solvents. Volume increases of over 50% are known. Pyridine can extract up to 25% of the mass of a coal sample. Clearly the pore structure of the coal is instrumental in this behaviour. The breaking up of coal by solvent adsorbtion takes on both chemical and physical aspects. That the most effective solvents are nucleophiles, such as pyridine and ethylenediamine, suggests a chemical approach[15,16]. Cross links between coal fragments may be broken by nucleophilic substitution reactions occurring on the bridges and by the disrupting of hydrogen bonding. As the links break so the coal fragments can move apart, causing swelling and releasing small fragments into solution.

The physical approach can illustrated by the following[17]. When coal is exposed to a vapour, such as benzene, uptake continues without reaching equilibrium even after weeks of exposure.

Benzene vapour condenses in the pores. It then extracts material from the coal, the resulting solution has a lower vapour pressure than the pure benzene outside the coal. This drives even more benzene into the coal. The invading benzene sets up stresses that eventually cause the coal structure to re-adjust, with coal-coal bonds breaking where necessary.

The two pictures shown above are obviously both complementary and simplistic. They do not easily account for the observation that only around 50% of adsorbed toluene can be removed by exposure to high vacuum[14]. The re-adjusting coal framework may well trap pockets of solvent in some way. Coal is unique in showing entrapment to this degree.

Investigation into the way in which solvents may bind to coal and what material can be extracted by said solvents can be conducted in many ways. Infra-red spectroscopy can follow the absorptions of those functional groups in both coal and solvent that may be interacting, in this way the sites and strengths of bonds formed may be studied. Electron Spin Resonance (ESR) spectroscopy can study some of the more rare components of coal, the transition metals, and see whether or not they are extracted into solution. Details of both of these types of experiment are presented in Chapters 2 (ESR) and 3 (IR).

1.5. ESR Studies of Coal

1.5.1. Overview Of ESR

Electron spin resonance (ESR) is a spectroscopic technique that is similar in principle to the more familiar NMR (nuclear spin resonance) technique. In the ESR experiment microwave radiation is absorbed by electrons in an applied magnetic field changing their spin states. As with NMR the observed absorption is the net absorption due to electrons moving to a higher energy state over and above those dropping back to the ground state and emitting energy whilst so doing. Only unpaired electrons give ESR spectra, as pairs of electrons occupying a single orbital may not have the same spin quantum number. This restriction severely limits the applicability of the technique to organic radicals and transition metals with an odd number of d electrons. The nature of the ESR spectrum is dependent upon the type and magnetic environment of the orbital containing the excited electron. The parameters used to describe the spectrum are outlined below.

g-values

The g-value is the rate of divergence of the possible spin levels (usually +/- 1/2) in an applied magnetic field (of strength B), and is given by the equation

$$h\upsilon = g\mu_\beta B$$

This value can be considered as analogous to the chemical shift in NMR. For those electrons coupled to other spins by spin-spin,

rather than spin-orbit interactions the value is close to 2 (2.0023), such signals are termed 'free-spin'. With transition metal complexes g can be shifted up or down *via*. spin-orbit coupling because the d orbital levels are close together and coupled by a magnetic field.

Manganese(II) is a d^5 high-spin complex so each d orbital contains one electron, giving an S-state radical. Δg is therefore small and g is approximately 2. With vanadium the strong V-O bond splits the levels of the d^1 complex so g-values are shifted by spin-orbit coupling, but not very far.

Hyperfine Coupling

Hyperfine coupling represents the effect of electron-nuclear coupling with magnetic nuclei. As such it is analogous to nuclear spin-spin coupling in NMR. The electron experiences a variety of local magnetic field strengths depending on the state of nearby magnetic nuclei. In the case of ^{55}Mn, with I = 5/2, six lines are produced, one each for the six possible M_I values; +5/2, +3/2, +1/2, -1/2, -3/2 and -5/2. ^{51}V has I=7/2, giving eight lines. ^{57}Fe, the only magnetic iron nucleus, is in very low abundance and is not seen. Hyperfine coupling is a tensor quantity and will often be resolved into parallel and perpendicular features for complexes with axial symmetry. The hyperfine structure of many spectra serve as useful fingerprints.

Zero-Field Splitting

This occurs when the possible electron spin-states are not degenerate with a zero external magnetic field. This splitting may cause additional splitting of the observed spectrum. If small, as in the case of symmetrical octahedral complexes like manganese(II), then satellite lines are seen either side of the main lines. Where the zero field splitting gets large compared to the resonance field strength only some of the possible lines may appear. Others may be of very low intensity or shifted beyond the range of the spectrometer. This situation occurs with iron (III), where lines characteristic of square planar and rhombic splittings can readily be identified.

1.5.2. Introduction to ESR Studies of Coal

Coal has been studied by ESR since the earliest days of the technique, the first studies being published in 1954[18,19]. By the end of the 1950's ESR studies of coal had been reported from around the world. The results of these early studies were reviewed by Tschamler and De Ruiter in 1962[20]. At this stage all work referred to a singlet close to free-spin, referred to subsequently as the free-spin signal. The effect of air, solvents, acetylation, chlorination, oxidation, reduction and even γ-irradiation on this signal have been reported. Correlations between coal composition and ESR spectra have also been extensively investigated.

Work has continued to concentrate on the free-spin signal to the point where the origins and interpretation of this signal are quite well understood. More recent work has been reviewed by Retcofsky[21].

A variety of other signals can be found in the ESR spectra of coals. These are of low intensity compared with the free-spin signal. As a result they will not usually be seen if room temperature spectra of the free-spin signal are being recorded. At higher spectrometer gain settings and at low temperatures these additional features become visible. They are due to transition metals. Manganese(II), vanadium (IV) (as vanadyl) and various forms of iron(III) can all be identified.

The probable reason for the neglect of these features is that the study of trace components does not attract much interest from beyond the academic community. By comparison the behaviour of the bulk 'organic' component is of possible economic and environmental importance and so research is concentrated in this area, particularly in the USA where such workers as Retcofsky[22], Petrakis and Grandy[23] have contributed to the understanding of coal combustion processes.

While this state of affairs is understandable on economic grounds, it is important to remember that other aspects of coal are potentially fruitful areas for ESR research.

1.5.3. The 'Free-Spin' Signal

1.5.3.1. Introduction

In this section the accepted interpretation of the free-spin signal in the ESR spectrum of coals is discussed. This signal dominates the ESR spectrum, so much so that in most cases the signal must be allowed to overload in order to see anything else. This signal is due to the organic bulk of coal, all other signals are due to trace transition metals.

1.5.3.2. Intensities

The intensity of an ESR signal is proportional to the number of unpaired spins in the sample[24], so it is possible to calculate the spin density in the sample from the intensity measurements. When plotted against carbon composition the spin densities show a near exponential growth up to around 94% carbon[20]. The spin densities are in the region of 10^{18} to 10^{19} spins per gram. Beyond 94% carbon the spin density tails off sharply. The interpretation of this[20] is that the size of the aromatic regions increases with increasing carbon content, slowly up to around 90% and rapidly above. It would be expected that the degree of stabilisation of a radical would increase with the size of the aromatic systems. As a result the high carbon content coals contain a higher concentration of stabilised radicals. The reduction of the signal at very high carbon content is due to the increase in conducting graphitic regions and the linking of aromatic regions. Discrete

radicals are then lost into conduction bands and large delocalised systems.

1.5.3.3. Line Widths

The linewidth of the free-spin signal in coal varies between about 0.6 G and 8.6 G. Measurements on a large number of coals, mostly American, show the line width to be a function of the hydrogen content[21]. This leads to the hypothesis that the linewidth is due to unresolved hyperfine interactions between the unpaired electrons and hydrogen nuclei. However, certain anthracites and meta-anthracites with less than 1% hydrogen have much larger line widths (up to 63 G). This is thought to be due to the beginnings of graphitic behaviour.

Other mechanisms are also thought to contribute to the observed linewidth. These include electron exchange narrowing[25] and g-value anisotropy.

1.5.3.4. g-Values

The earliest systematic investigation of g-values from the free-spin signal was published in 1966[26]. Studies show that the g-value is a function of the oxygen and sulphur content[21]. The nitrogen content is seemingly not a factor. The implication of this is that the organic radicals are stabilised by heteroaromatic systems containing oxygen and sulphur. Numerous studies have taken place of radical anions and cations based on these systems which give g-value in the range exhibited by coals. Extrapolation

of the results to zero sulphur and oxygen content gives g-values around those seen in neutral aromatic hydrocarbon radicals[27,28].

1.5.3.5. Conclusions

The free-spin signal in the ESR spectrum of coals is due to radicals stabilised by heteroaromatic systems in coal. Models exist to explain the intensity, linewidth and g-value of this feature in terms of the composition of the coal. Work has now progressed to studying these parameters whilst the coal undergoes chemical and/or physical treatments.

1.5.4. Other Signals

Three transition metals can be identified in ESR spectra of coals, vanadium(in the form of vanadyl), manganese(II) and iron(III). The intensity of these signals is less than that of the free-spin signal by at least two orders of magnitude.

It is only in the 1980s that any workers have produced publications concentrating on ESR spectra of transition metals in minerals separated from coals[29,30]. This work has the objective of identifying the location of the metals in coals by matching the spectra of coal derived mineral matter with the spectra of minerals or doped crystals. Progress with vanadyl and manganese(II) signals has been made as accurate A value measurements allow matching to be attempted. Iron(III) spectra do not lend themselves to such treatment and so the distribution of iron within coal is unclear, particularly with respect to the

possibility of iron being held within the 'organic phase' rather than within mineral matter.

The importance of the mineral matter in coals as catalytic sites for pyrolysis has also been investigated[31]. Related work on ESR spectra of metals in petroleum and tar sands[32] as well as on soil derived humic acid complexes[33,34] has also been published.

1.6. IR Studies

1.6.1. Introduction

Possibly the most widely known property of coal is its colour, typically black for bituminous and anthracitic coals. This is held to be due to the sum of the myriad electronic absorption bands that merge into a nearly continuous absorption that decreases towards longer wavelengths. The furthest extension of this band reaches into the near-infrared region, a region widely used by chemists to elucidate the composition of organic compounds.

Coal, as an optically dense solid, is not ideal material for infrared absorption spectroscopy. Severe surface scattering means that some form of sample preparation is required. Two principle routes exist, either the particle size can be reduced and the powder held in a suitable medium, or smooth coal surfaces can be prepared. Possible approaches were reviewed by van Krevelen[35]. The approaches considered there include:

Cut thin sections
Nujol mulls

Hexachlorbutadiene mulls
Bromoform paste
Potassium bromide pressed disks

Other techniques subsequently used include pressed disks of pure coal[17] and reflectance spectroscopy of diamond cut surfaces[36]. All of these techniques have disadvantages. In the case of suspension techniques there is the problem of spectral obscuration by the suspending medium. Cut sections take time to prepare and allow oxidation to take place. All techniques make it difficult to study the reactions of coals as the adsorbtion of most reagents leads to swelling, as discussed in Section 1.4. Modern advances in spectrometer design and computerised data processing have improved the quality of results achieved.

1.6.2. Results

Infrared studies have produce important positive and negative evidence about the chemical structure of coals. The information obtained comes from the presence, or absence, of absorption bands characteristic of a specific bonds. A typical spectrum and the assignment of its major bands is presented in Chapter 3. The technique can be used to follow reactions which alter specific bands. An example of this is presented in Chapter 3 which shows the absence of non hydrogen-bonded hydroxyl groups in a coal extract.

Infrared spectroscopy can be used to study the interaction between coal and solvents. Larsen[37] and Portwood[17] have reported studies of the breaking of intra-coal hydrogen bonds by adsorbed solvents.

This approach is extended in Chapter 3 to include the study of the solvent molecule themselves after adsorption into the coal.

References

[1] Voght, E.G. and White, R.R., *Ind. Eng. Chem.*, **40**, 1731, (1948)

[2] Pattersky, K. and Teichmüller, M., *Brennstoff-Chem*, **41**, 79, (1960)

[3] Austin, D.E.G., Ingram, D.J.E., Given, P.H., Binder,C.R. and Hill, L.W. in *Coal Science, Adv. Chem. 55*, American Chemical Society 1966

[4] Nelson, J.B., *Fuel*, **33**, 153, (1954)

[5] Hirsh, P.B., *Res. Conf. on Science in the Use of Coal*, 1958, Inst. of Fuel, London

[6] Chapter 18 in: Anderton, R., Bridges, P.H., Leeder, M.R. and Sellwood, B.W., *A Dynamic Stratigraphy of the British Isles*, Allen & Unwin, 1983

[7] p 36-37 in: Van Krevelen, D.W., *Coal*, Elsevier, 1961

[8] Chapter 11 in: Anderton, R., Bridges, P.H., Leeder, M.R. and Sellwood, B.W., *A Dynamic Stratigraphy of the British Isles*, Allen & Unwin, 1983

[9] Figure adapted from Figure 11.23 of Anderton, R., Bridges, P.H., Leeder, M.R. and Sellwood, B.W., *A Dynamic Stratigraphy of the British Isles*, Allen & Unwin, 1983

[10] Calver, M.A., Westphalian of Britain, C.R. *6me Cong. Int. Strat. Geol. Carb*, , **1**, 233, (1967)

[11] Teichmüller, M. and Teichmüller, R., in *Coal Science, Adv. Chem. 55*, American Chemical Society, 1966

[12] Davidson, M.R., in *Coal Science Vol. 1*, eds. Gorbarty, M.L., Larsen, J.W. and Wender, I. Academic Press New York 1982 and Retkofsky, H.L. in same publication

[13] Green, T., Kovac, J., Brenner, D. and Larsen, J.W., in *Coal Structure*, ed. Meyers, R.A., 1982, Academic Press

[14] Given, P.H., Marzec, A., Barton, W.A., Lynch, L.J. and Gerstein, B.C., *Fuel*, **65**, 155, (1986)

[15] Marzec, A., Juzwa, M., Betlej, K. and Sobkowiak, M., *Fuel Process. Technol.*, **2**, 35, (1979)

[16] Szeliga, J. and Marzec, A., *Fuel*, **62**, 1229, (1983)

[17] Portwood, L., Ph.D. Thesis, Leicester, 1987

[18] Uebersfeld, J., Etienne, A. and Combrisson, J., *Nature*, **174**, 614, (1954)

[19] Ingram, D.J.E., Tapley, J.G., Jackson, R., Bond, R.L. and Murnaghan, A.R., *Nature* **174**, 797, (1954)

[20] Tschamler, H. and De Ruiter, E. in *Chemistry of Coal Utilisation (Supplementary Volume)* ed. Lowry H.H., John Wiley, 1963

[21] Retkofsky, H. L., in *Coal Science Vol. 1*, eds.Gorbarty, M. l., Larsen, J. W. and Wender, I., Academic Press, New York, 1982

[22] Retcofsky, H.L., Hough, M. R., Maguire, M.M. and Clarkson, R.B., in: *Advances in Chemistry Series no. 192 - Coal Structure*, eds. Gorbarty,M.L. and Ouchi, K., American Chemistry Society, 1981

[23] Petrakis, L., Grandy, C.W. and Jones, G.L., *Chemtech*, **14**, 52, (1984)

[24] Austen, D.E. G., Ingram, D.J.E. and Tapley, J.G., *Trans . Faraday Soc.*, **54**, 400, (1958)

[25] Kwan, C.L. and Yen, T.F., *Anal. Chem.*, **51**, 1255, (1979)

[26] Toyoda, S. and Honda, H., *Carbon*, **3**, 527, (1966)

[27] Stone, A.J., *Mol Phys.*, **6**, 509, (1963)

[28] Segal, B.G., Kaplan, M. and Fraenkel, G.K., *J. Chem. Phys.*, **43**, 4191, (1965)

[29] Seehra, M.S. and Srinivasan, G., *Fuel*, **61**, 396, (1982)

[30] Malhotra, V.M. and Graham, W.R.M., *Fuel*, **64**, 270, (1985)

[31] Seehra, M.S. and Srinivasan, G., *Fuel*, **62**, 792, (1983)

[32] Graham, W.R.M., *Prepr. Am. Chem. Soc. Div. Pet. Chem.*, **31**, 608, (1986)

[33] McBride, M.B., *Soil Science*, **126**, 200, (1978)

[34] Mangrich, A.S. and Vugman, N.V., *Sci. Tot. Environ.*, **75**, 235, (1988)

[35] p 363-370 in: Van Krevelen, D.W., *Coal*, Elsevier, Amsterdam, 1961

[36] Thomas, K.M., Personal communication

[37] Larsen, J.W. and Baskar, A.J., *Energy & Fuels*, 1, 230, (1987)

2. ESR STUDIES OF COAL

2.1. Introduction

As discussed in the previous chapter electron spin resonance (ESR) can be a useful aid in investigating the detailed structure of coals. ESR requires unpaired electrons to be present for any signal to be seen. As a result the environments of any species with unpaired electrons present can be probed. Fortunately the organic bulk of coal only generates a single signal, representing those aromatic structures with an odd number of π-electrons. This signal is further discussed in Section 2.3.1 below. Those transition metal nuclei that are present and ESR active therefore dominate the ESR spectrum away from the single organic signal. The purpose of this work is to use ESR to investigate the chemical environment of the three such nuclei, iron(III), manganese(II) and vanadium(IV) detectable in coal samples.

2.2. Experimental

Within the British coal industry coals are generally known by the name of the mine from which they were extracted. As mines frequently work several seams at different depths simultaneously it is impossible to give precise geological horizons for coal samples defined in this way. The following coals were provided for study by British Gas, all are from the Westphalian except for Loyyan, for which no age was given.

- Snibston
- Hucknall

- Manton
- Gedling
- Markham Main
- Manvers Swallow-Wood
- Nantgarw
- Loyyan

All of them are English bituminous coals from the East Midlands, except for Nantgarw, which is Welsh, and Loyyan, which is an American lignite.

All coal samples were stored in screw top jars as supplied by British Gas. Particle size varied from about 10 mm to 1 mm. Coal samples were dried in an oven at 353 K for 24 hours before use. At this time they were ground with a mortar and pestle to an even size. Samples prepared in this way are termed 'ground'.

The Loyyan coal was provided as a fine powder and was kept in a zip-lock bag; it also was dried before use. The particle size of some samples was further reduced by use of grinding equipment in the Department Of Geology, Leicester University. These samples are fine powders with particles too small to visually distinguish. These samples are termed 'powdered'.

All ESR experiments conducted in this work, except where indicated otherwise, were conducted at 77 K with the sample immersed in liquid nitrogen. The sample was placed in a 4 mm quartz ESR tube which was itself immersed in a finger dewar of liquid nitrogen. After nitrogen boiling had reduced to a steady rate the finger dewar was located within the ESR spectrometer cavity, a stream of nitrogen gas was used to flush the cavity of excess moisture.

Solvent extract experiments were carried out by adding a small quantity of coal to a sample tube of the selected solvent. The tube was shaken and left standing for a period of one week at room temperature. After this time a sample of the liquid was extracted with a pipette and filtered through cotton wool. ESR experiments on solvent extracts were conducted by dropping solution into a dish of liquid nitrogen to form beads. The beads were then transferred to a finger dewar of liquid nitrogen suitable for use with the ESR spectrometer. Only Snibston coal was used for the solvent extract work.

2.3. Results

2.3.1. Line Shapes

Whilst conducting ESR experiments with coal looking for transition metal signals it became clear that some samples would give a clear spectrum whilst others would give indistinct 'bumps' in the expected region. Some coals tended to always give poor spectra. These may well contain a mixture of species that were giving overlapping features. Other coals, though, gave much better spectra when powdered, rather than ground.

Measured peak-peak line widths show no improvement but the lines appeared to the eye to be better resolved. The following results were obtained from Snibston coal. In all cases the peak-peak line width of the component of the manganese (II) sextet at the lowest field position was recorded.

Coal State	Temperature	Peak - Peak Linewidth
powdered	4 K	22 G
powdered	77 K	8 G - 20 G
ground	77 K	15 G - 20 G

Table 2.1 - Manganese (II) Linewidths from Snibston Coal

The cause of the apparent broadening may be a change in line shape rather than an actual linewidth change. Wertz and Bolton[1] say that unsymmetrical line shapes may be seen with solid state spectra where local magnetic fields are uneven. This could easily be the case for the transition metals in coal if they are present in clusters or in mineral grains.

Magnetic minerals form with their magnetic fields aligned with the earth's magnetic field at the time of formation, indeed this phenomenon is often used in paleogeographic studies to identify the magnetic latitude at the time of deposition. Iron containing minerals in coal fragments will have a local magnetic field which will disrupt the spectrometer's applied field, giving rise to extra anisotropies in the spectrum. Reducing particle size will involve randomly orientating all the local magnetic fields within the sample, so negating their effect on the spectrum.

2.3.2. Organic Signals

It is not intended that the organic derived ESR signal of coals be widely discussed here. In the previous chapter it was shown how these signals have been identified by other workers as

representing the unpaired electrons in heterogeneous polyaromatic systems. It was also shown how the parameters describing the ESR spectra obtained can be related to the chemical properties of the coals concerned. In an effort to gain new information from this spectrum experiments were conducted at 4 K (liquid helium temperature).

2.3.2.1. Nature Of The Signal

In some cases two distinct signals have been seen superimposed in the organic ESR spectrum of coal. This has only been seen in high grade coals and in some solvent modified coals, and consists of a narrow singlet superimposed on the usual broader singlet. The narrower line has been identified[2,3] as being due to line narrowing by exchange processes between radicals within coals. This behaviour increases with coal rank as the radical density increases, with a corresponding decrease in radical separation.

One possible way to get more detail from the organic ESR spectrum is to lower the temperature[4]. Signal amplitude is inversely related to the absolute temperature and T_1 spin-lattice relaxation processes are minimised with decreasing temperature. By minimising thermal relaxation linewidths can be reduced, giving a better resolution.

No reference to coal ESR conducted at liquid helium temperatures (ca. 4 K) could be found in published literature. It was therefore decided to conduct experiments under these conditions to see if any fresh information could be gained.

2.3.2.2. Results

Two spectra from this series are presented as Figures 2.1 and 2.2. Figure 2.1 shows the central singlet displayed under similar spectrometer settings to those previously used by Portwood[5] at room temperature. There is no sign of any additional detail in the spectrum. The same is true of Figure 2.2 which shows a wider spectrum looking for more detail from the transition metal signals. These spectra are essentially indistinguishable from those produced at the usual 77 K.

Measured linewidths for the organic signal at room temperature are typically between 4 G and 9 G[5]. The measured value from Figure 2.1 is 6.2 G.

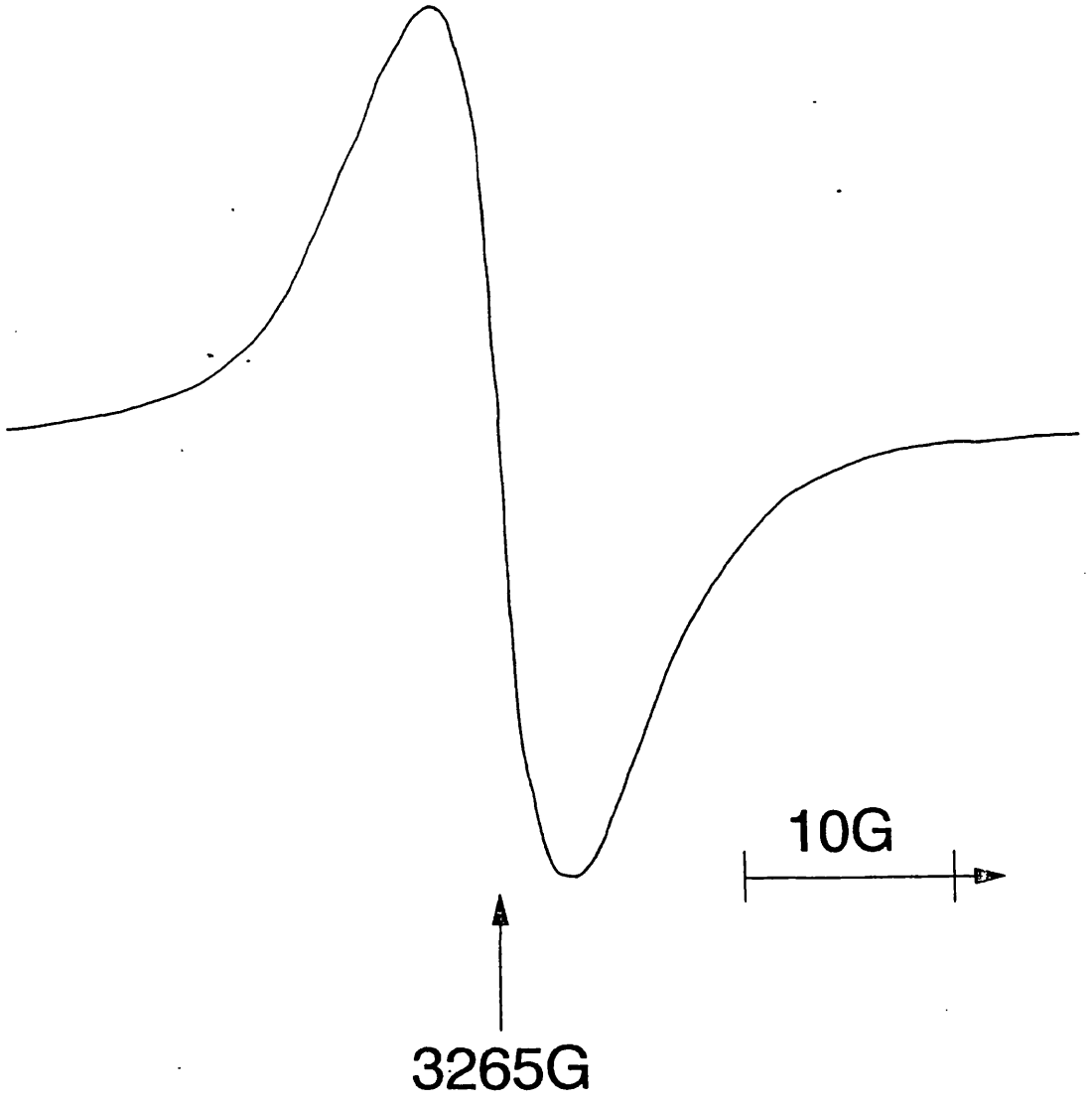

Figure 2.1 - Free Spin Region Of Snibston Coal at 4K

2.3.2.3. Interpretation

Reducing the operating temperature of the E109 spectrometer from ca. 77 K to ca. 4 K does not seem to produce any benefits. The line widths obtained are not noticeably narrower than those obtained at higher temperature. It must be concluded that thermal relaxation processes do not significantly contribute to the linewidth of the organic ESR spectrum of coal. Whatever variety of organic radicals does exist within coal, it is impossible by reduction of temperature to distinguish between any of them.

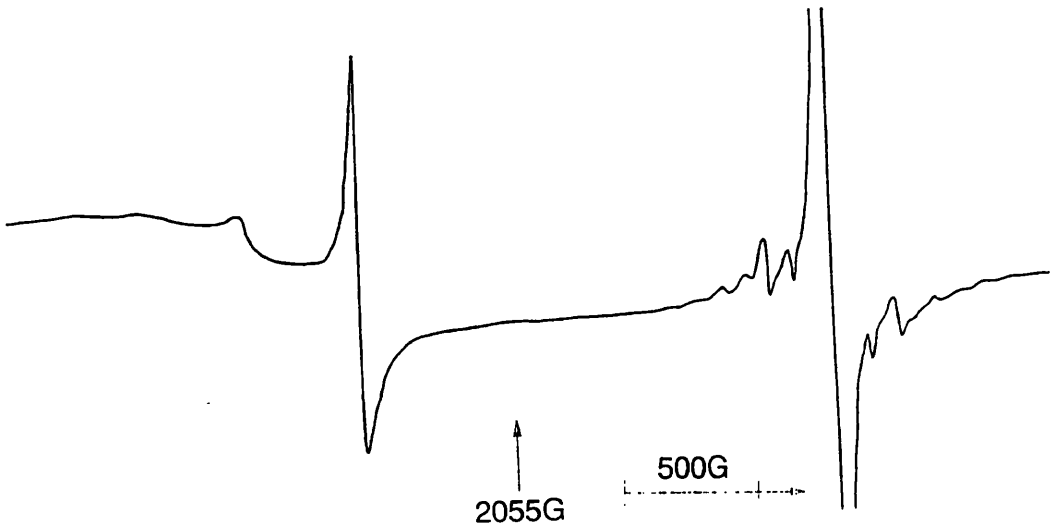

Figure 2.2 - ESR spectrum of Snibston Coal at 4K

2.3.3. Iron (III)

Iron is a very important element in both biochemistry and geochemistry. Of the common oxidation states only iron (III) has

the unpaired electrons necessary to produce an ESR signal. A Mössbauer study of iron containing minerals in coal was conducted by Montano[6] on West Virginian coals. He concluded that the iron containing minerals present were, in order of importance, pyrite, marcasite, clays (mainly illite), hydrated sulphates and carbonates. The only minerals containing iron (III) were the clays, and even they were reported as having far less iron (III) in them than is usually the case for samples not derived from coal. Iron oxides were found only in weathered coals although magnetite (Fe_3O_4) has been identified elsewhere by ferromagnetic resonance in fresh coals[7]. These observations confirm that the coals were formed in a strongly reducing environment. The magnetic nature of magnetite has prevented it from being detected by normal ESR experiments[8] so it cannot be considered as a source of any iron (III) ESR spectra.

2.3.3.1. Nature Of The Signal

Three separate iron (III) signals are seen in coal ESR spectra. Each represents iron nuclei in a different environment. Two of the signals seen in this study ($g = 6$ and $g = 4.3$) have been seen in studies of iron (III) in clays[9].

The strongest iron signal is seen at around $g = 4.3$. It represents iron (III) in an octahedral configuration[10] at the limits of rhombic distortion. It is a very common signal in geological[11,12] and biological samples[13] and, as such, is not particularly informative. One significant point about this signal

is that it represents, in both biochemistry and geochemistry, 'free' iron. Minerals containing a lot of iron (III) such as haematite (Fe_2O_3) only show this signal very weakly[11]. This signal has been identified with the iron (III) in octahedral sites in clays[9,14].

Similarly the signal at around g = 6 represents square planar iron (III)[10]. This signal is less common in coal than the g = 4.3 signal; it is also seen in clays[9].

The third iron (III) signal occurs around g = 3.25. This is a much more unusual spectrum and has been assigned to superparamagnetic iron/oxygen clusters[15,7]. These are discussed further below.

2.3.3.2. Results

Iron signals occurred in all of the coals studied. The g = 4.3 signal was always present and had a consistent appearance. The g = 6 signal was much less intense than the g = 4.3 signal, and was not always present. The g = 3.25 signal is even less intense and appears mostly as a broad 'bump' in the baseline. All of these features are labelled in Figure 2.3.

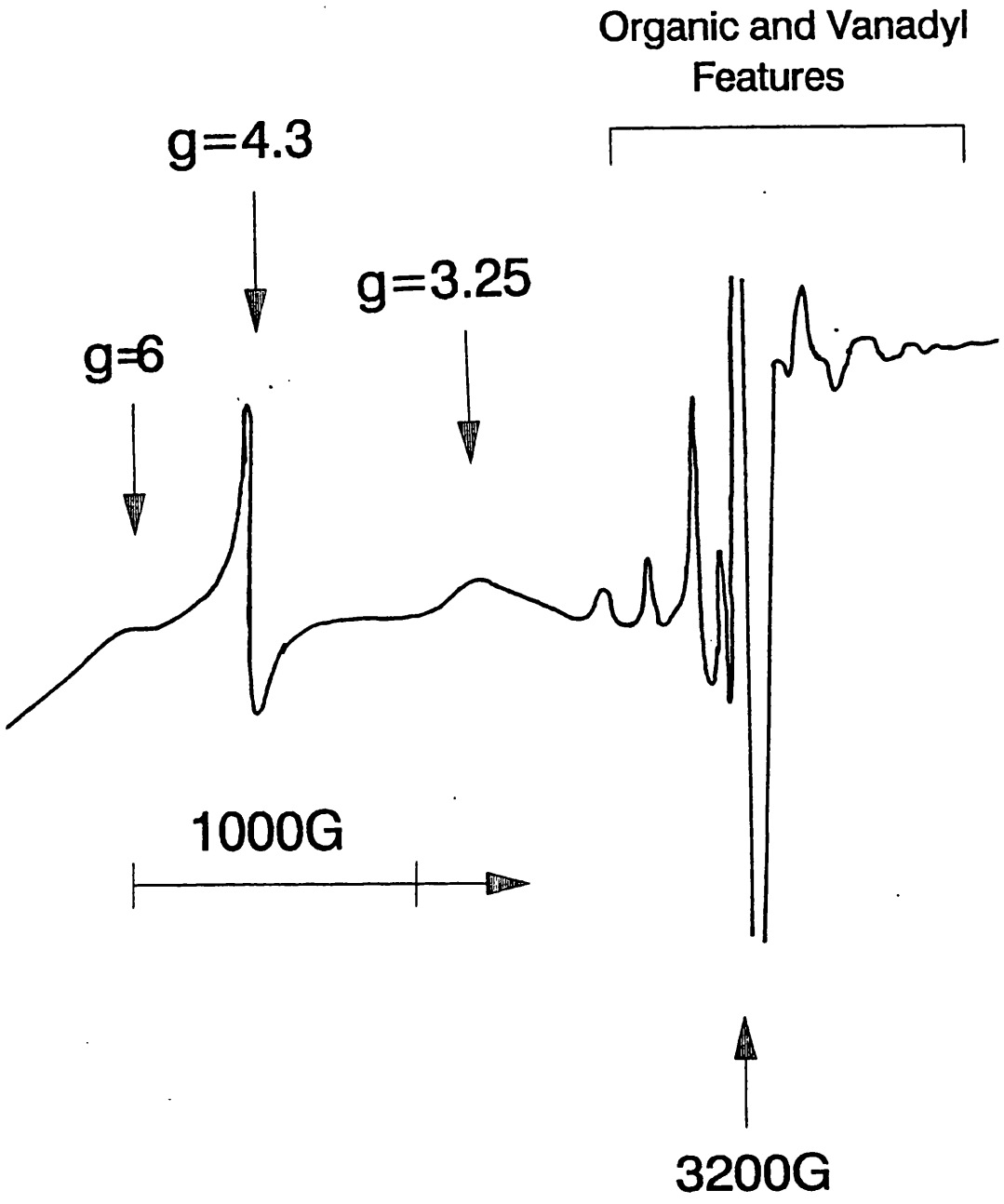

Figure 2.3 - ESR spectrum of Iron Features in Gedling Coal at 77K

2.3.3.3. Interpretation

The g = 4.3 and g = 6 signals are widespread within different coals and always take the same form. They are, therefore, of no use as fingerprints for specific coals. It is not possible from the information derived from pure coals to determine whether the iron is located within mineral grains or within the organic component. Iron environments are discussed further in Section 2.4.

The g = 3.25 signal is of far more interest, although appearing in only a few samples. Such signals have been attributed to clusters of FeOOH when seen in iron transport proteins[11]. The clusters have small enough masses to show superparamagnetic behaviour[16]. This occurs where a group of nuclei form a magnetic microcrystal and the resultant magnetic field is weak enough to undergo rapid thermally induced fluctuations. Two possible interpretations exist for the occurrence of such clusters in coal.

Firstly it is possible that the source of the signals is the same biological source as already described. If this were that case then the iron cores of biological macromolecules have been preserved from the original plant material.

The second possibility is that this is a sign of the development of secondary mineralisation since coal formation. The principle candidate must be goethite (essentially hydrous FeOOH). This would imply that the ground water passing through the coal has at

some stage been oxidising. There must also have been a source of iron for reworking, which would most likely be pyrite (FeS_2), the most common iron containing mineral in coal[7]. It is also possible that oxidation has occurred since extraction from the coal face.

2.3.4. Manganese (II)

A manganese (II) spectrum was only seen in Snibston coal. There was no sign of the vanadyl spectrum seen in all other coals studied. Manganese (II) occurs in many minerals, usually as a contaminant. ESR spectra of natural calcium salts such as calcite, aragonite (both polymorphs of $CaCO_3$), and haematite (anhydrous Fe_2O_3), frequently show a manganese (II) ESR spectra. Clay group minerals can also show manganese (II) spectra. The detection of manganese (II) is probably of little significance in itself, but its host mineral could be of significance as it has been suggested that calcium carbonate and/or calcium oxide may perform a significant catalytic role in coal pyrolysis[17].

2.3.4.1. Nature Of The Signal

Manganese (II) is a d^5 ion with a nuclear spin (^{55}Mn) of 5/2. This gives an easily recognised spectrum with six principle lines. Crystal field splitting of the manganese d orbitals causes parallel and perpendicular satellites to be seen. Study of these features yields zero field splitting (D) values, which are more sensitive to the environment than the hyperfine coupling (A) values calculated from the principle lines.

2.3.4.2. Results

The Snibston coal ESR spectrum is presented as Figure 2.5. The parameters calculated from the spectrum are presented below. In subsequent discussion D is taken as D_{para} to preserve compatibility with other studies[18,14] (the splitting from the last line of the principle sextet to the parallel feature is 2 D_{para}, this value is halved to yield D).

A_{iso}	-	95 G
D_{para}	-	185 G
D_{perp}	-	150 G
D_{iso}	-	D_{para} - D_{perp} = 55 G

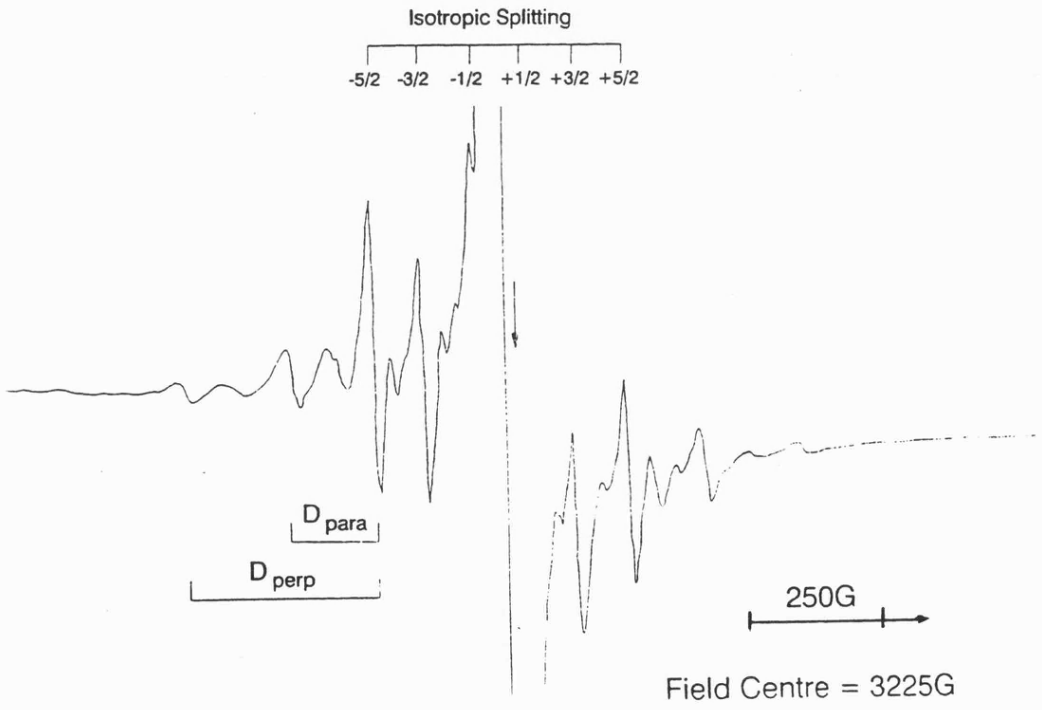

Figure 2.4 - ESR Spectrum of Manganese (II) in Snibston Coal

2.3.4.3. Interpretation

A study by Malhotra and Graham[18] identified calcite as the source of the manganese (II) spectrum in Pittsburgh No. 8 coal. The ESR parameters from that study and others are reproduced below.

Sample	A_{iso}	D
Coal Derived Pyrite[19]	95 G	60 G
Coal Derived Calcite[18]	96 G	75 G
Pittsburgh No.8 Coal[14]	96 G	77 G
Snibston Coal	95 G	185 G
Natural Calcite[18]	96 G	80 G
Laboratory $CaCO_3$[20]	95 G	85 G
Dolomite[14]	93 G	146 G
Modelling Clay[18]	95 G	113 G

Table 2.2 - ESR Parameters for Manganese (II) Environments

Clearly the ESR spectra indicate that the manganese (II) spectrum from Snibston coal is not in calcite. The laboratory calcium (II) carbonate sample gave a very similar spectra to those for natural and coal derived calcites presented in Reference 18. Further environments clearly need to be studied to identify the source of manganese (II) in Snibston coal.

2.3.5. Vanadium (IV)/Vanadyl

Vanadium (IV) in the form of the vanadyl ion, VO^{2+}, has been identified by ESR in a variety of coal related environments. These include porphyrins in asphaltene deposits[14], soils[21] and

carboxylate complexes in esturine sediments[22]. The purpose of this work was to identify the vanadyl environment in coals.

2.3.5.1. Nature Of The Signal

The vanadyl ESR spectrum in the solid state has been described in basic terms by Mc Bride[21]. ^{51}V has a nuclear spin of 7/2 and so an eight line spectrum is expected. In the solid state the axial anisotropy caused by the vanadyl oxygen causes the spectrum to appear as parallel and perpendicular features. The spectrum appears centred close to free-spin. It is, therefore, impossible to measure g-values as this part of the spectrum is dominated by the organic radical signal. Measurements of the parallel and perpendicular hyperfine coupling constants, A_{para} and A_{perp}, were made by measuring between the outermost component lines of the spectra and dividing by seven.

2.3.5.2. Results

All coals studied, except for Snibston, yielded a vanadyl spectrum. A spectrum from Manvers Swallow Wood coal is presented as Figure 2.5. In some cases the perpendicular features are insufficiently resolved for an A_{perp} value to be reported. Where both anisotropic **A** values are known it is possible to calculate the isotropic **A** value, A_{iso}, and the anisotropic interaction parameter, 2B. The values recorded and the A_{iso} and 2B values calculated from them, are tabulated in Table 2.2.

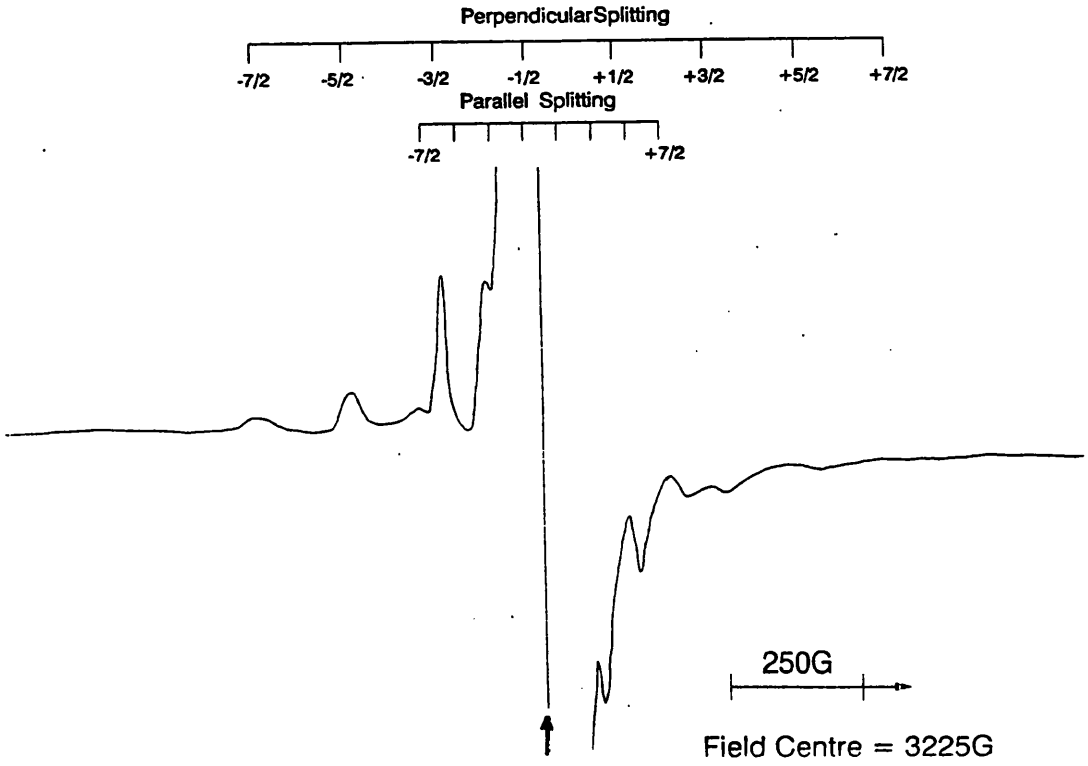

Figure 2.5 - Vanadyl Spectrum in Manvers Swallow-Wood Coal at 77K

Coal	$\|A_{para}\|$	$\|A_{perp}\|$	$\|A_{iso}\|$	$\|2B\|$
Manvers Swallow Wood	172G	62G	99G	73G
Manvers Swallow Wood	170G	67G	101G	69G
Markham Main	180G	-	-	-
Markham Main	170G	-	-	-
Loyyan	180G	66G	104G	76G
Manton	175G	64G	101G	74G
Manton	175G	58G	97G	78G
Hucknall	180G	-	-	-

Table 2.3 - Vanadyl ESR Parameters from Coals

Estimated experimental error on these values is ca. +/- 5 G. The main sources of error are the accuracy of measuring the width of the parallel feature, approximately 1200 G wide, and in defining the perpendicular features which are partly 'buried' by other lines. This means that the calculated values are within experimental limits of each other.

2.3.5.3. Interpretation

It is significant that the Loyyan sample gives a similar result to the others as it is an American lignite as opposed to a British bituminous coal. This would suggest that the environment of the vanadyl ion is not one that varies significantly with coal rank or geographical origin.

Other studies of vanadyl ions have produced a variety of results. Examples are presented it Table 2.3.

Sample	$\|A_{iso}\|$	$\|2B\|$	Reference
Circle Cliffs Asphaltene	98G	74G	9
Boscan Asphaltene	97G	76G	14
Vanadyl etiaporphyrin	97G	74G	14
vanadyl in humic acid	110G	79G	21
vanadyl in humic acid	114G	77G	12
vanadyl/oxalate	106G	82G	12
penta-aqua vanadyl	120G	83G	12
coal average	100G	74G	This Work

Table 2.4 - Non-Coal Vanadyl ESR Parameters

The environment of vanadyl in coal is clearly similar to the porphyrin environment found in asphaltenes. It is unlikely that porphyrin structures would form during the coalification process. This would suggest that the porphyrins were already present at the time of coal formation and that they are relics of some biochemical precursor. It is possible that the vanadyl group has displaced another ion from the porphyrin but vanadyl is known to occur in fungi[23] and similar primitive plants will have certainly lived in the coal swamps.

The important conclusion from this work is that the vanadyl in coal is located within the organic 'phase' rather than being present as a trace element in a mineral.

2.4. Coal Extracts

2.4.1. Introduction

The ability of solvents to penetrate coals and extract material from them has been an area of study for many years[24,25]. Some ESR work has been performed on solvent extraction, mostly at high temperatures and pressures. Most of these studies have concentrated on studying the organic ESR signal. It might be possible for ESR study of solvent extracts to help identify the location of metals within coal. Mineral grains should be highly insoluble in most organic solvents, whilst metal containing organic structures might be released from the coal into solution, and so be seen in the extract.

Duber *et al*[3] and Yokokawa[26] both claimed that the organic ESR signal was a composite of two lines, one with a line width of ca. 6 G, the other about 2 G. The narrower line is identified with radicals in the coal macromolecule that are capable of exchange interactions with each other whilst the broader line is due to radicals isolated from other radicals within the coal matrix. Duber *et al*[3] demonstrated that the apparent linewidth could be changed by preferential quenching of one or other of the radicals responsible. They found that the ESR spectrum of a pyridine extract contained none of the narrower feature, thereby apparently broadening. Seehra *et al*[27], however, using N-methyl pyrrolidone, found no radical quenching and therefore proposed that different extraction mechanisms must be considered.

2.4.2. Results

The extract spectra were found to contain the same features as the pure coal spectra. The changes were mostly in terms of different relative intensities of features. Sample spectra are presented as Figures 2.6 and 2.7. The results are presented in Table 2.5. The iron and organic peak heights refer to the peak heights of the g = 4.3 iron (III) signal and of the organic spectrum. Spectrometer power and field modulation were kept at the same values throughout these spectra, so the peak heights and their ratio serve as a rough guide to allow comparison of the extracts. No height is given for the pyridine organic peak because the feature was very strong and was not resolved on the chart paper.

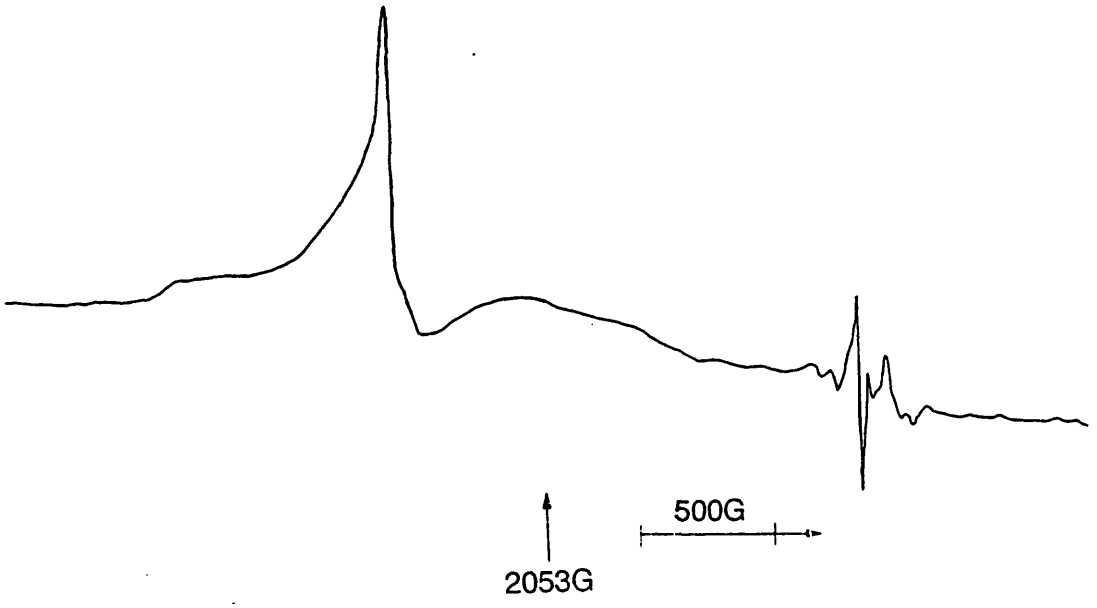

Figure 2.6 - ESR Spectrum of Benzene Extract of Snibston Coal

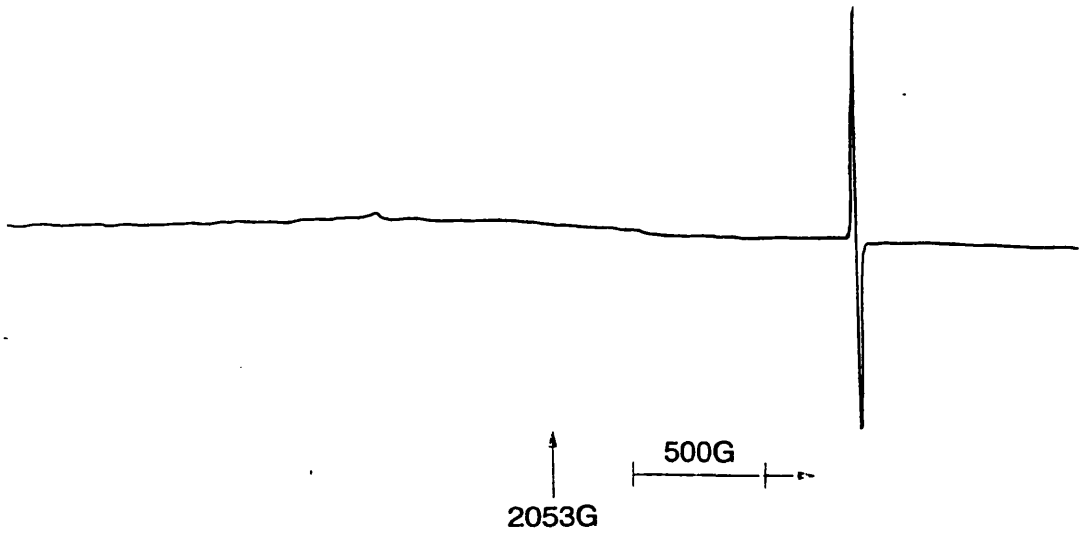

Figure 2.7 - ESR Spectrum of Acetone Extract of Snibston Coal

The procedures used to prepare these spectra were not intended to be quantitatively accurate. In qualitative terms the benzene results stands out as being significantly different. The most remarkable feature of these results is the enrichment in iron (III). This is shown by all samples, but particularly by benzene and, to a lesser extent, by pyridine. Only the benzene and pyridine extracts show any sign of other (non iron(III)) transition metal features centred on free-spin. In both cases the spectrum is insufficiently resolved to allow identification.

Solvent	Fe peak height	organic peak height	peak height ratio	recorder gain	organic peak linewidth
Untreated Coal	38	24320	640	$1.6*10^3$	6 G
Benzene	122	77	0.63	$1.6*10^4$	12 G
Acetone	2	151	75.5	$3.2*10^3$	8 G
DMSO	1.5	156	104	$5.0*10^3$	5 G
DMF	6	182	30.3	$2.5*10^3$	5 G
pyridine	60	n/a	n/a	$6.3*10^3$	12 G
trimethyl-benzene	0	36	n/a	$6.3*10^3$	6 G
nitro-benzene	0	89	n/a	$5.0*10^4$	10 G

Table 2.5 - ESR Data For Solvent Extracts

2.4.3. Discussion

2.4.3.1. Iron (III) Content

There are three ways in which the iron (III) content of the extracts could be enhanced. Firstly oxidation could be taking place of iron (II) minerals within the coal whilst the extraction takes place. The oxidising agent would have to be atmospheric oxygen dissolved in the solvent which does not explain why the final extract composition is so solvent dependent.

A second possibility is that the iron (III) containing environments are being preferentially extracted by the solvents. Confirmation of this explanation would require knowledge of the precise iron (III) environments. If they are evenly distributed throughout the organic phase then it is difficult to understand how the extraction can be selective. It could be understood if

the iron were localised, either in some form of iron rich cluster or in microcrystals, and those environments were preferentially extracted. It is recognised that coals can be modelled as two component systems[28]. One component is an insoluble macromolecule and the other a lower weight 'mobile' component trapped within, or bound to, the first component. The apparent concentration of iron in extracts would suggest that the iron is preferentially located in the mobile component. Iron present as mineral grains would clearly be a part of this component. Perhaps iron transporting organic compounds might be sufficiently stable to 'resist' inclusion in the macromolecule during coal formation.

A third possibility is that the phenomenon identified is not a preferential extraction of iron (III), but a quenching of the radicals in the organic matrix. Duber *et al*[3] claim a 30% loss of spin density whilst saturated with pyridine, which returns after washing with methanol and hydrochloric acid. This quenching process could certainly be operating but does not fully explain the observed results. Duber *et al* found that the radical quenching ability of a solvent was proportional to its ability to extract coal material. This was shown by Marzec *et al*[25] to be a function of the DN-AN value for the solvent, where DN is the Gutmann donor number and AN the Gutmann acceptor number. This too does not explain the results given that benzene performs best and better electron donors and acceptors are present amongst the solvents used. The Gutmann values and the iron (III)/organic peak height ratio are presented in Table 2.5.

Solvent	DN	AN	DN-AN	Peak Height Ratio
Benzene	0.1	8.2	-8.1	0.63
Acetone	17.0	12.5	+4.5	75.5
DMSO	29.8	19.3	+10.5	104
DMF	26.6	16.0	+10.6	30.3
Pyridine	33.1	14.2	+18.9	n/a

Table 2.7 - Gutmann Parameters For Solvents Used

Clearly the experimental results are difficult to explain and a more rigourous quantitative study is probably necessary to determine whether iron (II) is being oxidised during the extraction or if organic radical quenching is a significant mechanism.

2.5. Conclusions

ESR studies of transition metals in coal have produced few conclusive results. Certainly vanadyl is located within porphyrin-like structures in the organic phase. Iron (III) must be present in clays, is probably present as an oxidation product of iron (II) minerals, and its presence in the organic phase cannot be ruled out. Manganese (II) is present, but not in calcite where it has been found in Pittsburgh No.8 coal.

The brief solvent extract study seems to pose more questions than it answers. A rigourous study of extracts and residues may generate useful information, particularly if combined with studies of extracts with different analytical techniques. Room

temperature ESR of liquid extracts may give liquid phase spectra if the complexes are small, or solid phase spectra if the metals are still trapped within the coal matrix.

References

[1] Wertz, J., and Bolton, J., *Electron Spin Resonance*, Chapman & Hall, New York 1986, page 196

[2] Petrakis, L. and Grandy, D.W., *Prepr. Div. Fuel Chem. Amer. Chem. Soc.*, **23**, 147, (1978)

[3] Duber, S. and Wieckowski, A.B., *Fuel*, **63**, 1641, (1984)

[4] Wertz, J and Bolton, J., *Electron Spin Resonance*, Chapman & Hall, New York 1986, page 458

[5] Portwood, L., Ph.D. Thesis, Leicester 1987

[6] Montano, P.A. in *Coal Structure,* editors: Gorbarty, L.M and Ouchi, K., Advances in Chemistry Series no. **192**, American Chemical Society, Washington, 1981

[7] Malhotra, V.M. and Graham, W.R.M, *J. Appl. Phys* **57**, 1270, (1985)

[8] The author, unpublished results

[9] Meads, R.E. and Malden, P.J., *Clay Minerals*, **10**, 313, (1975)

[10] Dowsing, R.D. and Gibson, J.F., *J. Chem. Phys.*, **50**, 294, (1969)

[11] The author, unpublished results

[12] Mc Bride, M.A., *Soil Science*, **126**, 200, (1978)

[13] Deighton, N., Personal Communication

[14] Graham, W.R.M., *Prepr. Am. Chem. Soc. Div. Pet. Chem.*, **31**, 608, (1986)

[15] Weir, M.P., Peters, T.J. and Gibson, J.F., *Biochimica et Biophysica acta*, **828**, 298, (1985)

[16] Boas, J.F. and Troup, G.J., *Biochimica et Biophysica acta*, **229**, 68, (1971)

[17] Cypres, R. and Furfari, S., *Fuel*, **61**, 447, (1982)

[18] Malhotra, V.M. and Graham, W.R.M., *Fuel*, **64**, 270, (1985)

[19] Seehra, M.S. and Srinivasan, G., *Fuel*, **61**, 396, (1982)

[20] Spectra provided by Dr. J.L. Wyatt, University Of Leicester

[21] Mc Bride, M.B., *Soil. Sci. Soc. Am. J.*, **44**, 495, (1980)

[22] Mangrich, A.S. and Vugman, N.V., *Sci. Tot. Environ.*, **75**, 235, (1988)

[23] Chasteen, N.D., in Biological Magnetic Resonance vol 3, Plenum Press, New York, 1981, page 53.

[24] Hill, G.B., Hariri, H., Reed, R.I. and Anderson, L.A., in *Coal Science*, ed. Gould, R.F., Americal Chemistry Society, Washington, 1966

[25] Marzec, A., Juzwa, M, Betlej, K. and Sobkowiak, M., *Fuel Processing, Technology*, **2**, 35, (1979)

[26] Yokokawa, C., *Fuel*, **47**, 273, (1969)

[27] Seehra, M.S., Ghosh, B., Zondlo, J.W. and Mintz, E.A., *Fuel Processing Technology*, **18**, 279, (1988)

[28] Given, P.H., Marzec, A., Barton, W.A., Lynch, L.J. and Gerstein, B.C., *Fuel*, **65**, 155, (1986)

3. INFRA-RED STUDIES OF COALS

3.1. Introduction

Infra-red absorption spectroscopy is used extensively to study the bonding in many kinds of compounds. Its basis is the excitation of the vibrational modes possessed by the sample. A non-linear polyatomic molecule has 3n-6 vibrational modes, where n is the number of atoms. Linear polyatomics have 3n-5 modes. All modes are in principle features of the whole molecule. Fortunately many modes predominantly feature one specific bond or group, examples being the stretching of a carbonyl group or one of the six possible modes of a group of the form AX_2. Vibrational modes featuring the same kind of deformation of the same chemical group will tend to absorb at very similar frequencies. The exact frequency of the radiation absorbed is determined by the characteristics and environment of the group in question.

Coals are heterogeneous mixtures and so few specific bonds can be identified by infra-red absorption. In most cases only the general types of bonds can be identified. Infra-red absorption spectroscopy can be used to study in detail the effect that coals have on other compounds in contact with coal. This chapter presents an investigation of the way in which the spectra of organic solvent molecules are changed after being adsorbed by coals. The aim of the work is to determine the nature of the functional groups accessible to solvents within coals and to see how such groups change with different coals.

3.2. Experimental

Infra-red absorption spectroscopy faces many technical difficulties when performed on coals. Foremost is the difficulty in obtaining spectra of an opaque solid. The coal itself must be carefully prepared as elevated temperatures and chemical treatments will cause chemical alteration. For experiments where solvents are required to interact with coals it is necessary to expose the coal to solvent in such a way that the coal sample does not disintegrate and the spectrum is not overwhelmed by excess unbound solvent. These issues are addressed in the following sections.

3.2.1. Coal Samples

Coal samples were provided either as powders or as raw coal stored under deoxygenated water. Neither form is suitable for IR absorption spectroscopy. Even if they could be mounted in the spectrometer then the optically opaque nature of coal, and the scattering ability of the powder, would make spectroscopy impossible. Coal solutions cannot be used as studies have shown that the extraction of coal by organic solvents is a selective process. Mulls are likewise unusable as exposure to solvents would be problematical and the mulling agent might obscure significant spectral features.

Other workers have reported the used of cut thin sections and reflectance spectroscopy as solutions to the problems[1]. These

techniques are not available at Leicester and so new techniques had to be developed.

Portwood[2] reported the use of pressed discs of ground coal. These gave very good transmission spectra but they are extremely fragile and would disintegrate when exposed to solvent vapours that cause swelling of the coal. A better solution proved to be films of coal deposited from coal/water slurries.

3.2.1.1. Coal Slurry Preparation

All coal IR spectra presented in this work were recorded using films of coal deposited from a slurry, termed slides. Only water based slurries were used as most samples were supplied in water and coals are naturally saturated with water when underground. Solvents that would react with coal clearly could not be used. Dichloromethane, which does not react with coal, a fact established by ESR studies[3], was tried but it failed to form a slurry with coal.

Samples for preparation were ground with a mortar and pestle. The slurries were generated by grinding the coal with water in a McCrone Micronising mill fitted with agate elements. Approximately 1 g of coal was used with 10 cm^3 of water. The water was taken from the storage jars containing the coals as it should have been in chemical equilibrium with the coal, or de-ionised water if using powders. Grinding periods of 1-24 hours were used and were not found to make a difference to the spectra

obtained. Coal slurries were stored in sealed sample tubes until used. If kept for over a week slurries would start to settle out.

3.2.1.2. Coal Slide Preparation

Coal slides were prepared on 25 mm diameter calcium fluoride spectroscopic plates. Calcium fluoride was chosen because it does not have any absorption in the region selected for study, that of the stretching modes of carbonyl and hydroxyl groups. The preparation of slides from slurries require that the water is removed in such a way as to prevent cracking of the coal. Cracked slides may fall off the plate when held vertically and are likely to give a noisy spectrum if they do remain intact.

The most reliable way found to produce a film was as follows. The plate was heated in an oven at 85 °C. A single drop of slurry from a pipette was placed at the centre of the slide and spread thinly over the plate. The heat of the plate then dried the slurry within seconds. This usually produced an even slide that would not disintegrate. If the slide cracked then the plate was cleaned with acetone and returned to the oven. The fresh slides were allowed to stand for an hour before being returned to the oven, it having been found that a rapid return to the oven produced cracking of the film. Slides were left in the oven until required, the elevated temperature minimising the uptake of water by the coal.

The slide of a coal extract referred to in Section 3.3.2 was prepared in a similar way to those described above. The only

difference being that as acetone was the solvent heating the slide was not necessary to ensure rapid evaporation.

3.2.2. Spectrometer

All spectra were recorded on a Perkin Elmer 681 twin beam infra-red spectrometer used in absorption mode. Data capture and processing was performed in some cases on an attached microcomputer. This provided facilities for curve smoothing, calculation of difference spectra, differentiation and peak finding. The loss of this microcomputer facility forced a premature abandonment of this program of work.

The spectrometer cavity was flushed with nitrogen that had been passed through a dreschler bottle of molecular sieve. Removal of atmospheric water in this way improved the resolution of the spectra by removing minor water features from the 1550 - 1750 cm^{-1} region being used to study carbonyl stretching frequencies. These features re-occurred at the same frequencies and had previously been interpreted as fine detail of the solvent carbonyl stretch band[2].

3.2.3. Exposure To Solvents

Most of the experiments reported in this chapter involve the binding of a solvent to coal. It was found to be difficult to achieve solvent addition with the sample in the spectrometer as the sample was heated by the spectrometer beam. Change could be seen in the 3200 cm^{-1} region of the spectrum where hydrogen bonds

could be seen to be being lost as the spectrometer beam drove off solvent and/or water from the coal. It was decided to place the sample in the spectrometer only when the solvent adsorption had taken place. As a result the solvent lines produced represent the most tightly bound solvent molecules. Most of the unbound solvent is likely to have been removed by the nitrogen flow flushing the spectrometer or by heating by the infra-red beam. This side effect is in no way considered to be a disadvantage as the intention was to study coal-solvent bonding. Unbound solvent trapped in coal pores would serve only to obscure bound solvent.

Exposure to solvent was carried out in a desiccator. The coal slides were heated in a 85 °C oven for at least 24 hours before use. The spectra of the coal 'blank' was recorded on the computer and the slide was transferred to the desiccator. The top of the slide was marked so that it could be placed in the spectrometer with the same orientation after solvent exposure, this being necessary for the recording of difference spectra. The desiccator contained coal slides, a beaker of the chosen solvent and a beaker of molecular sieve and/or silica gel. The desiccator was flushed with nitrogen before being sealed for a period of at least a week. After this period of time the slide was taken from the desiccator and a new spectrum recorded, with the slide in the same orientation as before.

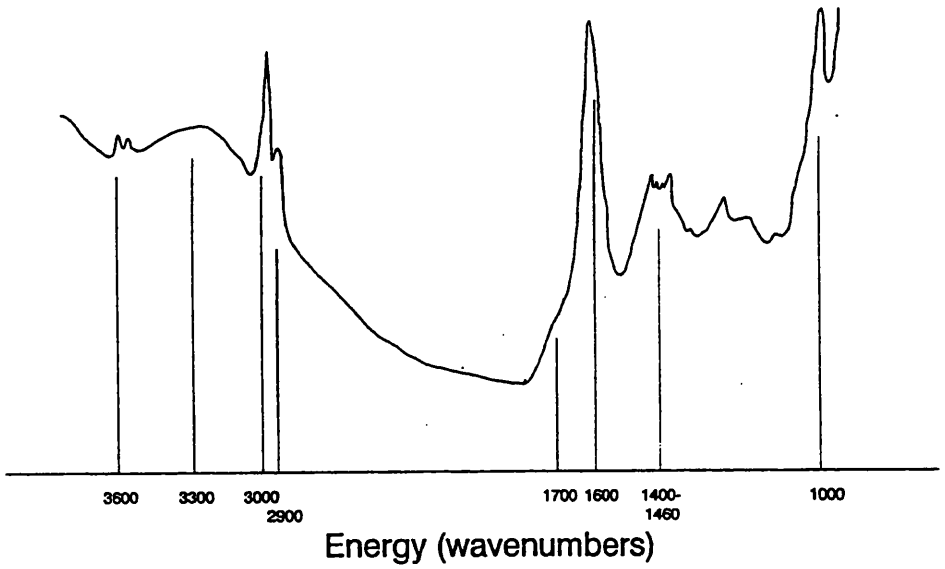

Figure 3.1 - IR Absorption Spectra Of Typical Coal

3.3. Pure Coals

An example infrared absorption spectrum of a coal slide is presented as Figure 3.1. Spectra achieved by other methods, such as thin sections[4], pressed discs[2], suspensions[5] or reflectance[6] show the same features except for the intense absorption due to the calcium fluoride. This absorption makes the spectra unusable to study features below about 1000 cm^{-1}. Above this point several features can be discerned. These are assigned below.

3.3.1. Assignment Of Features

The assignments of the bands within the IR spectrum were established during the 1940s and 1950s and were reviewed by van Krevelen[7].

3600 - 3700 cm^{-1}	Unbound phenolic and carboxylic O-H
3100 - 3600 cm^{-1}	Hydrogen bonded O-H and N-H
3000 cm^{-1}	Aromatic C-H stretch
2900 cm^{-1}	Aliphatic C-H stretch
1600 - 1700 cm^{-1}	C=O stretch
1600 cm^{-1}	Aromatic skeletal stretch
1400-1460 cm^{-1}	CH_2 scissors
	CH_3 deformation
	Aromatic skeletal stretch

Portwood[2] established that the coal spectrum does not differ significantly across a range of British bituminous coals, certainly not to the extent of individual coals having infra-red fingerprints.

3.3.2. Acetone Extract

A sample of coal was kept in a stoppered sample tube of acetone for a period of a month. After this time the solution was golden-brown in colour, a colouration which persisted after filtration.

A slide was formed according to the procedure described in Section 3.2. The resulting spectrum is presented as Figure 3.2. It shows identical features to Figure 3.1 across the complete spectrum, except for the sharp peaks above 3600 cm^{-1}, which are no longer present. These peaks are assigned to unbound hydroxyl groups. These groups could not exist in the presence of water which is known to saturate coals, as they would for hydrogen bonds to water. They are assumed to be in areas closed to water, located around 'blind' cavities within the coal structure that do not connect to the pore network.

This result indicates one of two possibilities. Firstly, it is possible that prolonged exposure to acetone has resulted in the breakup of the coal structure, allowing solvent to reach areas within the coal not penetrated by water. This seems unlikely given that this would probably require the breaking of carbon-carbon bonds by acetone. The second, and more likely, possibility is that the extraction by acetone is selective, with only smaller fragments being removed from the coal. This argument for selective extraction is supported by the results of the ESR study presented in Chapter 2. It is also supported by the reduced height of the band around 1600 cm^{-1}, which is assigned to the stretching modes of the aromatic skeleton. If would be expected that large polyaromatic systems would be the least soluble part of coals and the most resistant to attack.

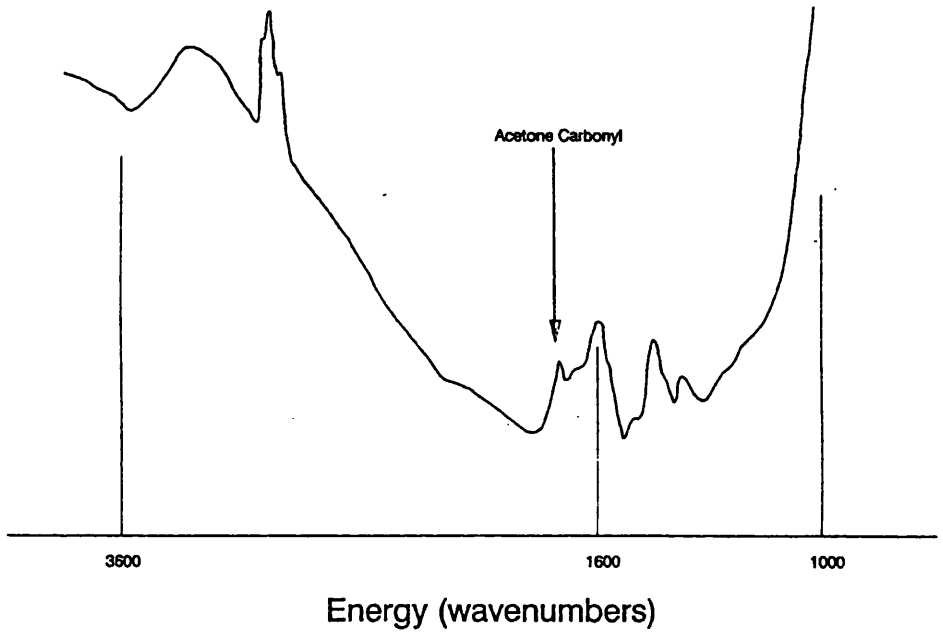

Figure 3.2 - IR Absorption Spectra Of Acetone Extract Of Coal

3.4. Solvent Addition

3.4.1. Introduction

Most models of coal assume that the hetero atoms present in the coal matrix are present either in hetero aromatic structures or in organic functional groups. These functional groups are the likely binding sites of any solvent molecules penetrating the coal pore network. The formation of new bonds will cause the loss or perturbation of existing bonds, both in the coal spectrum and in that of the solvent. Larsen[8] has studied the change in the OH stretch region of coals after adsorption and suggests that

hydrogen bonds are being lost from the coal. This must indicate that solvent molecules are breaking intra-coal hydrogen bonds and bonding to the former proton donating hydroxyl groups. In order to study the nature of these bonding sites it is easiest to study the changes to the IR spectra of simple solvent molecules. Use of solvents as probe molecules in solvation studies at Leicester has led to the accumulation of a large body of data detailing the behaviour of key solvent chromophores, particularly the carbonyl group, in a variety of environments. Probes used include acetone[9] and various amides[10,11] By introducing the same solvents into coal it may be possible to deduce the nature of the bonding sites present in coal and something of the mechanism of solvent reaction with coal.

Three coals were selected for study, two bituminous coals and a lignite. The two bituminous coals, Hucknall and Gedling, both have 80% carbon. They were selected to see if there are significant differences in functional group chemistry between coals of a nominally similar bulk composition. The lignite, Loyyan, allows comparison between the functional group behaviour of lignites and bituminous coals.

3.4.2. Experimental

The procedure used to expose the coal samples to solvent vapour has been described in detail already in this chapter. Once the spectra had been recorded a difference spectra was calculated to remove the coal features present. A peak finding routine was then

used on the second derivative of the difference spectrum to establish a wavenumber value of the centre of the peaks present.

3.4.3. Results

The experimental band positions for the selected solvents in the three coals are presented in Table 3.1. Where a solvent has two sets of data it is because that solvent shows two carbonyl stretching frequencies. An example difference spectrum and its second derivative is shown in Figure 3.3.

Solvent	Hucknall	Gedling	Loyyan
acetone	1666	1665	1663
1-methyl-2-pyrolidinone	1687	1684	1663
2-pyrolidinone a	1695	1691	1974
2-pyrolidinone b	1667	1669	1658
cyclopentanone a	1727	1726	1723
cyclopentanone b	1660	1654	1656
formamide	1694	1693	1690
DMF	1672	1668	1663
pentan-3-one	-	1666	1662

Table 3.1 Carbonyl Stretch (Wavenumbers) of Selected Solvents Bound To Coal

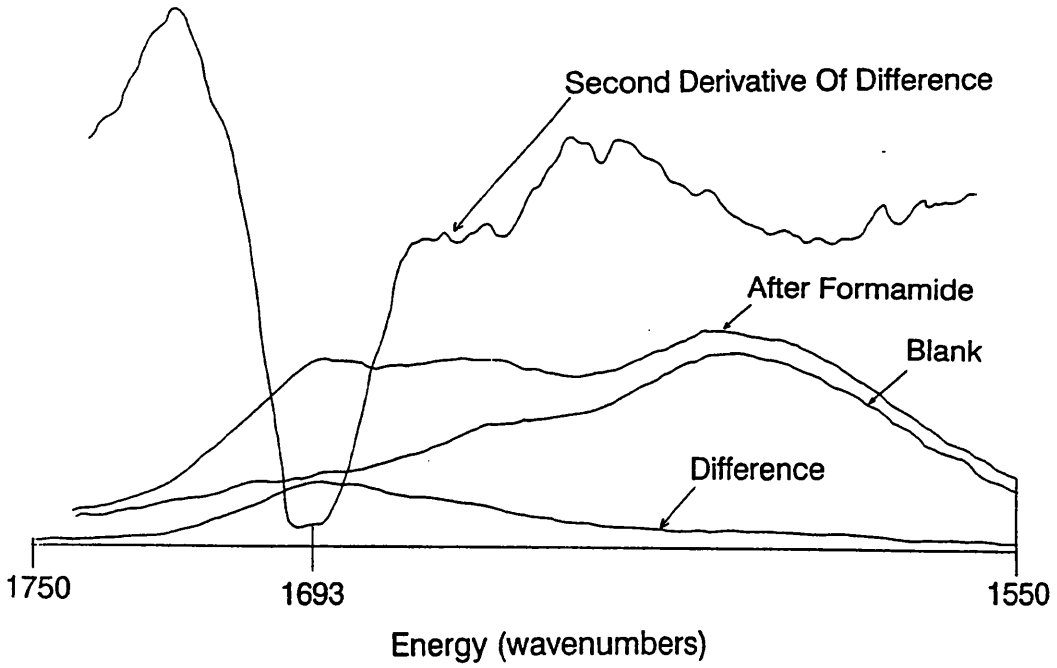

Figure 3.3 - IR Absorption Difference Spectrum Showing Change on Addition of Formamide to Gedling Coal

The carbonyl stretching modes of different solvents vary. This is a feature of the electronic structure of the solvents themselves and is of no concern here. In order to eliminate the characteristics of the solvents, but to show the changes brought about by the coal the experimental band positions need to be normalised. This is achieved by comparing the experimental results to the behaviour of the solvents in two control environments. The chosen environments are deuterium oxide (used to avoid water bending modes in the 1550 cm^{-1} - 1750 cm^{-1} region) and dichloromethane. These represent the solvent in environments

where it is likely to be fully hydrogen bonded (deuterium oxide) and without hydrogen bonds (dichloromethane).

The band positions in coal can then be viewed as being in a specific position in relationship to two known standards, deuterium oxide ('h-bonded') and dichloromethane ('free'). The coals can be considered to impart a shift to the carbonyl band, expressed as a percentage of the shift from the position in dichloromethane to the position in deuterium oxide. The band positions in the control environments and the shifts calculated are presented in Table 3.2.

Solvent	H-Bonded	Free	Hucknall	Gedling	Loyyan
acetone	1697	1718	248	252	262
1-methyl-2-pyrolidinone	1649	1686	-3	5	62
2-pyrolidinone a	1650	1690	6	15	50
2-pyrolidinone b	1660	1709	86	82	104
cyclopentanone a	1721	1750	79	83	93
cyclopentanone b	1727	1735	938	1013	988
formamide	1691	1707	81	88	106
DMF	1655	1674	11	32	58
pentan-3-one	1745	1798	-	249	257

Table 3.2 Coal Induced Carbonyl Shifts

It is important to remember that the experimental values quoted are the centres of quite broad bands, typical band half widths at half height are 20 cm^{-1}. Many bands are also unsymmetrical, extending further to lower wavenumbers than to higher. Formamide in particular shows identifiable shoulders giving approximate shifts of 230 for Hucknall and 295 for Gedling. Since coals are

highly heterogeneous the solvents are interacting with a variety of functional groups. All that can be said to be shown here are the strengths of typical interactions.

The results in Table 3.2 have two important features. Firstly the effect of the coals on different solvents varies considerably; secondly for any one solvent bond the three coals generally produce a general trend in shifts, increasing from Hucknall to Loyyan. This second trend indicates that the nature of the functional groups accessible to solvents is a function of the individual coal.

In the previous chapter it was noted that the ability of a solvent to extract material can be related to its acceptor/donor properties as measured by the Gutmann acceptor and donor values, specifically the quantity DN-AN[12] (donor number - acceptor number). Some similar property could control the great variation in the strength of coal-solvent interactions revealed in Table 3.2. Figures 3.4 - 3.6 show plots of coal carbonyl shifts against the quantities DN, AN and DN-AN for those solvents for which data is available[12,13]. The values used are presented in Table 3.3.

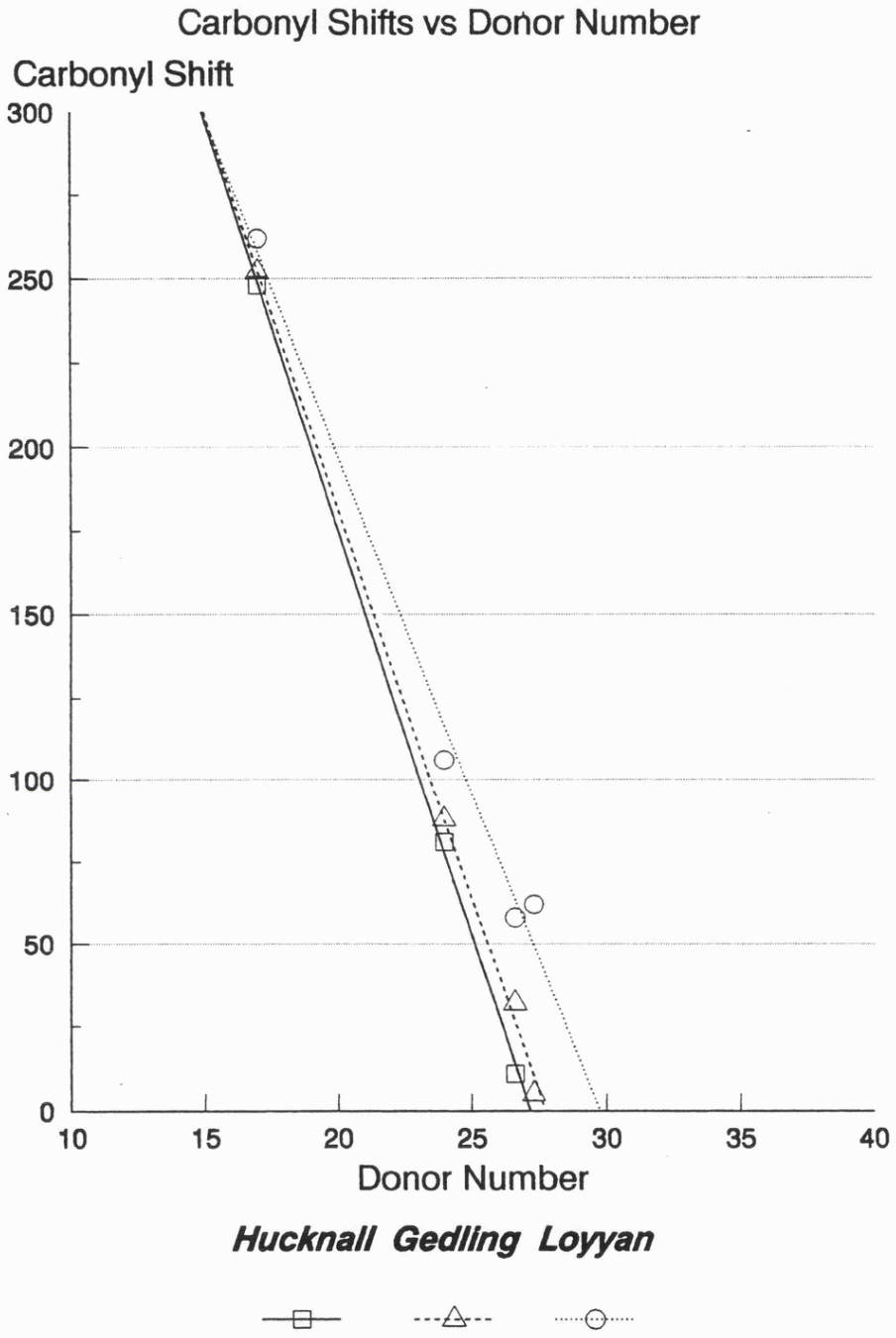

Figure 3.4 Carbonyl Shifts vs Solvent Donor Numbers

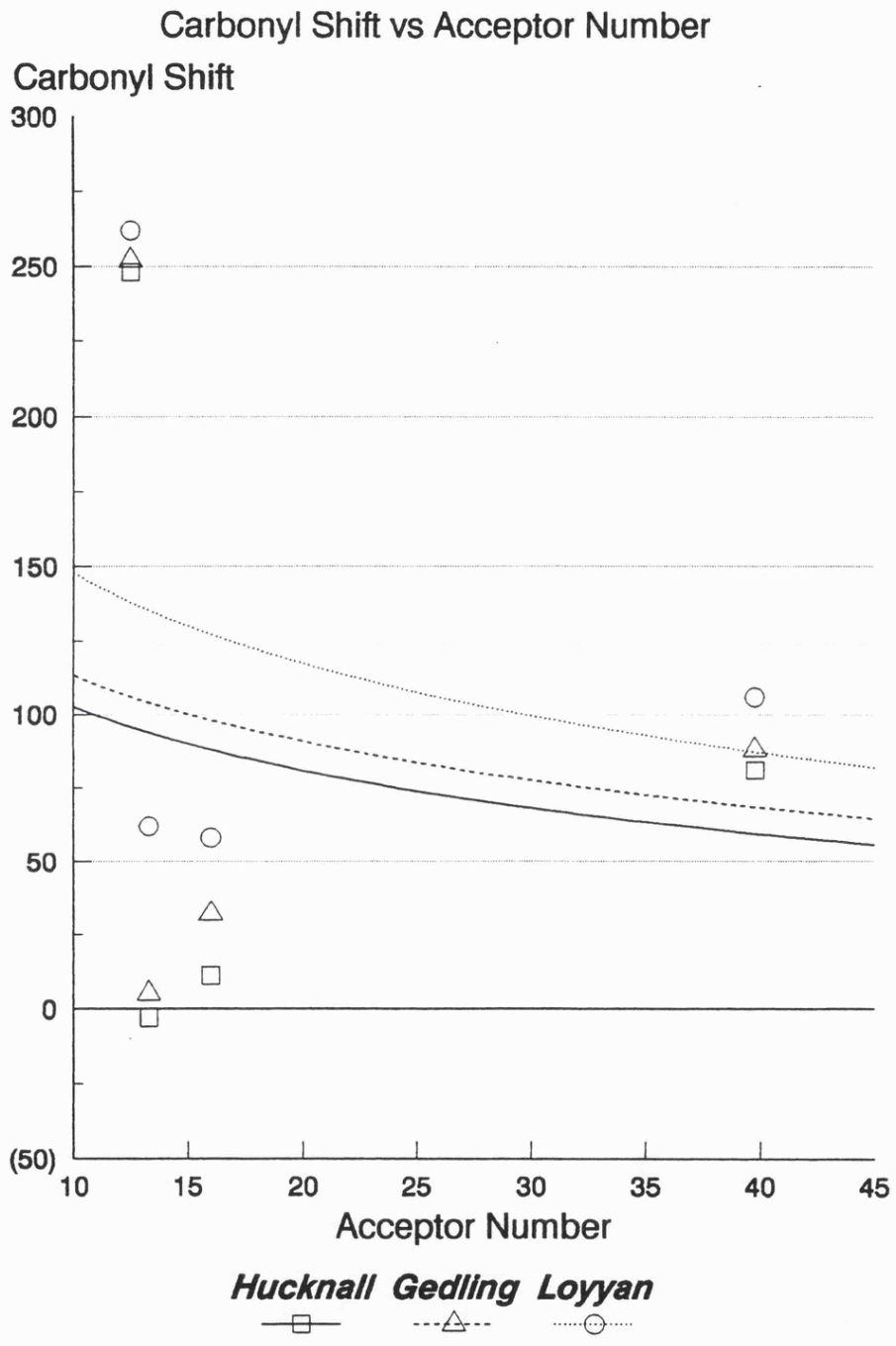

Figure 3.5 Carbonyl Shifts vs Solvent Acceptor Numbers

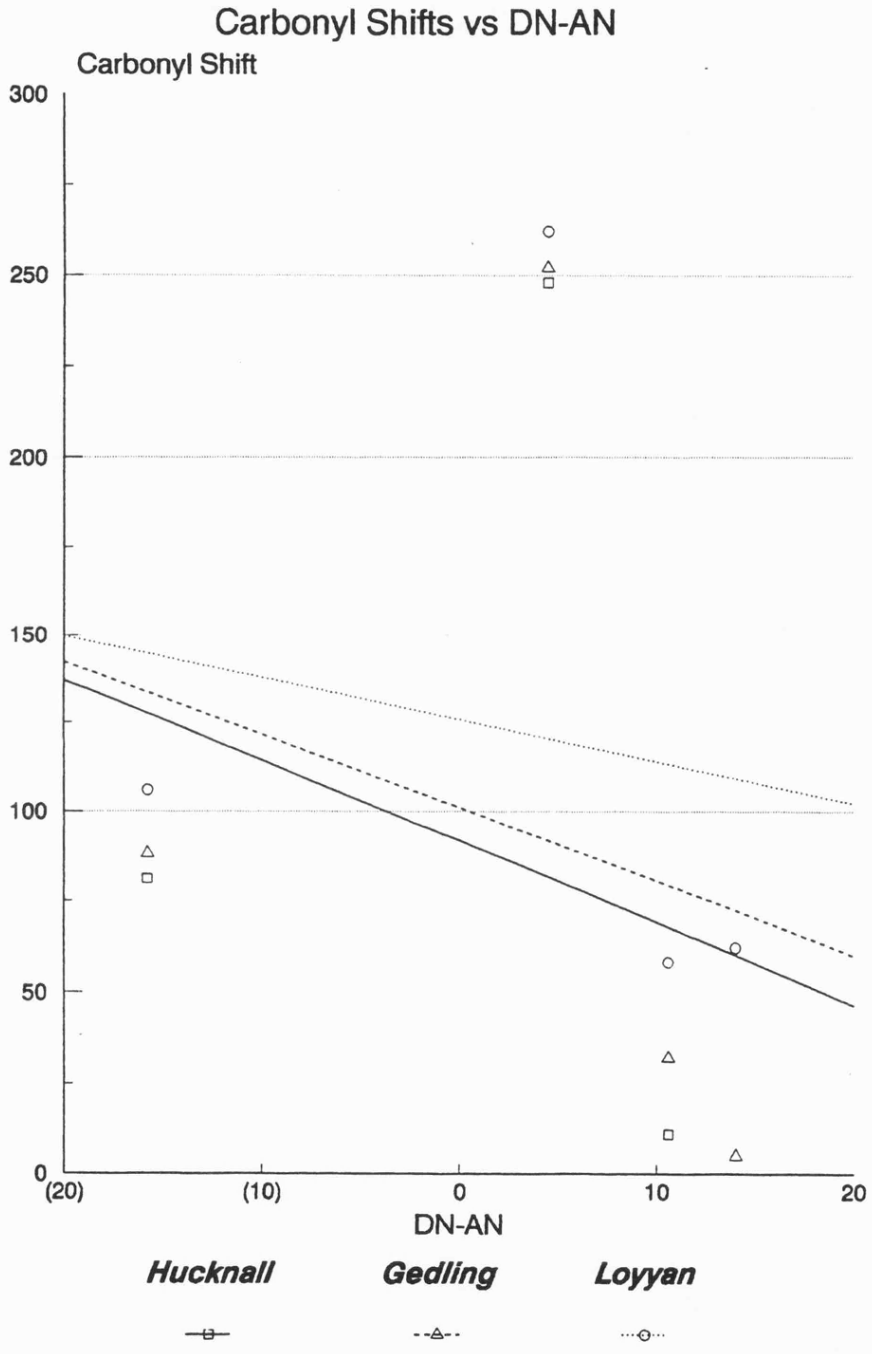

Figure 3.6 - Carbonyl Shifts vs DN-AN

Solvent	DN	AN	DN-AN
acetone	17.0	12.5	4.5
formamide	24.0	39.8	-15.8
1-methyl-2-pyrolidinone	27.3	13.3	14.0
DMF	26.6	16.0	10.6

Table 3.3 - Acceptor/Donor Properties Of Solvents

3.4.4. Discussion

Figures 3.4-3.6 do not show the expected pattern. The work in the previous chapter indicated that the quantity DN-AN (plotted against carbonyl shift in Figure 3.6) seemed to control extraction by solvents. Neither this plot or that of AN (plotted against carbonyl shift in Figure 3.5) show any kind of trend. Figure 3.4 (a plot of DN against carbonyl shift) shows an excellent linear trend. The plot suggests that the weaker electron donors form the strongest interaction with coal. This is in complete contradiction to Larsen's work on the ability of solvents to 'mop up' coal hydrogen bonds, which showed that amides were more effective than acetone, the reverse of the trend suggested by Figure 3.4.

Only the ketones among the solvents used produce shifts over 100 with bituminous coals. Lower values indicate that the solvents are in an environment offering no stronger binding sites than water. It is a distinct possibility that these solvents are not

interacting with the coal itself at all. They may have formed condensed droplets of solvent within the pores, or be interacting with water not removed by the sample drying process.

The different sizes of the solvent molecules can help to explain the spread of the results. If the solvents are divided into three groups, pyrolidinones, ketones and amides then within each group the smaller molecules have higher shifts (if the cyclopentanone-b band is ignored), although the trend is slight This suggests that a higher proportion of the smaller solvent molecules reach strong binding sites. This is supported by the general trend for Loyyan to induce larger shifts than the two bituminous coals. Lower grade coals would be expected to show a more open structure, with a larger pore size and less cross-linking, thus allowing better access to solvents. It then follows that as Gedling shifts are generally higher than Hucknall shifts then these two coals of similar carbon content have different pore structures and/or functional group compositions.

3.5. Exposure To Air

3.5.1. Introduction

In the previous section the nature of the interaction between certain solvents and coals was investigated. It was established that the strength of the interaction in many cases seemed very weak, certainly not of the strength expected if solvent molecules were interacting with the acidic hydroxyl groups known to be present (see Section 3.3.1). One possible cause of the apparent

low average strength of interaction is that the samples used were saturated with condensed solvent. In order to investigate this possibility a sample was left in the open air for a week so that water could return and excess solvent evaporate.

3.5.2. Results

The sample chosen for exposure to air was Gedling that had been exposed it formamide. It had already been noted that the difference spectrum of this combination showed a distinct shoulder at around 1660 cm^{-1}. The difference spectra before and after exposure to the air are shown in Figure 3.7

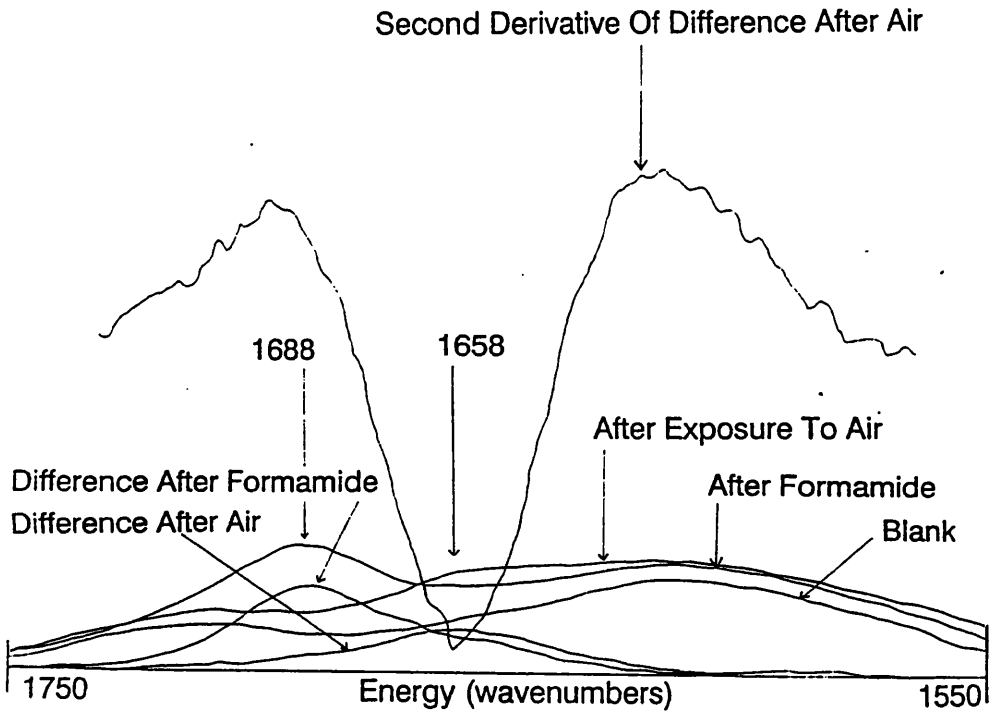

Figure 3.7 - IR Absorption Difference Spectrum Showing Change on Loss of Formamide From Gedling Coal

Figure 3.7 clearly indicates two important results. Firstly there is a major loss in the intensity of the formamide carbonyl band. The second is the significant shift of the band to lower wavenumbers.

3.5.3. Discussion

The behaviour of the formamide band after exposure to the air indicates that the bulk of the formamide in the sample after the period of exposure is weakly bound, if at all, to the coal. Once removed from the formamide rich atmosphere most formamide within

the coal escapes. There is no sign of significant amounts of formamide remaining with a shift of around 100, indicating bonding to water. This would be expected if formamide were being displaced by water from coal sites and ending up interacting with the returning water. That it does not simply demonstrates that water is unable to displace formamide bound to coal.

The position of the centre of the residual band is at 1658 cm^{-1}, the approximate position of the shoulder seen in the original difference spectrum. This gives a shift of 194. This is comparable to the values originally obtained for acetone.

It may therefore be that the shift values presented in Table 3.2 are determined by solvent volatility. The more volatile the solvent the higher the contribution to the carbonyl band from tightly bound solvent. As volatility decreases so more unbound solvent remains within the coal pore system, driving the shift to lower values.

3.6. Interactions Between Acetone and Aromatic Hydroxyl Groups

3.6.1. Introduction

In this section the term 'aromatic hydroxyl' is taken to apply to hydroxyl groups that are part of an aromatic molecule. Such groups are the likely binding sites of solvents within coals. Section 3.5 demonstrated that the strength of the interaction between coal and solvents was similar for both acetone and

formamide, indicating a common bonding mechanism to the same sites. If a molecule can be found that is able to reproduce the carbonyl stretching frequencies of solvents bound to coal then this molecule can be used as a model for typical functional groups in coal.

3.6.2. Experimental

Dilute solutions were prepared of selected compounds in dichloromethane. Infra-red absorption spectra were recorded between 1550 cm^{-1} and 1750 cm^{-1}. Acetone was then added to the solutions and a new spectrum recorded. In each case the positions of new bands, or shoulders, appearing were recorded. It was found to be important to keep the solutions at very low concentration, otherwise the acids tended to dimerize preventing interaction with acetone.

3.6.3. Results

The results obtained are tabulated below in Table 3.4. In most cases the carbonyl band was clearly a composite band indicating the presence of different acetone environments. The feature that gave the largest shift (which would be that representing the strongest bonding) was taken as the result. The known positions of acetone in Gedling coal, dichloromethane and water are also tabulated for reference.

Reagent	Acetone Carbonyl Band Position (cm^{-1})	Carbonyl Shift
Dichloromethane	1718	0
Deuterium Oxide	1697	100
Gedling Coal	1665	252
Salicylic Acid	1680	181
Phenol	1690	133
para-Fluorophenol	1691	129
Benzoic Acid	1692	124

Table 3.4 - Interaction Between Acetone and Aromatic Hydroxyl Compounds

Other reagents were used, including 2,6-di-tertiarybutyl phenol and 2,4,6,-trimethyl phenol. Neither of these delivered a shift above 100, which indicates a failure to detect acetone interacting with them.

3.6.4. Conclusions

The shifts produced by the aromatic hydroxyl compounds do not match the shifts produced by coals. It is possible that the dimerisation problems have not been overcome and that Table 3.4 does not accurately represent the interactions between acetone and the selected reagents. Evidence for this comes from work by Larsen *et al*[14] which suggests that the hydroxyl groups in coal typically behave like *para*-fluorophenol. Table 3.4 would not support the idea of *para*-fluorophenol being a model for coal hydroxyl groups.

A second possibility is that the coal pore environment cannot be re-created in solution. The sites that are available to solvents

are the functional groups pointing into the spaces of the pore system. Figure 3.1 shows that only a few of the hydroxyl groups within coal are 'free', the majority are interacting with some other group within the coal or with the water that saturates the pore system. Solvent molecules must break the existing bonds and either displace water molecules or insert themselves along the axes of existing bonds. Straight chain ketones and simple amides, such as formamide, could certainly be able to form this second kind of bond, bonds which would not be easy to reproduce in solution.

3.7. Conclusions

This work has been unsuccessful in developing a model for the behaviour of solvents binding to coals. The reasons for this are principally failures of experimental technique. Without removing all water from the coals it is impossible to allow solvents unhindered access to the pore system. Similarly removal of all unbound solvent is a pre-requisite for being able to study the bound solvents. Using higher temperatures to remove more water does, however, heighten the risk of structural alteration. Thermal alteration processes effecting carboxylic acid groups have been shown by Gethner[15] to be significant at 100°C, and the aim of the work has always been to study the properties of coal in its natural state, rather than to study altered or processed coals.

The ideal experimental arrangement would be to have the coal slides mounted in a gas cell attached to a vacuum line. This

would allow for removal of water and solvent by vacuum and the recording of spectra without having to expose the sample to the atmosphere.

The most reliable result produced by this work is the trend in the carbonyl shifts shown in Table 3.2. The result shows that Loyyan coal produces a larger shift in the carbonyl stretching band than the bituminous coals, of which Gedling produces a larger shift than Hucknall in most cases. Lignites, such as Loyyan, have a more open pore structure than higher grade coals (30% porosity for lignites, 1% for coals 87-90%C[16]). As such they will allow easier access to solvents, both entering and leaving the coal. This means that solvents will have an easier task in reaching the available functional groups, which will be in less constricted environments. It also means that unbound, or loosely bound, solvents can more easily escape and not contribute to the subsequent spectra.

This result is in agreement with the theory that coal hydroxyl groups are the binding sites for solvents. ^{13}C NMR studies clearly show that lower grade coals have a higher ratio of aliphatic to aromatic carbon atoms[17,18]. This implies that the proportion of functional groups on aliphatic side chains will be higher. Since aliphatic carboxylic acids tend to be stronger than their aromatic analogues then the carboxylic acid groups in lignites should be better electron acceptors than those in higher grades of coal, producing a greater influence on the carbonyl groups of neighbouring solvents. Typical carboxylic acid and phenol K_a values are presented in Table 3.5, with halogenated

forms present to illustrate the degree of induction derived strengthening possible[19].

Compound	K_a
ethanoic acid	1.75×10^{-5}
trichloroethanoic acid	23.2
benzoic acid	6.5×10^{-5}
para-chlorobenzoic acid	10.3×10^{-5}
phenol	1.1×10^{-10}
para-fluorophenol	1.1

Table 3.5 - K_a Values of OH Bearing Compounds

Alcohols, on the other hand, are much weaker acids than phenols. If alcoholic hydroxyl groups were the principle binding sites for solvents then lignites would interact less strongly than bituminous coals. This is clearly not the case so aliphatic carboxylic acid groups must dominate the bonding between solvents and lignites. In bituminous coals the predominance of aromatic structures leads to less acidic carboxylic acids and weaker interactions with solvents.

In summary, the evidence of this work points to carboxylic acid groups as being the most important functional groups for bonding to solvents. This is in agreement with the work of Larsen[8] and Portwood[2], which showed that basic solvents removed weakly hydrogen bonded hydroxyl groups from the infra-red absorption spectra of coals. The only way in which lignites could bond more

strongly than bituminous coals would be if carboxylic acid groups were the source of the hydroxyl groups, as aliphatic carboxylic acids are typically stronger than their aromatic analogues and aliphatic structures decrease in abundance with rank. Carboxylic acid groups are well known to be present in coals and in such precursors as peat. However, to date no model compound has been found which emulates in solution the perturbation of the solvent carbonyl groups produced by coals.

References

1 Thomas, K.M, Personal Communication

2 Portwood, L., Ph.D. Thesis, Leicester, 1987

3 The author, unpublshed results

4 Gethner, J.S., *Fuel*, **61**, 1273, (1982)

5 van Vucht, H.A., Rietveld, B.J. and van Krevelen, D W, *Fuel*, **34**, 50, (1955)

6 Thomas, K.M., Personal Communication

7 van Krevelen, D.W., *Coal*, Elsevier, Amsterdam, 1961

8 Larsen, J.W. and Baskar, A.J.,*Energy & Fuels*, **1**, 230, (1987)

9 Symons, M.C.R. and Eaton, G., *J. Chem. Soc., Faraday Trans. 1*, **81**, 1963, (1985)

10 Symons, M.C.R., Eaton, G. and Rastogi, P.P., *J. Chem. Soc., Faraday Trans. 1*, **85**, 3257, (1989)

11 Symons, M.C.R. and Eaton, G., *J. Chem. Soc., Faraday Trans. 1*, **84**, 3459, (1988)

12 Marzec,A., Juzwa, M., Betlej,K. and Sokowiak, M., *Fuel Proc. Tech.*, **2**, 35, (1979)

13 Czelia, J. and Marzec, A., *Fuel*, **62**, 1229, (1983)

14 Larsen, J.W., Green, T.K. and Kovac, J., *J. Org. Chem.* **50**, 4729, (1985)

[15] Gethner, J.S., *Fuel*, 64, (1985)

[16] Grimes, W.R. in *Coal Science*, volume 1 (Eds. Gorbarty, M.L., Larsen, J.W. and Wender, I), Academic Press, New York, 1982

[17] Wilson, M.A. and Pugmire, R.J., *Trends in Ananlytical Chemistry*, 3, 144, (1984)

[18] Davidson, R.M. in *Coal Science*, volume 1 (Eds. Gorbarty, M.L., Larsen, J.W. and Wender, I), Academic Press, New York, 1982

[19] Morrison, R.T. and Boyd, R.N., *Organic Chemistry* (4th ed), Allyn and Bacon, Boston, 1983

Part 2

Solvation Studies

4. BINARY SOLVENT SYSTEMS

4.1. Introduction

The binary solvent systems studied in this work all have three components; two are solvents and the third a solute in low concentration. In such systems the interactions between the solute and the solvents may cause the composition of the liquid in the vicinity of the solute to be different from the 'bulk' composition of the solution. This is termed 'preferential solvation' and its study is important in understanding the interactions between species in the liquid phase.

In 1960 Grunwald *et al*[1] described a thermodynamic treatment of solvation. Subsequently, in a series of papers, Covington *et al*[2,3,4,5,6] related a similar thermodynamic treatment to spectroscopic techniques, notably NMR, allowing details of preferential solvation to be extracted from spectroscopic work. The principles behind this treatment are presented in Section 4.3. The model has subsequently been widely accepted and cited in subsequent years[7,8,9,10,]. The model has not been without criticism[11,12] on theoretical grounds and at least one alternative treatment has been proposed[13,14]. The original papers contained a mathematical error which was corrected by Engberts[15]. The corrected treatment is used throughout the work described in this Chapter.

This work is an attempt to test the model proposed by Covington for the behaviour of probe species in binary solvent systems. The objective is to test the assumptions of Covington's model by finding how closely Covington's model follows experimental results and how it compares to an alternative model that lacks many of its assumptions. The work has been carried out by using a series of computer programs to calculate equilibrium constants and to derive solvation numbers for probe species. The programs use, as inputs, experimental nmr chemical shifts of probe molecules in binary systems.

The equilibrium constants thus calculated are compared to equilibrium constants estimated from infra red studies of the same systems. It is hoped to show a correlation between the results of the two spectroscopic techniques.

4.2. Definition of Terms

Included here are the principal terms referred to in this work.

Free Fit : Any reference to free fit means that no relationship is assumed between the equilibrium constants in a given system. The data fitting software treats all equilibrium constants as independent variables.

Fixed Fit : Any reference to a Fixed Fit or Covington fit means that the equilibrium constants in a given system are mathematically related. The data fitting software treats the equilibrium constants as a series of values with a defined relationship between members.

Solvation Number : The number of solvent molecules specifically associated with the probe molecule. This is generally referred to as n.

Probe Molecule : A molecule present in low concentration relative to that of the solvents in the system. It must have an active chromophore to allow its environment to be probed.

Most probe molecules, and some solvents, used are referred to by abbreviations. These include :

TEPO : Triethylphosphine oxide

DMA : N,N-Dimethylacetamide

NMA : N-Methylacetamide

DMSO : Dimethylsulphoxide

THF : Tetrahydrofuran

MeCN : Cyanomethane

As an aid to understanding the symbols used in this work are the same as used by Covington in his papers[2,3,4,5,6]. Unfortunately the letter K is used in several guises and this can cause confusion. These uses are as follows:

k_i : The equilibrium constants of all reactions considered are denoted by a k. The subscript refers to which step of the overall reaction sequence this specific value refers to, thus k_2 is the equilibrium for the second stage in the sequence.

$K^{1/n}$: This is one of the Covington fitting parameters. It describes the overall degree of preferential solvation shown in the system. If 1 then there is no preferential solvation, the composition of the solvent close to the solute molecules is the same as the bulk composition of the solvent.

k : This is the other Covington fitting parameter. It describes the way in which the degree of preferential solvation changes with solvent mole fractions. This represents the degree by which it gets easier (or harder) to remove successive molecules of a specific solvent from the solute.

4.3. Covington's Theory

The kind of system that is under investigation is one where a probe molecule, X, is in a mixture of two solvents, W and P. The

probe molecule has a fixed solvation number, n, and can be in any one of n+1 solvation states.

$$XW_n\ ,\ XW_{n-1}P\ ,\ XW_{n-2}P_2\ ,\ \ldots,\ XWP_{n-1}\ ,\ XP_n$$

Initially Covington proposed[2] that all the steps along the sequence had an equal energy change associated with them. From this a model was proposed that allowed the equilibrium constants for the changes along the chain to be calculated from the values of n and the overall equilibrium constant K (ie. the equilibrium constant controlling the change from XW_n to XP_n).

In order to check the validity of this model an equation was presented that allowed the prediction of NMR chemical shifts from the equilibrium constants k_i to k_n. The experimental results used were the chemical shifts of a suitable nucleus of the probe molecule. Where TEPO is the probe then ^{32}P NMR was used and for amides the ^{13}C NMR signal of the carbonyl carbon was used. The assumption that allows this calculation is that the chemical shift of a species is proportional to its position between the two end members of the sequence ie. that the chemical shift of XW_2P_2 is half way between those of XW_4 and XP_4. This takes advantage of the fact that the lifetime of the solvation states is very short compared to the lifetime of the excited nuclear spin state. The observed chemical shift thus represents a probe molecule in a weighted average solvation state.

This model was modified by making the energy change vary with each successive step[5] ie. removing the first W molecule makes it

easier to remove the second, the removal of which makes it easier to remove the third, and so on. It was proposed that this change should be a factor of RT ln k, where k is a constant that gives the magnitude and direction of change in the energy change involved in exchanging solvent molecules. This gives a new equation for deriving the chemical shift of the probe in a solution of a given mole fraction of solvent

$$\frac{d}{dp} = \frac{\sum_{i=1}^{n} (K^{1/n}Y)\, i \left(\frac{i}{n}\right) k_i \left(\frac{i-n}{2}\right) \prod_{j=1}^{i} (n+1-j)/j}{1 + \sum_{i=1}^{n} (K^{1/n}Y)\, i \left(\frac{i}{n}\right) k_i \left(\frac{i-n}{2}\right) \prod_{j=1}^{i} (n+1-j)/j}$$

where d is the chemical shift relative to XW_n, dp is the chemical shift of XP_n relative to XW_n and Y is the ratio of the mole fractions of the solvents ie. $\frac{X[P]}{X[W]}$, where X[P] is the mole fraction of P and X[W] the mole fraction of W.

4.4. Experimental

Except where noted below all experimental results where taken from work by Eaton[16], who studied the NMR shifts of selected probe molecules in a range of binary solvent systems. The experimental chemical shifts for TEPO in H_2O/MeCN were determined in conjunction with Mr. G. Archer.

The starting point for this work was a program written by K. Remerie of the University of Groningen[15,17]. This was written in FORTRAN to run on a CDC CYBER computer. The program required

the mole fraction ratios and chemical shifts for the experimental points and the solvation number to produce values for $K^{1/n}$ and k by a least squares fit. A version of this program running on Leicester University's VAX computer was named BNMR1. It proved impossible to modify BNMR1 so that the equilibrium constants could vary freely.

To this end a completely new program was written from scratch in a mixture of PASCAL and MODULA 2. This program was called SHIFTER. It was noticed that the program was occasionally producing 'nonsense' solutions. Plotting of the calculated data showed a good fit to the experimental data but the equilibrium constants were sometimes either negative or increased in the sequence k_1 to k_n. Equilibrium constants are expected to decrease in the sequence k_1 to k_n, for the following reason:

The equilibrium expression for any equilibrium constant k_i is

$$k_i = \frac{[XP_iW_{n-i}][W]}{[XP_{i-1}W_{n-(i-1)}][P]}$$

When the two probe states are in equal concentrations they cancel from the expression which becomes :

$$k_i = \frac{[W]}{[P]}$$

This gives the composition of the solution when the probe states are in equal concentration. The larger the value of i the larger must be [P] at this 'cross-over' point in the concentrations of the probe states. If [P] is increasing then

[W] is decreasing and so k_i becomes smaller with increasing values of i.

The program seemed to produce 'nonsense' solutions at high solvation numbers. The program was modified to start at a solvation number of one and to run repeatedly until a maximum number was reached or a 'nonsense' solution was detected. In most cases it was found that this produced the solvation number of the probe determined by other techniques. This version of the program was called MSHIFTER (the 'M' standing for 'multiple').

The final version allows the user to compare the results from a free fit run with the results of the fixed fit model. The program runs as MSHIFTER to determine the solvation number and the free fit results and then calculates the Covington parameters for this solvation number. This version is called CSHIFTER.

The results of these computer runs were compared to those from infrared work carried out on the same systems[16]. It has already been noted that when two probe states are in equal concentration the equilibrium constant for their conversion can be calculated from the mole fractions of the two solvents. These points where two probe states are in equal concentration, 'cross-over points', can be estimated from plots of infrared band area against solvent composition. Clearly this assumes that the extinction constants for all probe states are equal.

From the plots of species concentration against solvent composition, points could be estimated where the concentrations of

two probe states were equivalent. These points are presented alongside the equivalent points calculated from the equilibrium constants from the computer for comparison.

4.5. Results and Discussion

4.5.1. Equilibrium Constants

			Free Fit		Fixed Fit		IR
SYSTEM	n	i	k_i	Cross-Over	k_i	Cross-Over	Cross-Over
TEPO in H_2O/DMSO	3	1	3.63	22%	3.67	21%	13%
		2	1.18	46%	1.16	46%	49%
		3	0.36	74%	0.55	65%	87%
TEPO in H_2O/THF	3	1	2.73	27%	2.59	28%	17%
		2	0.23	81%	0.29	78%	77%
		3	0.086	92%	0.024	98%	96%
TEPO in H_2O/MeCN	3	1	2.56	28%	2.22	31%	19%
		2	0.21	83%	0.32	76%	90%
		3	0.078	93%	0.025	98%	95%
DMA in H_2O/MeCN	2	1	1.12	47%	1.12	47%	71%
		2	0.11	90%	0.11	90%	94%

Percentages refer to the percentage of the second solvent named in the solution (mol fraction x 100) at the indicated cross-over point.

Table 4.1 - CSHIFTER results

The results of running CSHIFTER are tabulated in Table 4.1. Plots of the experimental and computer generated data for these systems are included in Figures 4.1, 4.2, 4.3 and 4.4.

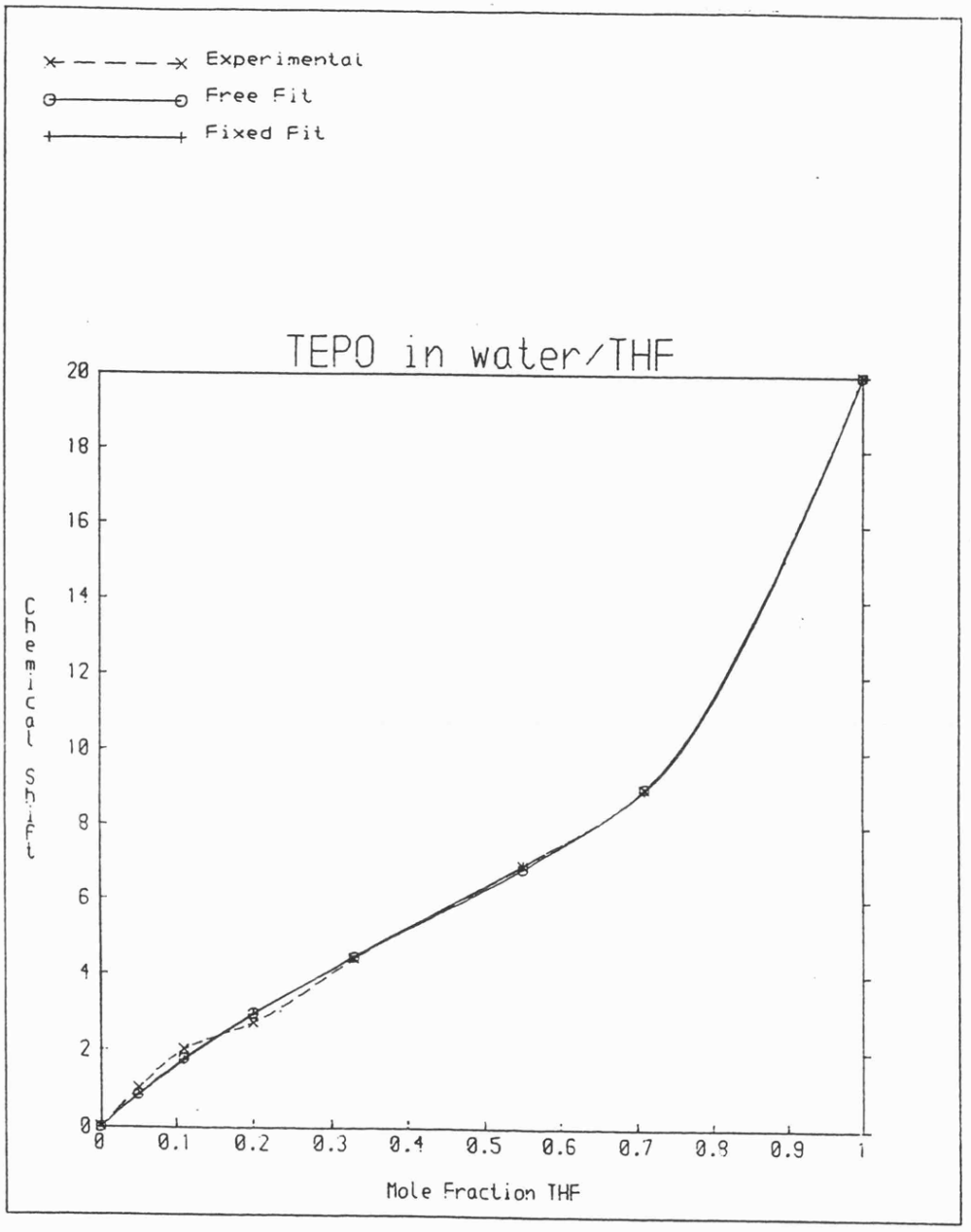

Figure 4.1 - CSHIFTER plots for TEPO in H_2O/THF

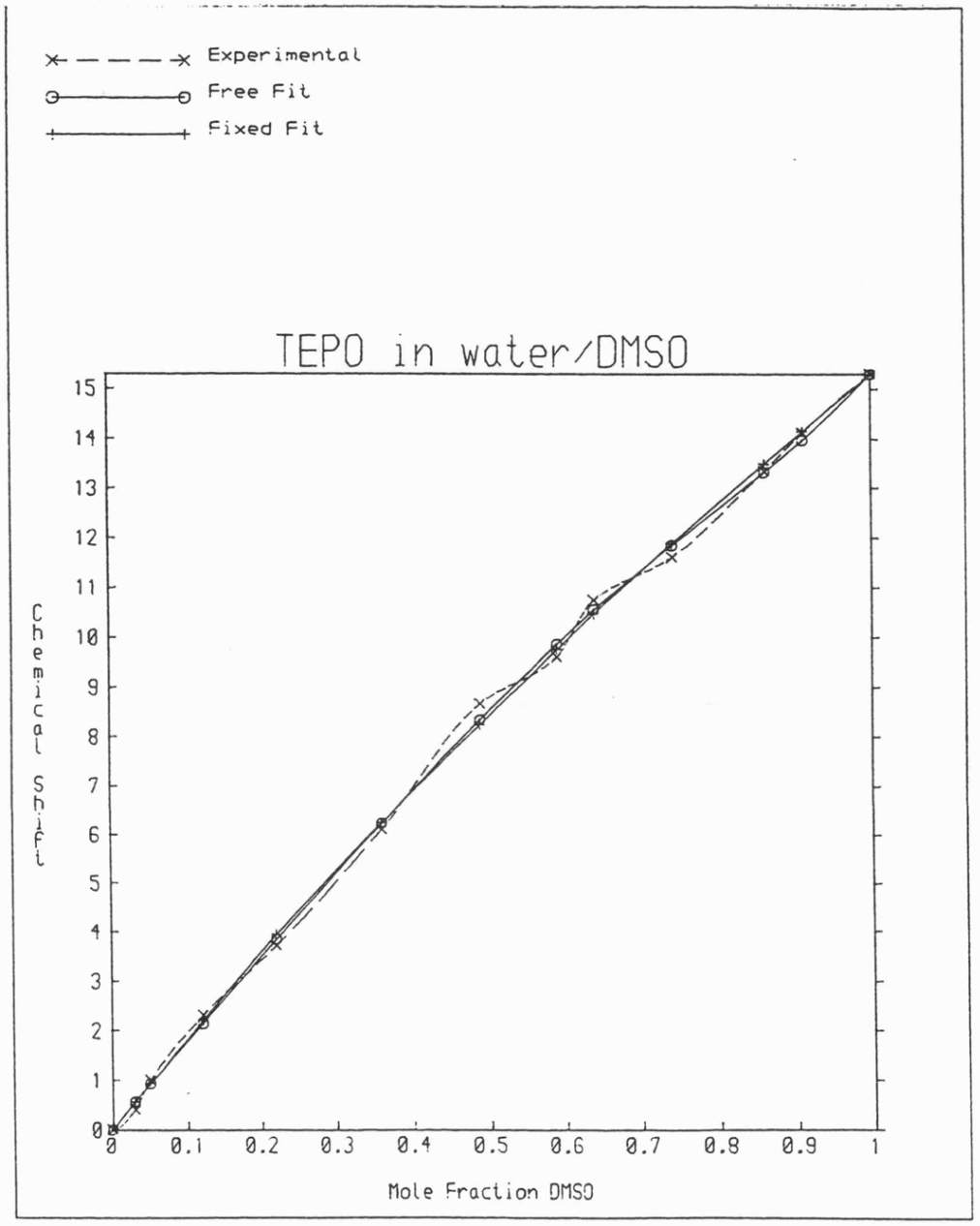

Figure 4.2 - CSHIFTER plots for TEPO in H_2O/DMSO

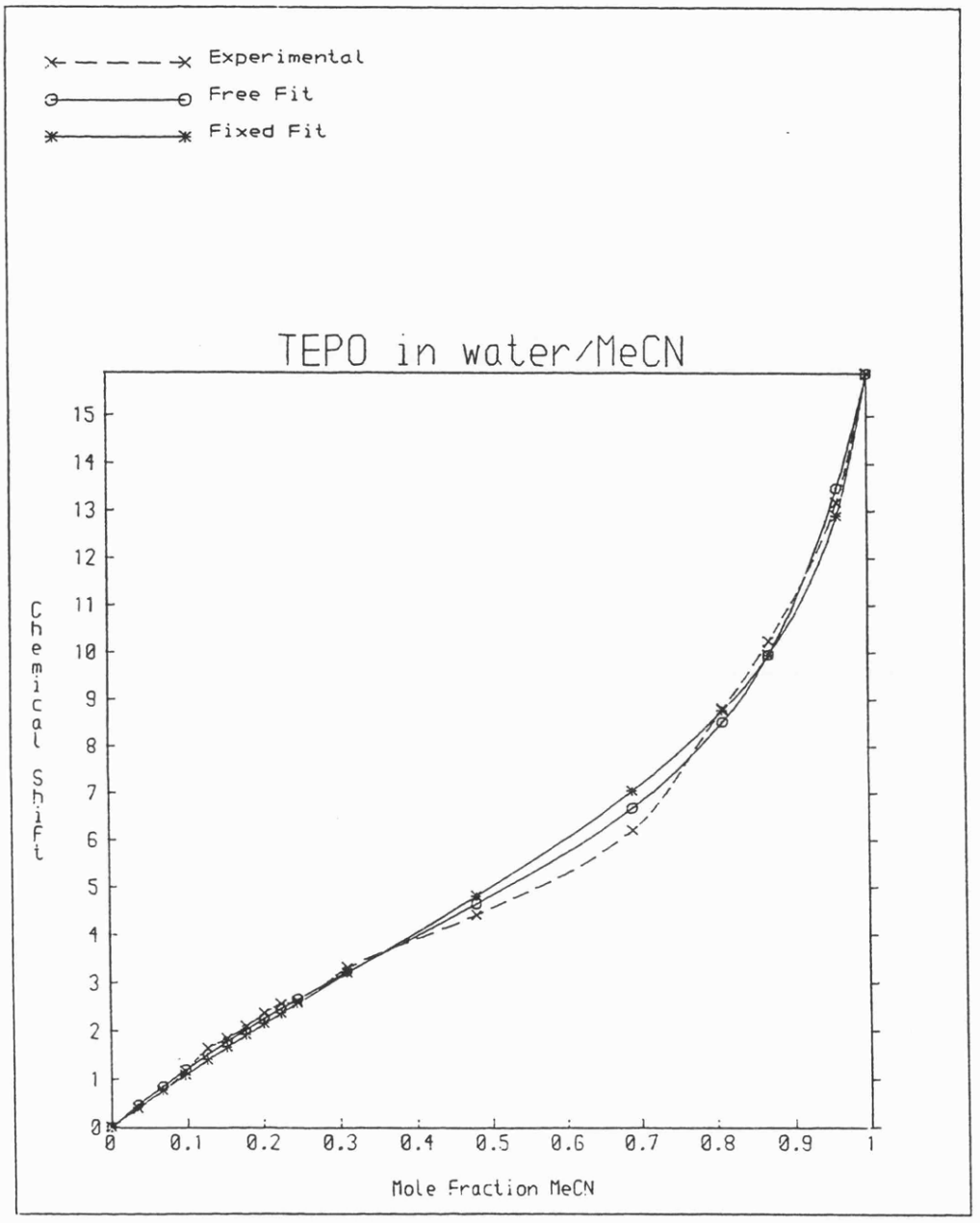

Figure 4.3 - CSHIFTER plots for TEPO in H_2O/MeCN

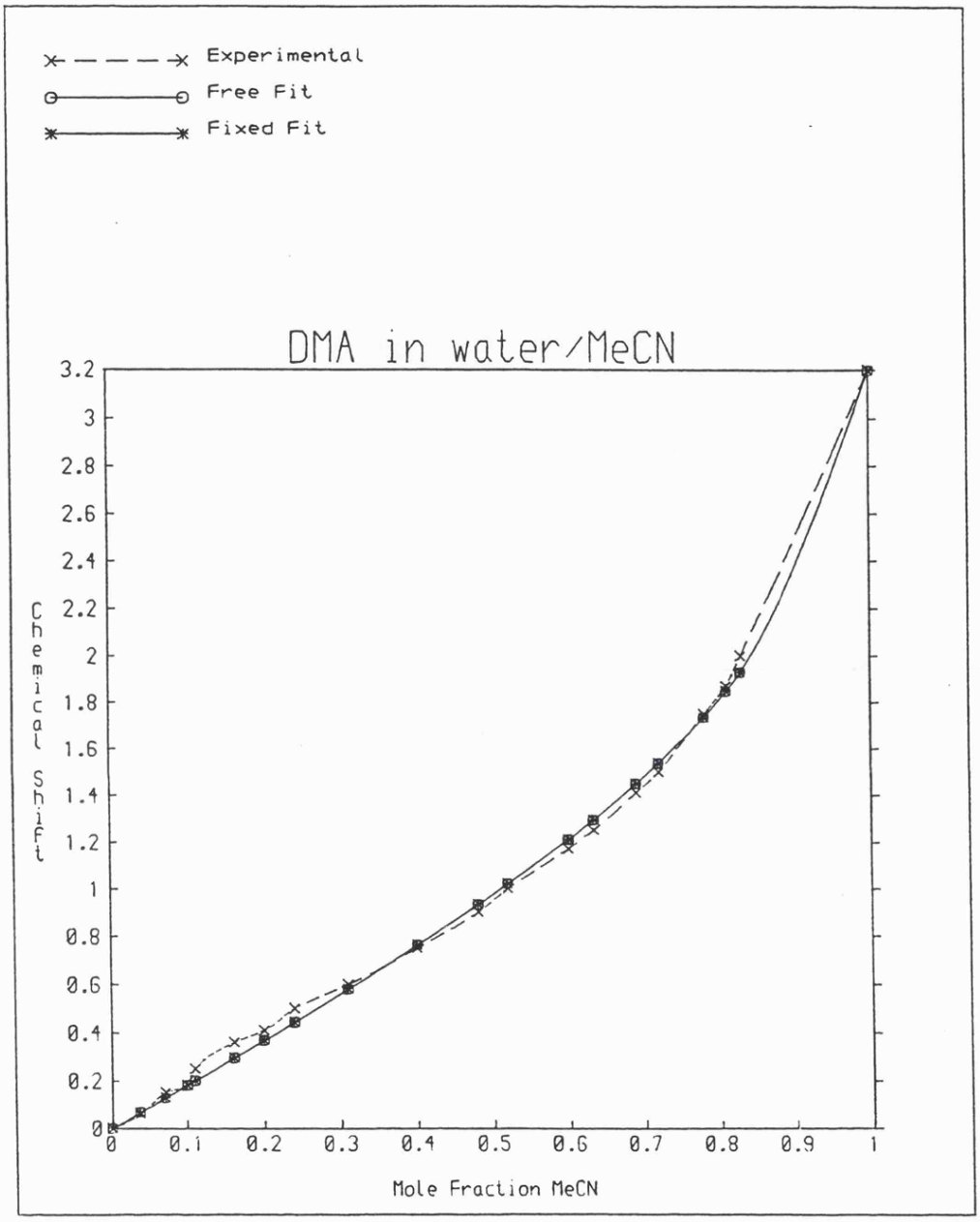

Figure 4.4 - CSHIFTER plots for DMA in H_2O/MeCN

It should be noted that any situation where n=2 is going to cause the free fit and fixed fit models to produce the same answer. This is because in each case there are two degrees of freedom in the least squares fit. In the case of the fixed fit model k_1 is a variable and its relation to k_2 is a second variable. In the free fit case k_1 and k_2 are both independent variables. As a result both models can and will optimize to the same solution.

In general it can be seen from the equilibrium constants above that both models have produced similar results that are in approximate agreement with the IR results. In the case of the water/DMSO system agreement is good. In the case of the other systems agreement is not so good. It is important to note that the more extreme the degree of preferential behaviour (the more curved the experimental plots) the worse the agreement. A more exaggerated shape will require more degrees of freedom to match accurately if it is not following a simple equation. This is an indication that there are either errors present in the experimental data, or that both models break down when a high degree of preferential solvation occurs.

4.5.2. Trends

In all cases where n has a value of three the free fit model has three degrees of freedom whilst the fixed fit model has two (see explanation above of the n=2 case). Examining the results from those systems where n = 3 a pattern can be seen. The k_1 values run in the order DMSO > THF > MeCN. This is the same order as the

base strengths. This is reasonable as it means that stronger bases compete more effectively with water. In terms of k_2 values the same pattern is maintained by the free-fit model but not by the fixed-fit. With k_3 two fixed-fit values are the same (THF and MeCN), otherwise the pattern holds.

It can be seen that the strengths of the bases used are reflected in their ability to compete against water for TEPO. The cross-over points do not compare well with those predicted from the infra-red work. Agreement is not good in any of the systems. It is especially noteworthy that the k_1 values are consistently higher than those from the infra-red work. This is considered further below.

4.5.3. Covington Parameters

In addition to the equilibrium constants shown in Table 4.1 the program also produces two additional parameters of use, these are as follows:

$K^{1/n}$ This is calculated from the free fit equilibrium constants. It essentially shows which solvent the probe shows a preference for. If the value is greater than 1 then preference is shown to the solvent being added progressively by k_1 to k_n. If the value is less than 1 then preference is shown to the starting solvent. A value of 1 shows that there is no preferential solvation.

k This parameter indicates the nature of the change in energy change between successive equilibria. A value of k less than 1 indicates increasing preference for the added solvent. A value of 1 would indicate that there was no change in the energy change between steps. A value greater than 1 indicates increasing preference for the solvent being removed (This interpretation is not obvious but study of Figure 1 of Reference 5 shows it to be true.).

SYSTEM	$K^{1/n}$	k
DMA in H2O/MeCN	0.352	0.392
TEPO in H2O/MeCN	0.346	0.432
TEPO in H2O/THF	0.377	0.344
TEPO in H2O/DMSO	1.16	0.948

Table 4.2 - $K^{1/n}$ and k Values Calculated By CSHIFTER

The values of these parameters gained from these runs are tabulated in Table 4.2. The results for $K^{1/n}$ show that in all systems except for TEPO in H2O/DMSO preference is shown for water as the value is less than one. DMSO is the preferred solvent in the TEPO in H2O/DMSO system. This can be seen from the results in Table 4.1 by looking at the k2 results of those systems where n=3.

Where k2 is less than 1 the cross-over concentration is over 50% ie. more than half of the bulk solvent must be replaced before 50% of the solvation sphere is replaced. In the case of TEPO in H_2O/DMSO k2 is just greater than 1 and the cross-over point is close to, but less than, 50% indicating preference for DMSO. The values of k produced are all less than one. This indicates that preference for the non-aqueous component of the system increases in all cases. This would seem to be just a feature of those systems studied as Covington reports[5] systems where k>1.

Interpretation of k values must involve the concept of weakening the binding between the probe and the less favoured solvent with the presence of more of the favoured solvent. When two probes have been used in the same solvent (as with H_2O/MeCN) the parameters obtained differ. This shows that preferential solvation behaviour is a function of the solute. This would be expected as different types of molecule in terms of polarizability, charge, geometry etc. are going to have different affinities for the same solvents. However, the influence of the interactions between the two solvents are not explicitly considered in the model, and they are likely to be significant. This point is further developed later.

4.5.4. Accuracy of Fits

The computer also produces two indications as to the quality of the fit achieved. These are the sum of the squares of the deviations between the computer generated and experimental curves

and the IFAIL flag that indicates the confidence in the quality of the fit. All results had either an IFAIL value of 0 indicating complete confidence in the solution or a value of 5 indicating high confidence but the result is not proven to minimize the difference between calculated and experimental data. The least squares results show a consistent, if marginal, advantage to the free-fit result. This is doubtless a reflection of the additional degree of freedom allowed in the TEPO cases as has already been discussed. The results are tabulated in Table 4.3.

SYSTEM	Free Fit	Fixed Fit
DMA in H2O/MeCN	0.0262	0.0262
TEPO in H2O/MeCN	0.603	1.26
TEPO in H2O/THF	0.147	0.166
TEPO in H2O/DMSO	0.0828	0.0831

Table 4.3 - Residual Sum Of Squares for Computer Fits

If the Covington model is assumed to be correct then any deviation between the fixed fit and experimental curves in the plots represents experimental error. The free fit curve then represents only the limitation of the experimental error by introducing an unwarranted degree of freedom into the model. It the Covington model is assumed to be flawed in its assumptions then the difference between the free fit and experimental curves represent experimental errors whilst the difference between the fixed fit and free fit curves shows the degree of error introduced by

Covington's assumptions. It should be noted that the value of the residual least squares value depends heavily on the exact number of data points in use. As a result these values should be used to compare the results of the two models on a particular data set, rather that to compare between the accuracy achieved with different systems.

4.5.5. N-methylacetamide in water/cyanomethane

One experiment that did not generate good results was NMA in water/cyanomethane. This molecule poses a problem because the probe is the carbon atom of the carbonyl group and solvation may occur at the amide proton (1 potential bond) as well as at the oxygen (2 potential bonds). These two forms of bonding create a problem because of the assumption that all the different solvated states form a sequence. With two different sorts of solvent bond being formed (solvent-oxygen and solvent-amide proton) the fixed-fit model cannot cope. The free fit model does not assume that the energy changes in swapping solvent molecules form a regular sequence (changing by RT ln k each time), so it should be able to cope with a situation like this.

The results do not bear this out, the free fit model producing a value of n=2. When forced to produce a solution with n=3 it turned out that k_2 and k_3 were very close in value, the additional degree of freedom not yielding a viable solution. It must be assumed that the strength with which changes at the nitrogen atom are reflected in the ^{13}C NMR spectrum of the carbonyl carbon is

weak compared to the effect of binding to oxygen, which will be transmitted to the carbon by polarization of the carbonyl π-system. In conclusion the NMA experiment shows that ^{13}C NMR spectroscopy of amides is insensitive to solvation at the amide nitrogen. As such the Covington model cannot cope with amides (as probes) that do solvate at the amide proton. The results for this system are in Table 4.4 and the plots in Figures 4.5 and 4.6.

			Free Fit		Fixed Fit		
SYSTEM	n	i	k_i	Cross-Over	k_i	Cross-Over	Sum of Squares
NMA in H_2O/MeCN	2	1	1.26	44%	1.26	44%	0.041
		2	0.14	88%	0.14	88%	
	3	1	2.57	40%			0.0089
		2	0.22	82%			
		3	0.23	81%			

Table 4.3 - CSHIFTER Results for NMA in Hydrogen Peroxide

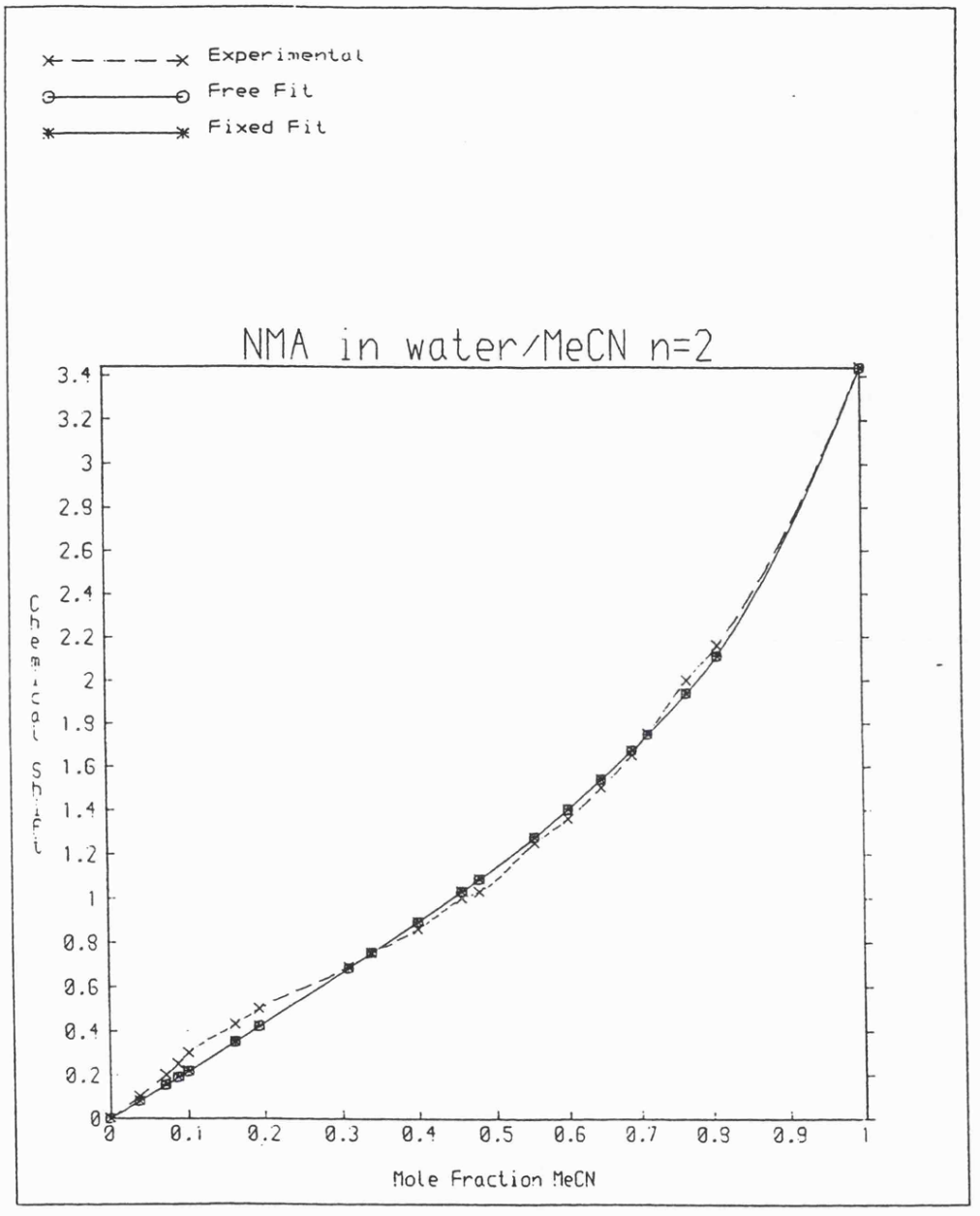

Figure 4.5 - CSHIFTER plot for NMA in water/cyanomethane: n = 2

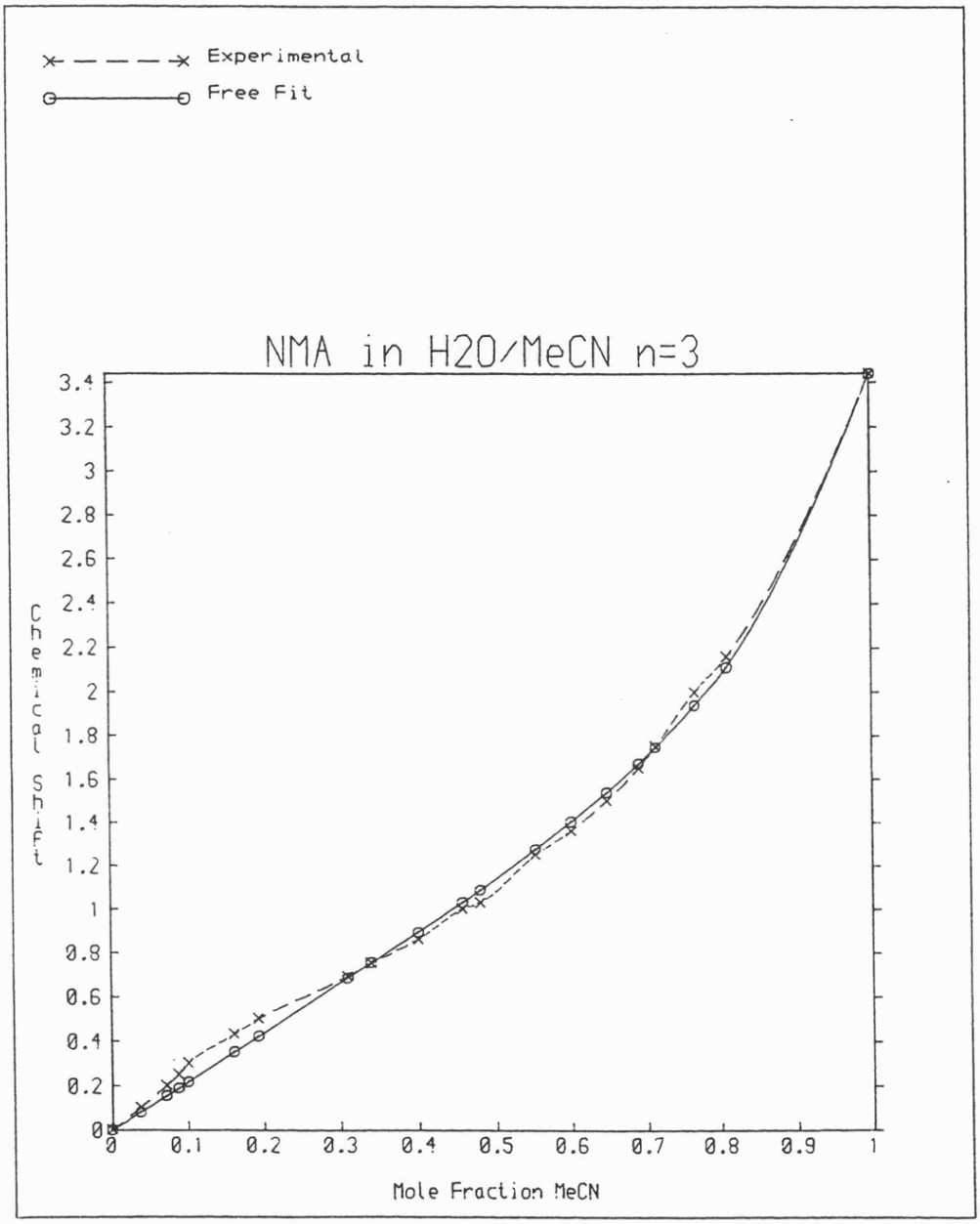

Figure 4.6 - CSHIFTER plot for NMA in water/cyanomethane: n = 3

4.6. Comparison with Infra-Red Studies

The NMR experiments and infra-red studies of the systems studied above have been published by Symons and Eaton[18,19].. In these publications are the diagrams from which the infra-red values in Table 4.1 were taken.

It was demonstrated in Section 4.4 that it is possible to extract the solvent composition that will lead two probe states to be in equal concentration. From the resultant mole fractions of the solvents an approximate value for the equilibrium constant can be calculated. This has been carried out for all the systems for which data is available. The corrected Covington equation, presented in Section 4.3, relates chemical shifts to equilibrium constants and concentrations. It has been used in reverse to predict chemical shifts from the equilibrium constants calculated from the infrared data. Plots of these predicted chemical shifts are included as Figures 4.7 to 4.10.

These plots were generated using the same equations used in CSHIFTER. If these equations, and, by implication Covington's model, are accurate these curves should reproduce the experimental NMR data. The IR results are considered to be reliable as they have been shown elsewhere[18] to correlate with the NMR data used in this Chapter.

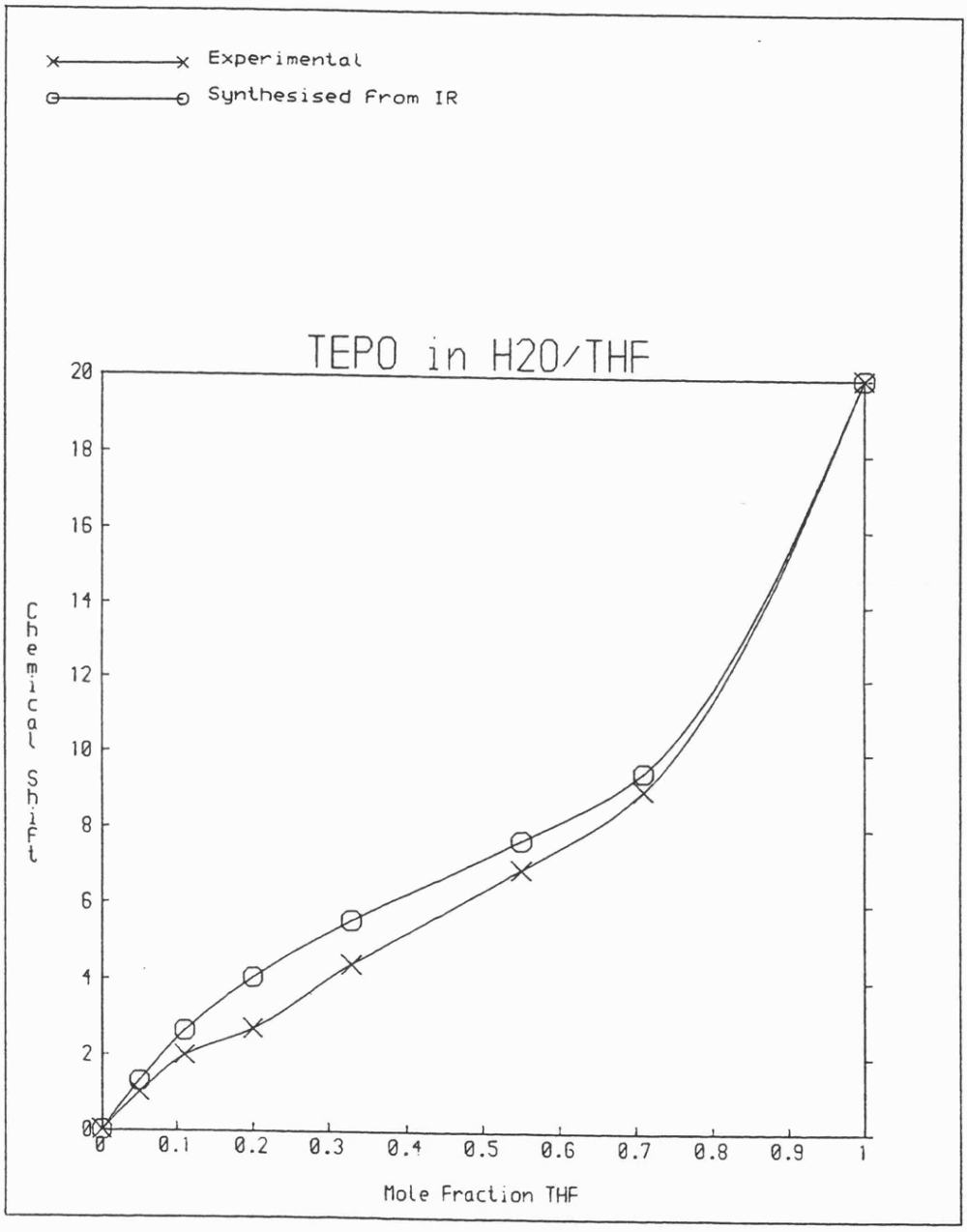

Figure 4.7 - Chemical Shift Curve Reconstructed from IR results : TEPO in H_2O/THF.

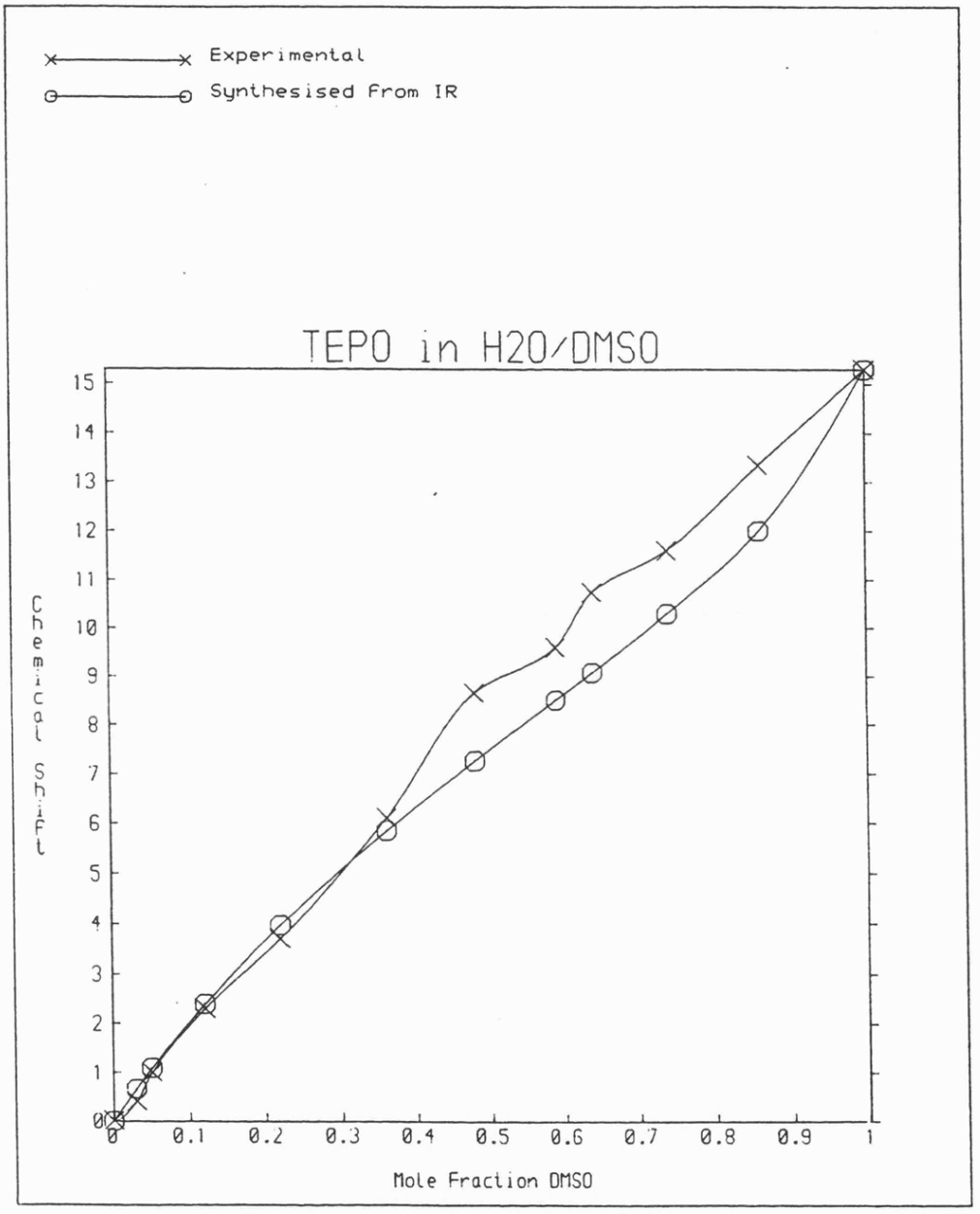

Figure 4.8 - Chemical Shift Curve Reconstructed from IR results : TEPO in H_2O/DMSO

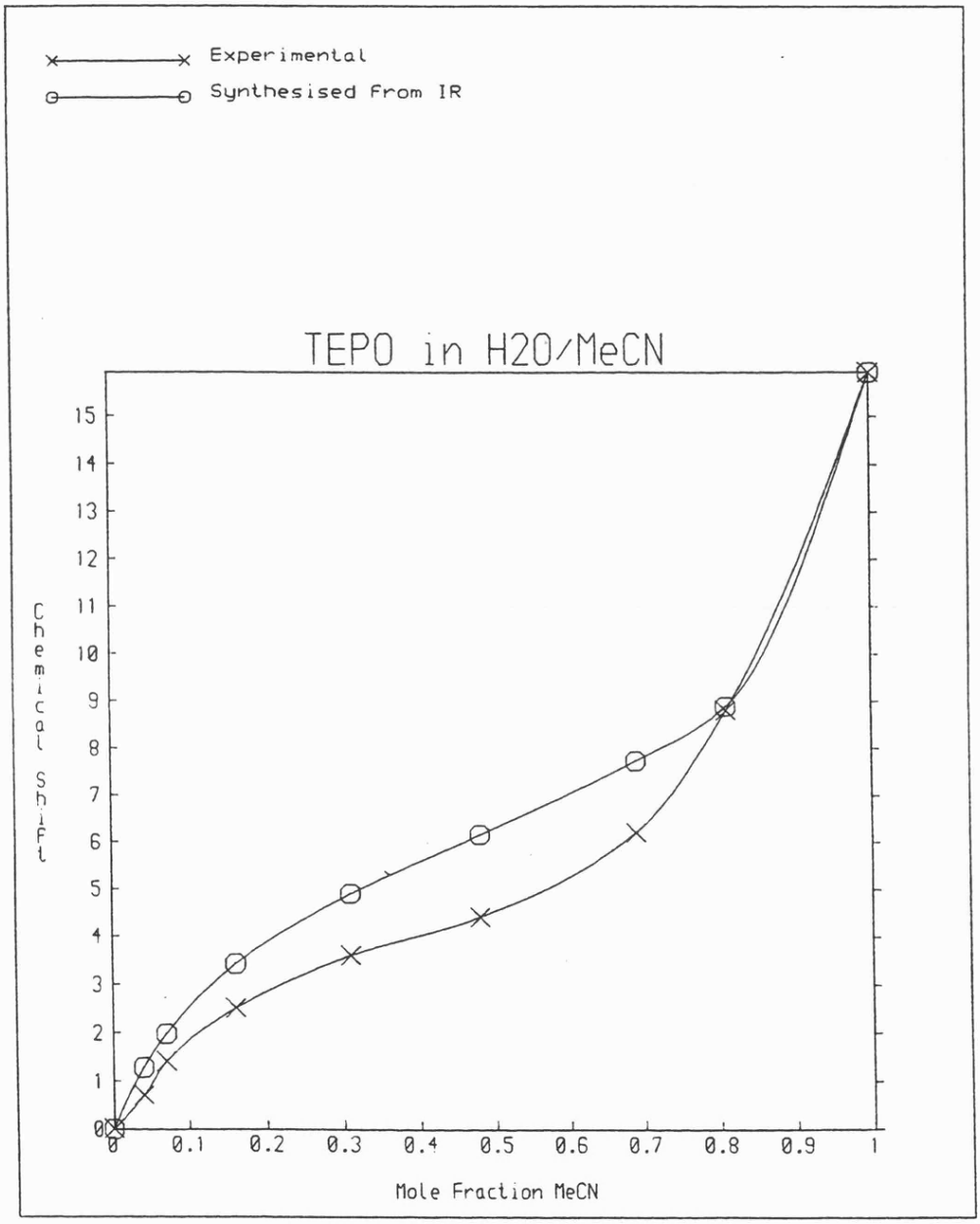

Figure 4.9 - Chemical Shift Curve Reconstructed from IR results : TEPO in H_2O/MeCN.

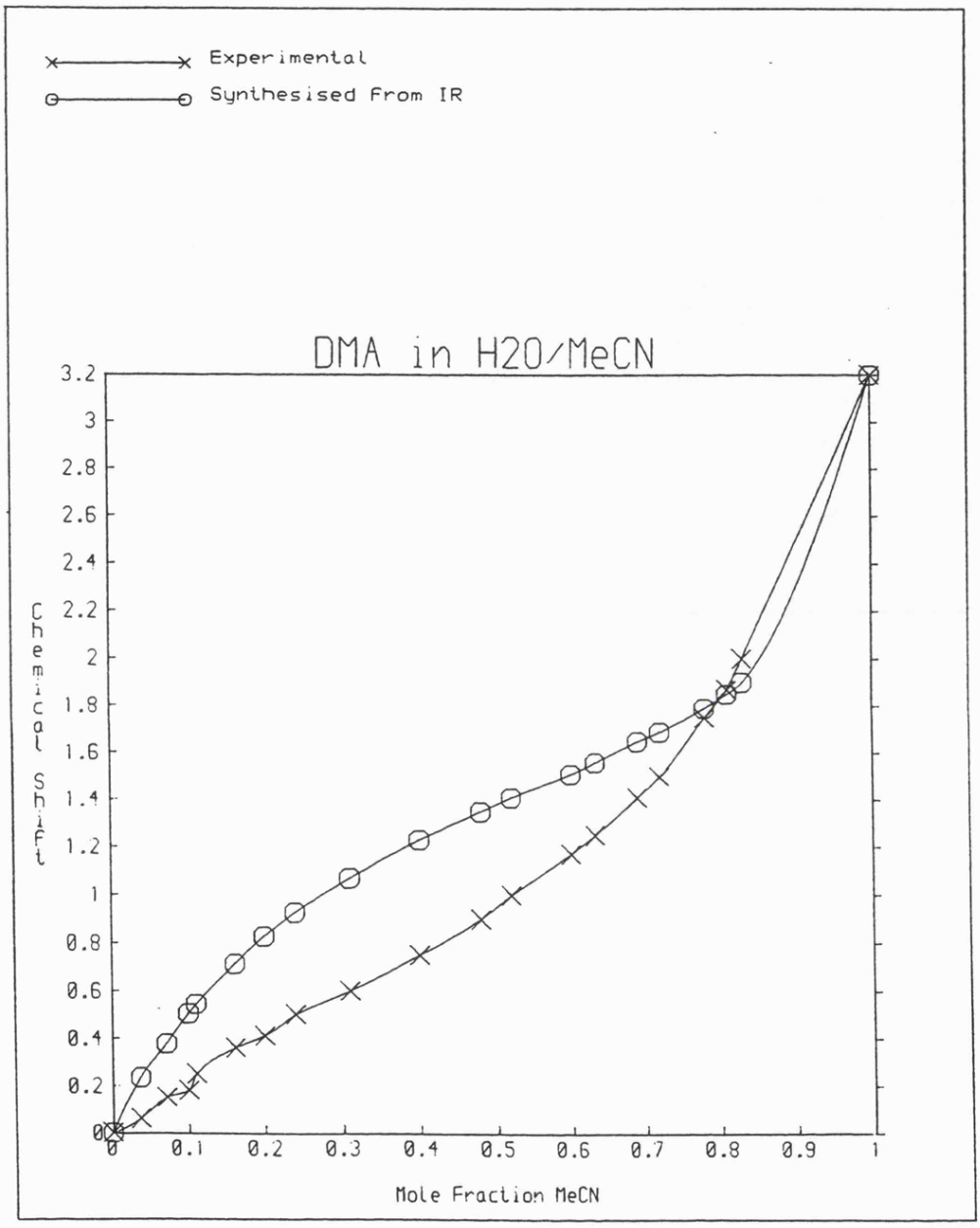

Figure 4.10 - Chemical Shift Curve constructed from IR results

DMA in H_2O/MeCN

It is clear that these synthesized plots do not agree with the experimental NMR results shown. In each case the synthesized plots show a more exaggerated curvature than the experimental data. There are two possible causes :

- Cross-overs do not generate correct equilibrium constants. This would be the case if the systems cannot be approximated to ideal behaviour, as concentrations are being used rather than chemical potentials.

- It is impossible to describe the behaviour of these systems purely in terms of a series of equilibrium constants.

In one diagram, reproduced as Figure 4.11, it can be see that the IR peaks due to the different probe molecule states do not have constant wavenumber positions. Each of the states generates a peak that moves slowly with changing solvent composition. This is attributed to the inductive and/or cooperativity effects of secondary solvating solvent molecules. Changing the position of an infra-red band implies changing the distribution of electrons along the bond. This in turn must change the chemical shift of a nucleus at one end of the bond.

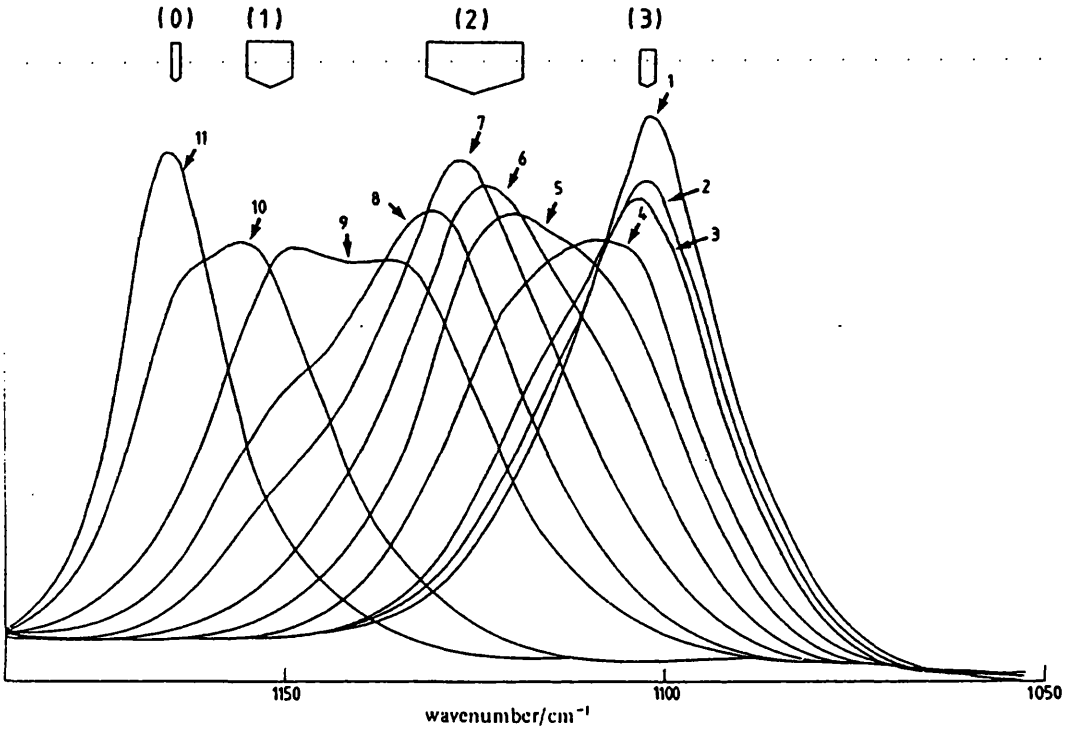

Key (in mole fractions):
1 = 0.00, 2 = 0.03, 3 = 0.07, 4 = 0.16, 5 = 0.36, 6 = 0.65, 7 = 0.79, 8 = 0.95, 9 = 0.97, 10 = 0.99, 11 = 1.00. Band maxima are indicated by broad arrows which span their shifts, the numbers indicating the postulated number of water molecules.

Figure 4.11 - Infrared spectra for dilute solutions of TEPO in water/MeCN systems.

Covington's model assumes that each probe state has a constant chemical shift. In reality it would seem that these chemical shifts are, in fact, functions of solvent composition. This undermines the basis of both fixed-fit and free-fit models.

It is noticeable that the behaviour of all of the TEPO in water/base systems the behaviour at high water mole fraction is the same in terms of absolute chemical shifts (linear to 3 ppm at 0.2 mole fraction). This would imply that behaviour in this region is determined by properties of the water and that the nature of the base is unimportant. This brings a return to the idea, mentioned earlier, that solvent-solvent interactions and not

solvent-probe interactions are determining the behaviour of these systems. This behaviour is not seen with methanol/base systems[18]. The explanation for this observation is as follows.

Water forms a three dimensional hydrogen-bonded structure in the liquid phase. When water dominates the solvent composition it will tend to dominate the binding sites on the probe. As water-water interactions are stronger than water-cosolvent interactions a zone of pure water will form a 'shell' around the probe binding sites which the cosolvent cannot easily penetrate. The only way for the cosolvent to remove a water molecule from the primary solvation shell is for the water structure to break up. The proposed mechanism for this is the generation of broken hydrogen bonds within the water 'shell', in other words OH_{free} and LP_{free} groups must form within the shell[19]. This may allow the base access to the primary solvation shell where it can remove a solvating water molecule.

This mechanism is independent of the properties of a basic cosolvent, provided that water-water interactions are stronger than water-base interactions. In the methanol-base systems this behaviour is not seen. Methanol forms a chain structure in the liquid phase. Base molecules are not, therefore, denied access to the primary solvation shell by stearic blocking in the way that the three dimensional water structure can. They may 'unhook' the methanol chains from the probe molecule, and their ability so to do *will* be a function of the nature of the base.

This mechanism explains the nature of the experimental results. It also happens to have nothing to do with the model of solvation behaviour proposed by Covington and would, therefore, further invalidate his model, at least in systems where one component is water.

4.7. Conclusions

The Covington model is capable of fitting the selected NMR data quite accurately. Certainly the added freedom of the free-fit model, where no assumption is made as to the relationship between the equilibrium constants, does not significantly improve the quality of the fits.

Covington's model is nonetheless flawed because it ignores the effects of all solvent species outside the primary solvation shell. It does remain a viable model as the fits to experimental data are generally good and the equilibrium constants generated shows the expected trends due to base strength.

It must also be remembered that all of the systems studied here have water as a component. Water is a unique solvent in its behaviour[20] and Covington's approach may well be valid with solvents that do not show such a well developed three dimensional structure. In order to produce a better model it would be necessary to calculate the effect of all the solvent molecules beyond the primary shell on the primary shell members and to then calculate the effect on the probe. Presumably it is possible to

develop a statistical treatment that could produce the required result.

The attempt to correlate the experimental chemical shifts to those predicted from infra-red work clearly failed. The binary solvent systems are not behaving in an ideal manner and the assumed relationship between probe concentrations and equilibrium constants would seem not to hold. The differences between the experimental chemical shifts and those predicted from infra-red are significant.

It must also be noted that the limitations of computer applications in any field where experimental data is used as raw data are shown up here. A least squares fitting routine, no matter how elegant and well designed, cannot make intelligent interpretations of results. If any one experimental point is wrong it will be considered an equal of points that are accurate. The routine has one objective - to produce parameters that minimize the difference between experimental points and the points generated by the equation used as a model. If the experimental points are only slightly in error then the equilibrium constants obtained may have no bearing on the true equilibrium constants, they just show the best mathematical solution to the problem.

References

1 Grunwald, E., Baughman, G. and Kohnstan, G., *J. Am. Chem. Soc.*, **82**, 5081, (1960)

2 Covington, A.K., Lilley, T.H., Newman, K.E. and Porthouse, J.A., *J. Chem. Soc., Faraday Trans. I*, **69**, 963, (1973)

[3] Covington, A.K., Lilley, T.H. and Newman, K.E. *J. Chem. Soc., Faraday Trans. I*, **69**, 973, (1973)

[4] Covington, A.K, Lantzke, I.R. and Thain, J.M., *J. Chem. Soc., Faraday Trans. I*, **70**, 1869, (1974)

[5] Covington, A.K. and Thain, J.M., *J. Chem. Soc., Faraday Trans. I*, **70**, 1879, (1974)

[6] Covington, A.K. and Covington, A.D., *J. Chem. Soc., Faraday Trans. I*, **71**, 831, (1975)

[7] Covington, A.K. and Newman, K.E., *Pure Appl. Chem*, **51**, 2041, (1979)

[8] Marcus, Y., *Aust. J. Chem.*, **36**, 1719, (1983)

[9] Marcus, Y., J. Chem. Soc., Faraday Trans. I, **84**, 1465, (1988)

[10] Parbhoo, B. and Nagy, O.B., *J. Chem. Soc., Faraday Trans. I*, **82**, 1789, (1986)

[11] Langford, C.H. and Tong, J.P.K., *Acc. Chem. Res.*, **10**, 258, (1977)

[12] Langford, C.H. and Tong, J.P.K., *Pure Appl. Chem.*, **49**, 93, (1977)

[13] Muanda, M., Nagy, J.B. and Nagy, O.B., *Tetrahedron Lett.*, **38**, 3421, (1974)

[14] Muanda, M., Nagy, J.B. and Nagy, O.B., *J. Chem. Soc., Faraday Trans. I*, **74**, 2210, (1978)

[15] Remerie, K. and Engberts, J.B.F.N., *J. Phys. Chem.*, **87**, 5449, (1983)

[16] Eaton, G., Ph.D. Thesis, Leicester, 1982

[17] Program listing provided by Dr. J.B.F.N. Engberts

[18] Symons, M.C.R. and Eaton, G., *J. Chem. Soc.,Faraday Trans. I*, **78**, 3033, (1982)

[19] Symons, M.C.R. and Eaton, G., *J. Chem. Soc.,Faraday Trans. I*, **84**, 3459, (1988)

[20] Symons, M.C.R. *Chem. in Brit.*, **25**, 491, (1989)

5. FAST EXCHANGE IN INFRARED SPECTROSCOPY

5.1. Introduction

It is possible that if a reaction results in a balanced equilibrium, rather than a one way conversion, then it can proceed so fast that spectroscopic studies of the equilibrium system can show features/characteristics determined by the reaction rate. In the case of NMR work this will happen if the lifetime of the reacting species is similar to, or shorter than, the relaxation time of the nuclear spin state. This generates two regimes for spectroscopy, fast exchange and slow exchange. In the fast exchange regime the spectrum seen is the average of those of the product and of the reagent. This happens because the chemical environment of the nucleus changes during the lifetime of the spin state. In the slow exchange regime the chemical environment does not change during the lifetime of the spin state and so two distinct chemical environments are seen. There is inevitably a transitional regime between fast and slow exchange. The sharp lines of the slow exchange system broaden and merge before sharpening up again as a fast exchange spectrum. The lifetime of the excited spin state in most proton NMR work needs to be of the order of 10^{-1}-10^{2} seconds in order to be within the slow exchange regime[1].

In infrared absorption spectroscopy the critical event is the vibration of the chemical bond. This is a very much faster event than nuclear spin relaxation, in the region of 10^{-12}-10^{-15} seconds.

It is generally considered that infrared spectra are always within the slow exchange regime. This study shows that in at least one system infrared spectra seem to show behaviour usually associated with NMR spectra moving between fast and slow exchange regimes.

5.1.1. Background

The use of infrared and Raman band shape analysis to study fast dynamic processes in liquids is well established[2]. Work has been attempted on other processes such as ionisation reactions[3,4,5,6,7], hydrogen bonding reactions[8], methyl group rotations[9] and donor-acceptor complex formation[10]. Theoretical approaches to the interpretation of such work have only recently been investigated[11,12]. Such interpretations when applied to data generated by work such as that contained in this Chapter may reveal useful information about hydrogen bonding in solution.

5.1.2. Cyanomethane and Methanol System

In solvation studies at Leicester much use is made of probe molecules. A probe is a molecule added to a solution that has a bond or nucleus sensitive to the way in which the species is solvated. Infrared or NMR techniques can then be used to examine the behaviour of the solution. Cyanomethane is heavily used as a solvation probe.

It has been shown in the course of such work[13] that when dissolved in methanol it assumes one of two states. These are termed 'free' where there are no hydrogen bonds between probe and solvent, and

'bound' where a single hydrogen bond is formed between a cyanomethane nitrogen and an alcoholic proton.

A study has been made of the way in which the proportions of the two species changed with temperature. The fundamental infrared absorption bands due to the CN triple bonds of cyanomethane in the two solvation states were studied at different temperatures. This study revealed that not only were the bands changing in relative intensity, as expected, but that they were moving relative to each other as well.

5.2. Experimental

The spectrometer used in this work is a Perkin Elmer 580 infrared spectrophotometer. Temperature control was maintained by a Specac 20.00 variable temperature unit attached to a Beckman demountable cell holder. The sample was prepared as a thin film between calcium fluoride plates in Beckman RIIC FH-01 cells. Spectra were recorded at various temperatures between 203K and 343K. Below 203K the solution froze, above 343K it boiled. This is, therefore, the maximum temperature range possible without the introduction of pressure control equipment. In order to obtain the most reliable temperatures the readings below room temperature were made by cooling the sample to below the desired temperature and then letting it warm up to the correct temperature. The spectra were recorded between 2280 cm^{-1} and 2240 cm^{-1}. The solutions used were of 0.06 ml cyanomethane in 1 ml of methanol.

Both reagents came from samples stored over drying agents (calcium hydride for cyanomethane and molecular sieve for methanol).

5.3. Data Handling

The spectra from the Perkin Elmer 580 were transferred to Leicester University's VAX cluster using a Calcomp digitiser. A program was written to convert files from the digitiser into usable digitised spectra. The digitiser created too many data points for the available spectral simulation programs to handle. The conversion program therefore used interpolation routines to produce a smooth curve through the available data. This caused some problems as spurious points were created by the interpolation, these had to be removed from the files 'by hand' to leave smooth curves. The conversion program also performed an automatic baseline subtraction. The baseline line subtracted was the straight line with the largest gradient that passed through the first data point and went below, or through, ever other point. A second conversion program was written to convert the digitised spectra into the correct file format for the simulation program VIDCA. This program, written by N. Pay[14] at Leicester, was used to perform a simulation of the digitised spectra. VIDCA requires the user to specify a height, width, position and gaussian percentage for each band of the simulation. The bands so described, their sum and the experimental spectrum are plotted on the terminal screen (Pericom MX2000). There is no computer assistance in refining the simulation, all modifications are made interactively by the user.

Using VIDCA, simulations were made of all the spectra generated. In each case two bands only were used. Some problems were encountered fitting a curve to the experimental data in the wings of each spectrum. It is assumed that this is due to errors caused by the automatic baseline subtraction. Subtraction of a quadratic, rather than linear, baseline may have improved matters. Once simulations were completed plots were made of line width, band shape (percentage gaussian) and band position against temperature. A plot was also made of the difference in band position against temperature.

5.4. Results

All the spectra consist of two bands. Those at lower temperature are quite distinct, whilst those at higher temperature appear as a single asymmetric band. These bands are assigned[15] to the free and mono-bound states of cyanomethane. The higher energy band is assigned to the bound species, as hydrogen bonding to the nitrogen strengthens the carbon-nitrogen bond in cyanides[13], stronger bonds requiring more energy to excite. This assignment is supported by the observation that addition of dimethylformamide (acting as a non-hydrogen bonding diluent) leads to a decrease in the high energy band and an increase in the low energy band. This shows that the low energy band is due to a non-hydrogen bonded species.

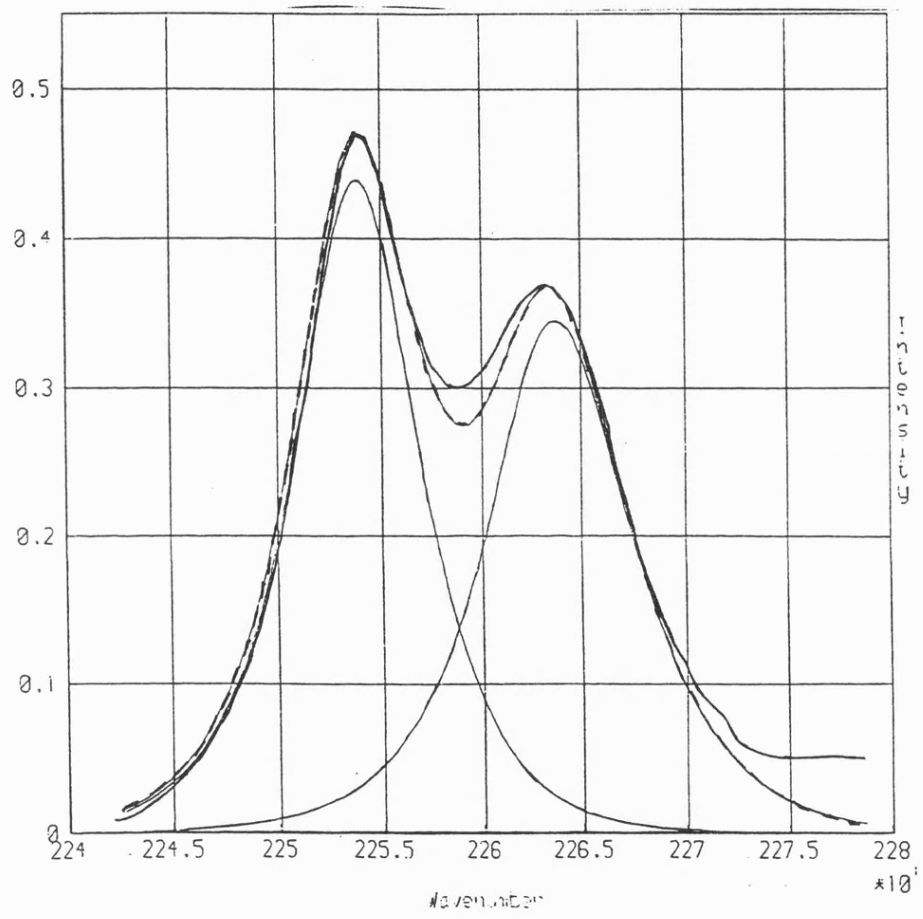

Dashed line represents the synthesized envelope produced by the two component bands. Bold line represents the experimental spectrum

Figure 5.1 - CN stretch of MeCN in Methanol at 203K

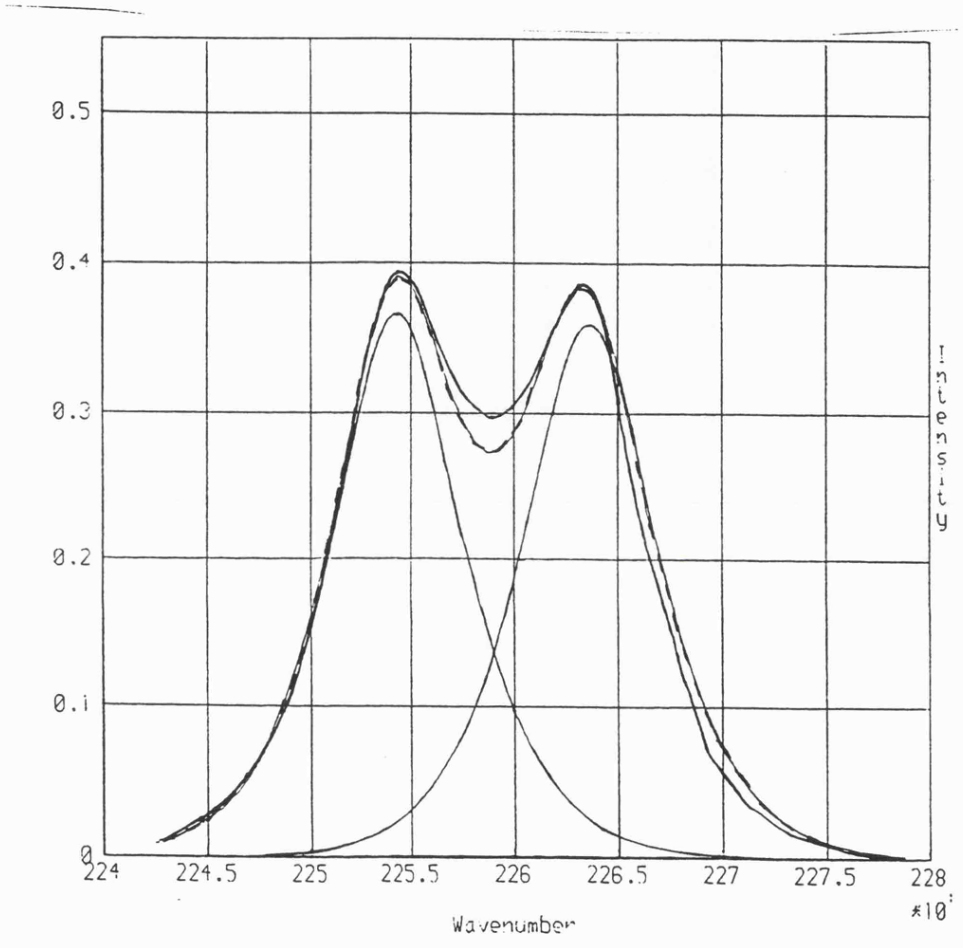

Dashed line represents the synthesized envelope produced by the two component bands. Bold line represents the experimental spectrum

Figure 5.2 - CN stretch of MeCN in Methanol at 223K

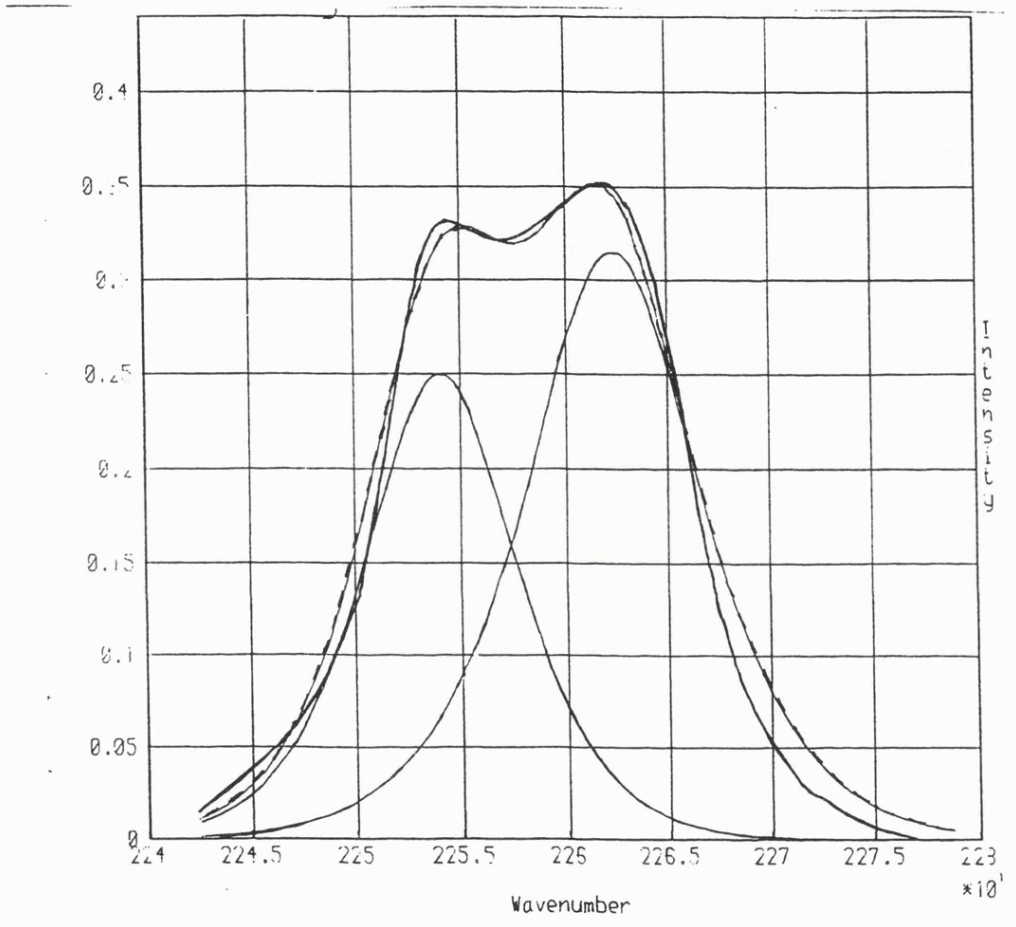

Dashed line represents the synthesized envelope produced by the two component bands. Bold line represents the experimental spectrum

Figure 5.3 - CN stretch of MeCN in Methanol at 248K

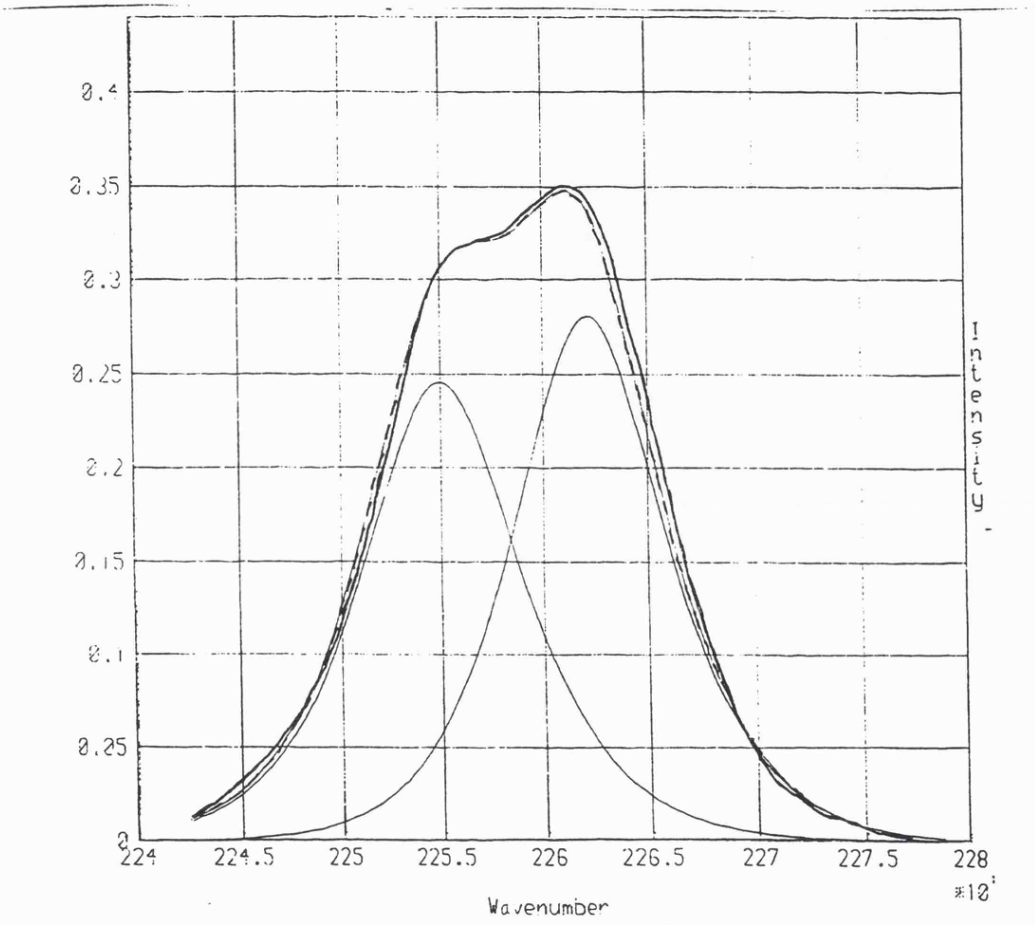

Dashed line represents the synthesized envelope produced by the two component bands. Bold line represents the experimental spectrum

Figure 5.4 - CN stretch of MeCN in Methanol at 273K

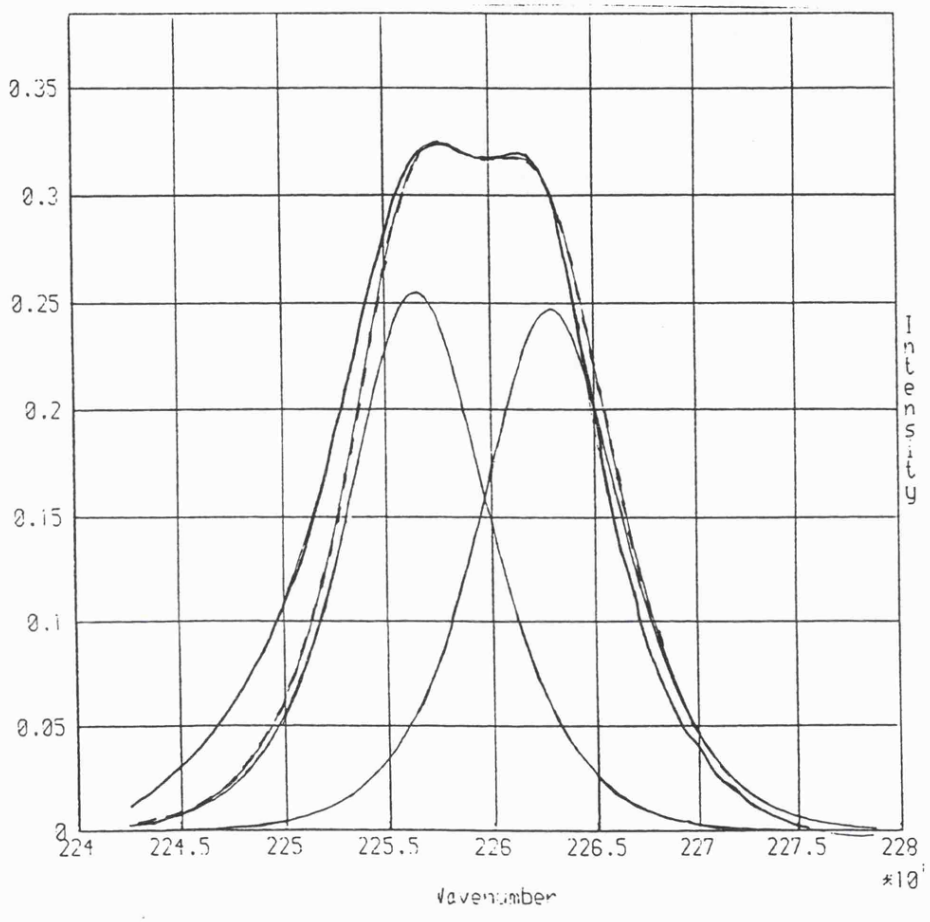

Dashed line represents the synthesized envelope produced by the two component bands. Bold line represents the experimental spectrum

Figure 5.5 - CN stretch of MeCN in Methanol at 298K

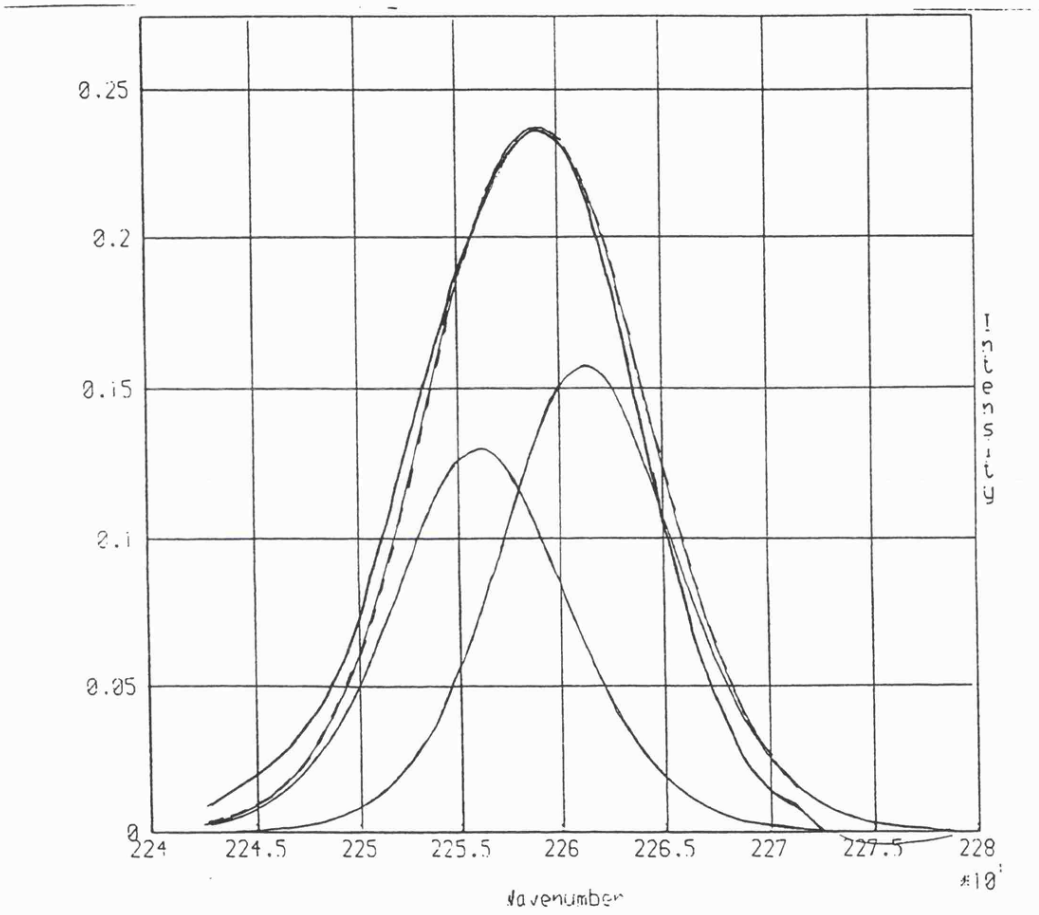

Dashed line represents the synthesized envelope produced by the two component bands. Bold line represents the experimental spectrum

Figure 5.6 - CN stretch of MeCN in Methanol at 323K

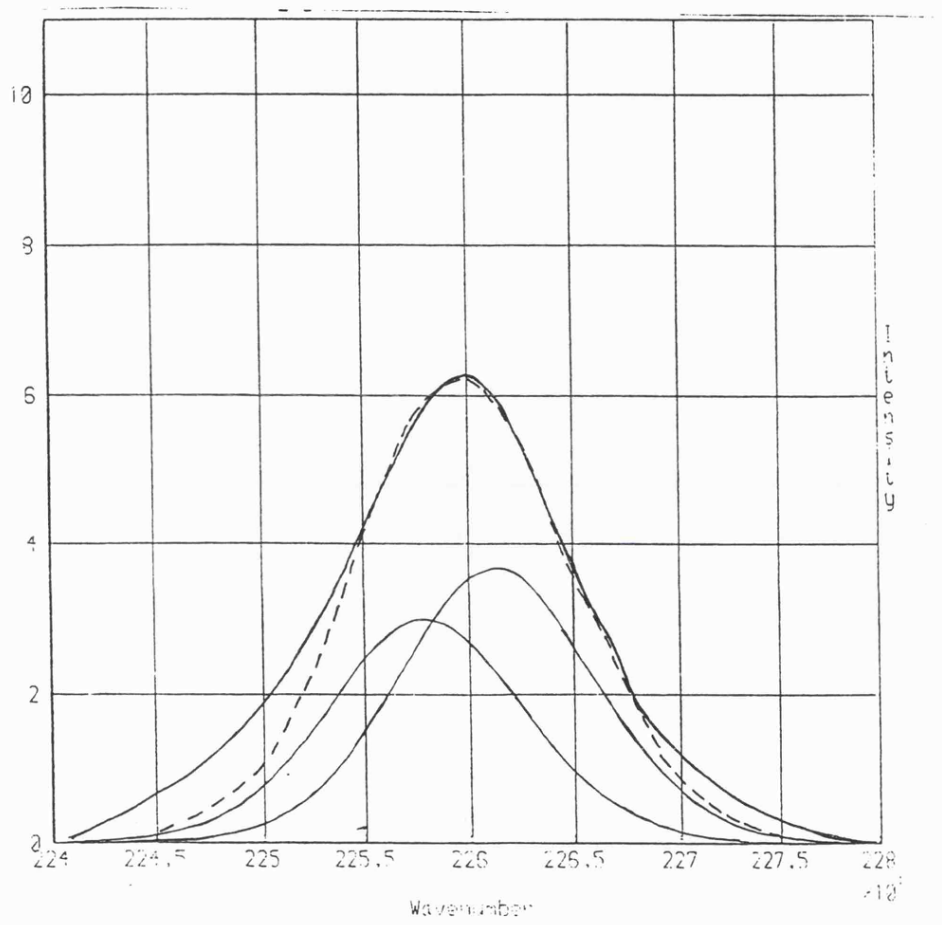

Dashed line represents the synthesized envelope produced by the two component bands. Bold line represents the experimental spectrum

Figure 5.7 - CN stretch of MeCN in Methanol at 333K

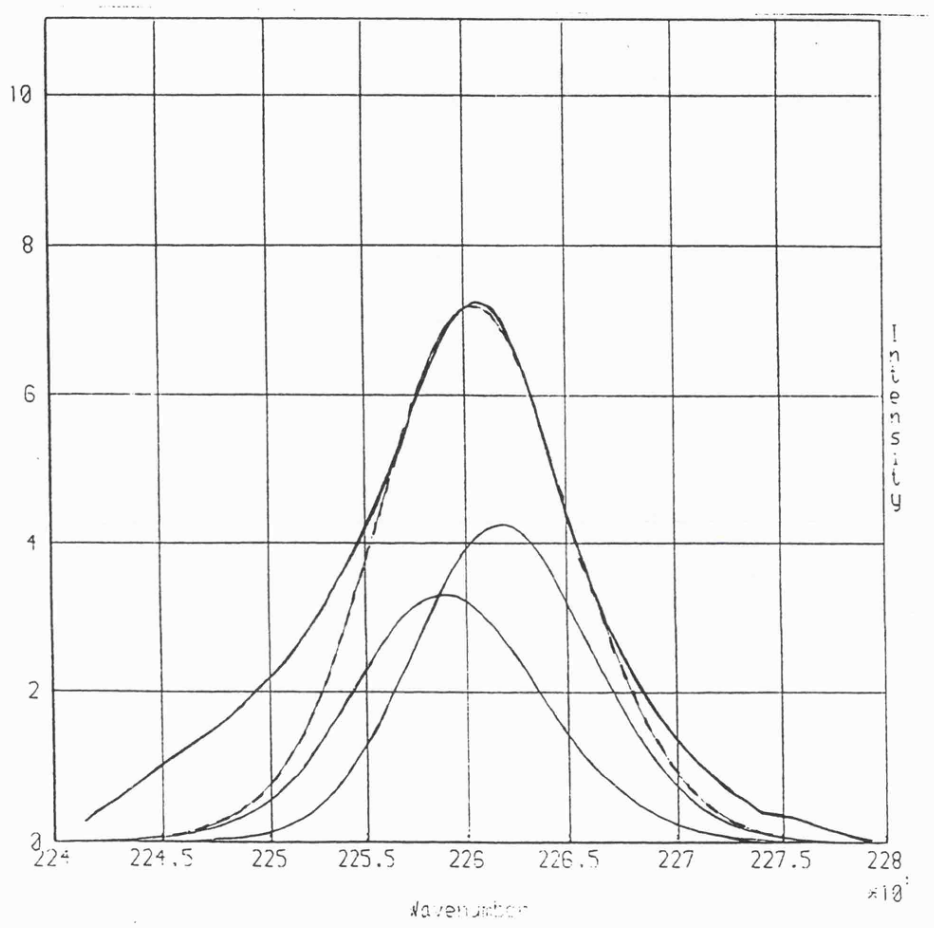

Dashed line represents the synthesized envelope produced by the two component bands. Bold line represents the experimental spectrum

Figure 5.8 - CN stretch of MeCN in Methanol at 343K

Simulations were successfully made of all the digitised spectra (Figures 5.1 to 5.8). It proved impossible to perform all the simulations with bands that were in the same position for each spectrum. This demonstrates that the observed change in the experimental envelope cannot be attributed to simple thermal broadening of the absorption bands, which would have allowed fitting of all spectra with changes to linewidth and possibly line shape.

The simulation shown in Figure 5.1 could not be performed using bands of the same width and shape. It is therefore proposed that these bands are taken as representative of the slow-exchange regime, with no significant contribution from fast exchange phenomena. The simulations shown in Figures 5.7 and 5.8 have insufficient intensity in the wings, suggesting that a single Lorentzian band could have fitted better than the two highly Gaussian components used. This would indicate that Figures 5.7 and 5.8 represent systems fully in the fast exchange regime. If this is the case then the reported fitting parameters for these two cases are meaningless.

Details of the line shape, linewidth and position parameters for the simulations are tabulated in Tables 5.1, 5.3 and 5.4 and plotted in Figures 5.9, 5.11 and 5.12. In all cases band 1 is assigned to the 'free' CN group and band 2 to the 'bound' group.

5.4.1. Errors

All of the above data show inconsistencies and, as a result Figures 5.9, 5.11 and 5.12 do not show smooth shapes. This is almost certainly as much due to the pitfalls of interactive curve fitting as to any experimental errors. The simulations are always capable of further refinement and accuracy is derived as much from patience or intuition as from skill. It is also possible to introduce errors by trying to 'force' a fit to a pre-conceived pattern. To avoid this kind of contamination no reworking of the simulations was attempted after the first graphs of the results had been drawn.

The curves in Figures 5.9 - 5.12 were drawn by exponential regression functions that form a part of the drawing package used to prepare the graphs (Lotus Freelance 3.0). The curve in Figure 5.13 was drawn by the author.

Errors in the data could be introduced by the spectrometer, by condensation in the cell or by errors in the digitisation (the digitiser cursor is moved by hand). The errors introduced by computer processing have already been alluded to. It is accepted that the data set is quite sparse given the temperature range covered, further data would improve confidence in the plots made.

5.4.2. Line Widths

The linewidths generated for the two bands are tabulated in Table 5.1 and plotted in Figure 5.9. The bands gradually broaden

Temperature (K)	Half Width at Half Height (wavenumbers)	
	Free Band 1	Bound Band 2
203	3.50	4.20
223	3.75	3.75
248	4.80	5.10
273	4.60	4.30
298	4.40	4.40
323	5.10	5.10
333	5.50	5.50
343	5.50	5.10

Table 5.1 - CN Stretch Half Linewidths (wavenumbers)

with increasing temperature. At lower temperatures any differences between the bands will be due to the maintenance of the slow-exchange regime preserving the different inherent line widths of the two bands. At higher temperatures there is less reason why the two bands should show different line widths so those occasions where they are different are probably due either to experimental error or to errors in the simulation.

Figure 5.9 shows that the two bands appear to have increasingly similar linewidths, merging at around 310K-320K thus supporting the suggestion that the 333K and 343K (Figures 5.7 and 5.8) cases represent a single merged band.

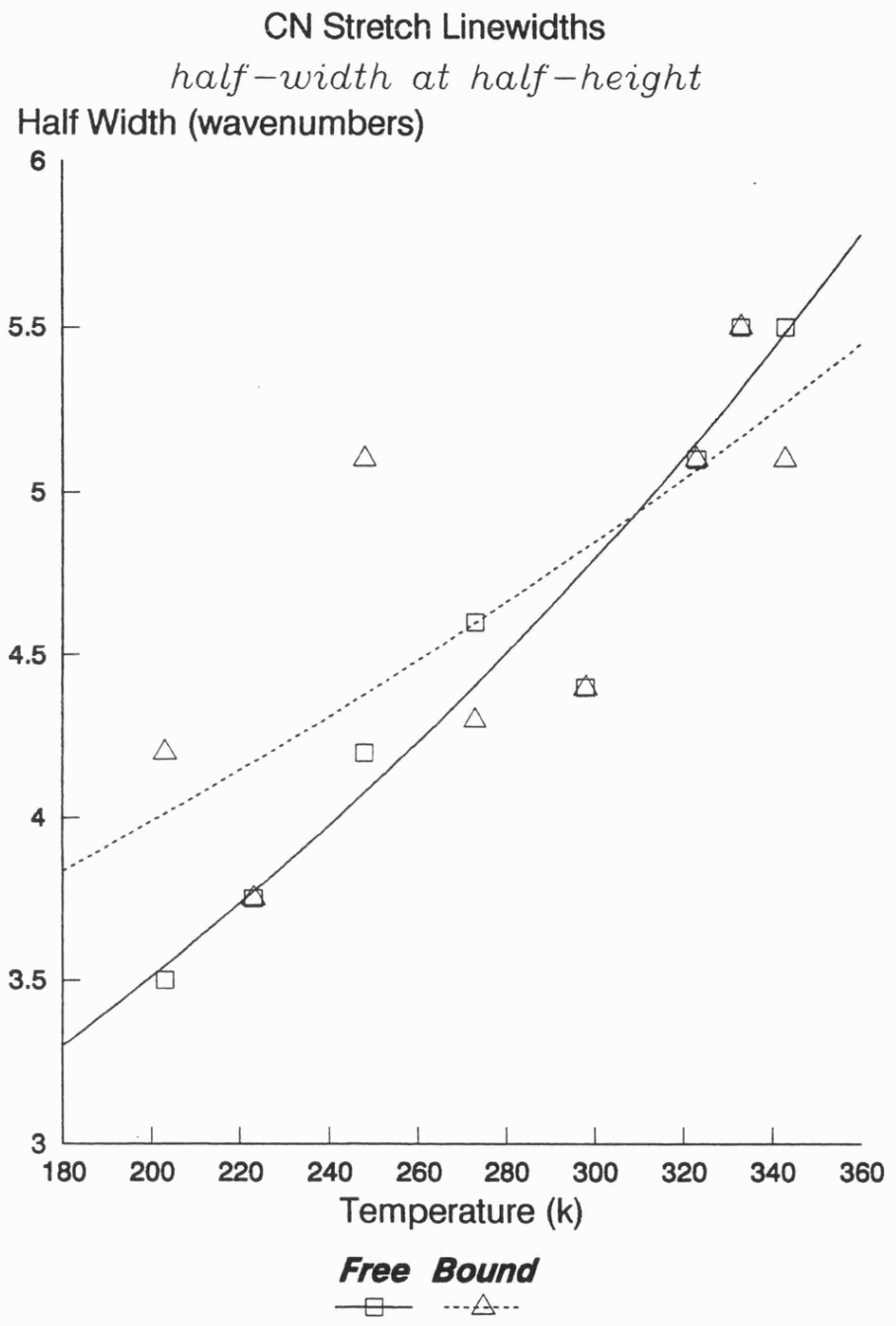

Figure 5.9 - CN stretch linewidths of MeCN in Methanol

If a band is lifetime broadened and a width for the unbroadened line is available then it is possible to calculate the lifetime of the short lived species. Clearly this is only a valid approach where a line width is available for a band which has no lifetime contribution to its width. In practise this does not occur, it is assumed here that the broadening of the lowest temperature (203K) bands in this work have negligible lifetime broadening.

This approach can be applied to the equilibrium between hydrogen bonded and free cyanomethane using the data from this work. The band width of the bound species at 203K will be taken as the unbroadened width. The approximate equation for this relation is[16] :

$$\delta E = \frac{h}{2\pi\tau}$$

where δE is the increase in linewidth (full width at half-height) and τ the halflife. When converted to wavenumbers and with lifetime as the subject it becomes :

$$\tau = \frac{5 \times 10^{-12}}{\delta \upsilon}$$

where $\delta \upsilon$ is the increased linewidth in wavenumbers. The lifetimes for the cyanomethane - methanol hydrogen bond have been calculated using linewidths for the bound species taken from Figure 5.9. They are displayed in Table 5.2 and plotted as Figure 5.10.

Temperature (K)	Line Width Increase (cm^{-1})	Half Life (s)
220	0.33	1.5×10^{-11}
248	0.78	6.4×10^{-12}
273	1.21	4.1×10^{-12}
309	1.88	2.7×10^{-12}
323	2.20	2.3×10^{-13}

Table 5.2 - Lifetimes of cyanomethane - methanol hydrogen bonds

This result is in very good agreement with results from recent molecular dynamics calculations on the same system which give a value of 10^{-12}s at 298 K[17].

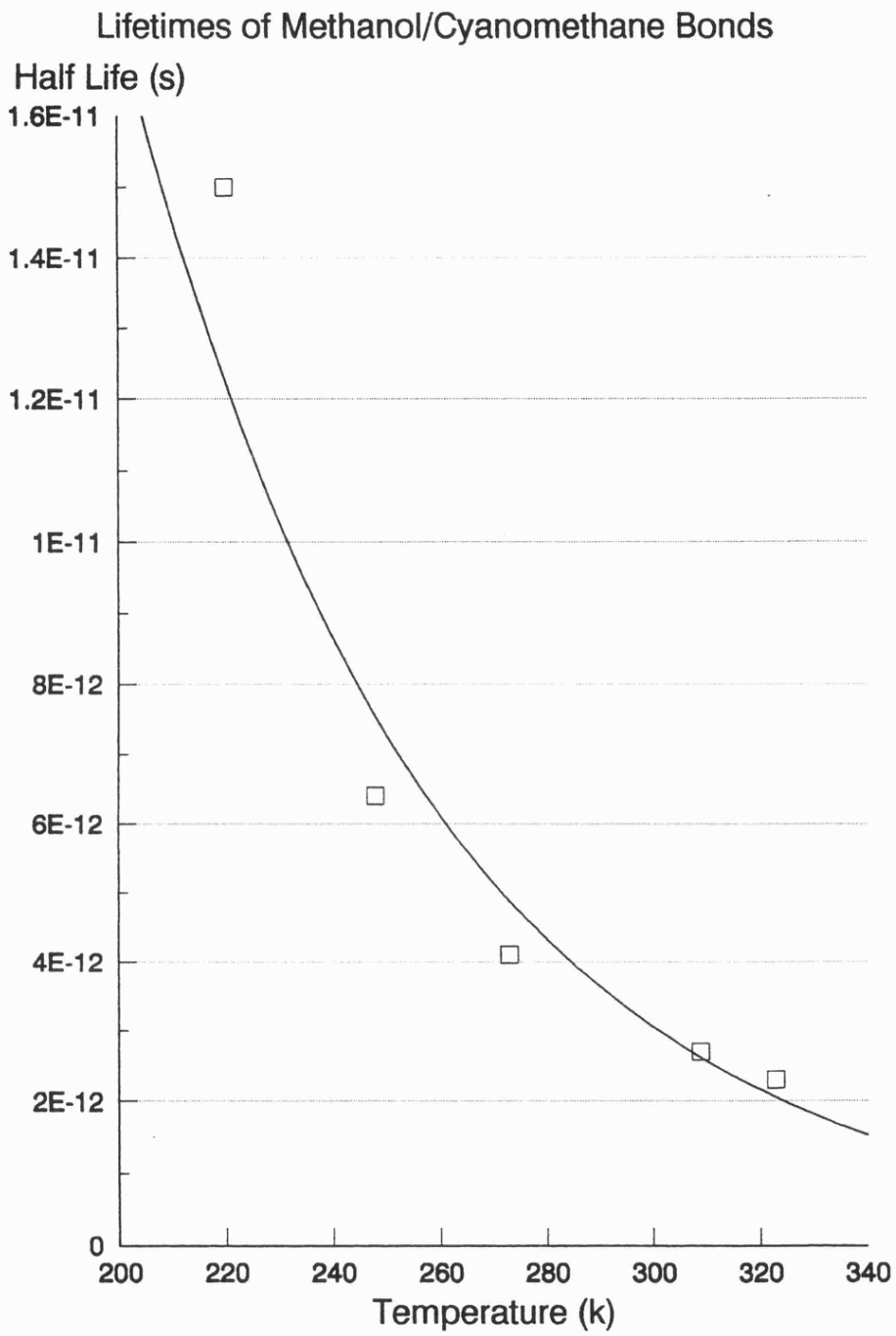

Figure 5.10 - Lifetimes of cyanomethane - methanol h-bonds

5.4.3. Line Shapes

The bands generated by the computer are a combination of two lineshape functions, one lorentzian and one gaussian. The user specifies a percentage contribution for the gaussian, the complement is a lorentzian contribution. The line shape data is presented in Table 5.3 and plotted against temperature in Figure 5.11.

The simulations show an increasing gaussian character to the bands as temperature increases. As temperature increases the rate of collisions will increase. This would, in most circumstances, lead to an increased degree of kinetic control on the vibrational relaxation function. In other words the curve should become *more* lorentzian in nature[18,19]. In the case of this work it would seem that the lines become *less* lorentzian with an increase of temperature. This tends to suggest that fewer collisions are occurring and that the vibrational relaxation function is more controlled by gas-phase like relaxation processes such as translational diffusion.

This can be explained if it is remembered that the reaction studied here is proceeding very fast. It is significant that the calculated lifetimes of the h-bonds in this work is of the same order of magnitude as the theoretically predicted cut-off between Gaussian and Lorentzian domains, 0.5×10^{-12} s[19]. This would make a significant change of lineshape in this system quite plausible

Temperature (K)	Line Shape (% Gaussian)	
	Free Band 1	Bound Band 2
203	17.5	18.5
223	25.0	25.0
248	30.0	30.0
273	27.0	27.0
298	30.0	35.0
323	55.0	55.0
333	62.0	62.0
343	70.0	70.0

Percentage of line shape function contributed by gaussian function

Table 5.3 - CN Stretch Line Shape

if the hydrogen bond lifetime is changing significantly around the 0.5×10^{-12} region.

Rotational correlation times for cyanomethane in water / 1-propanol mixtures have been calculated from both theory and from ^{14}N NMR derived transverse relaxation times[20]. These values vary between 1.58×10^{-12} s and 4.5×10^{-12} s with composition of the solution. In pure 1-propanol the values calculated were 4.41×10^{-12} s (theoretical) and 4.3×10^{-12} s (experimental). As noted already above these values are very close to the bond lifetimes and coupling between processes may well be occurring[21].

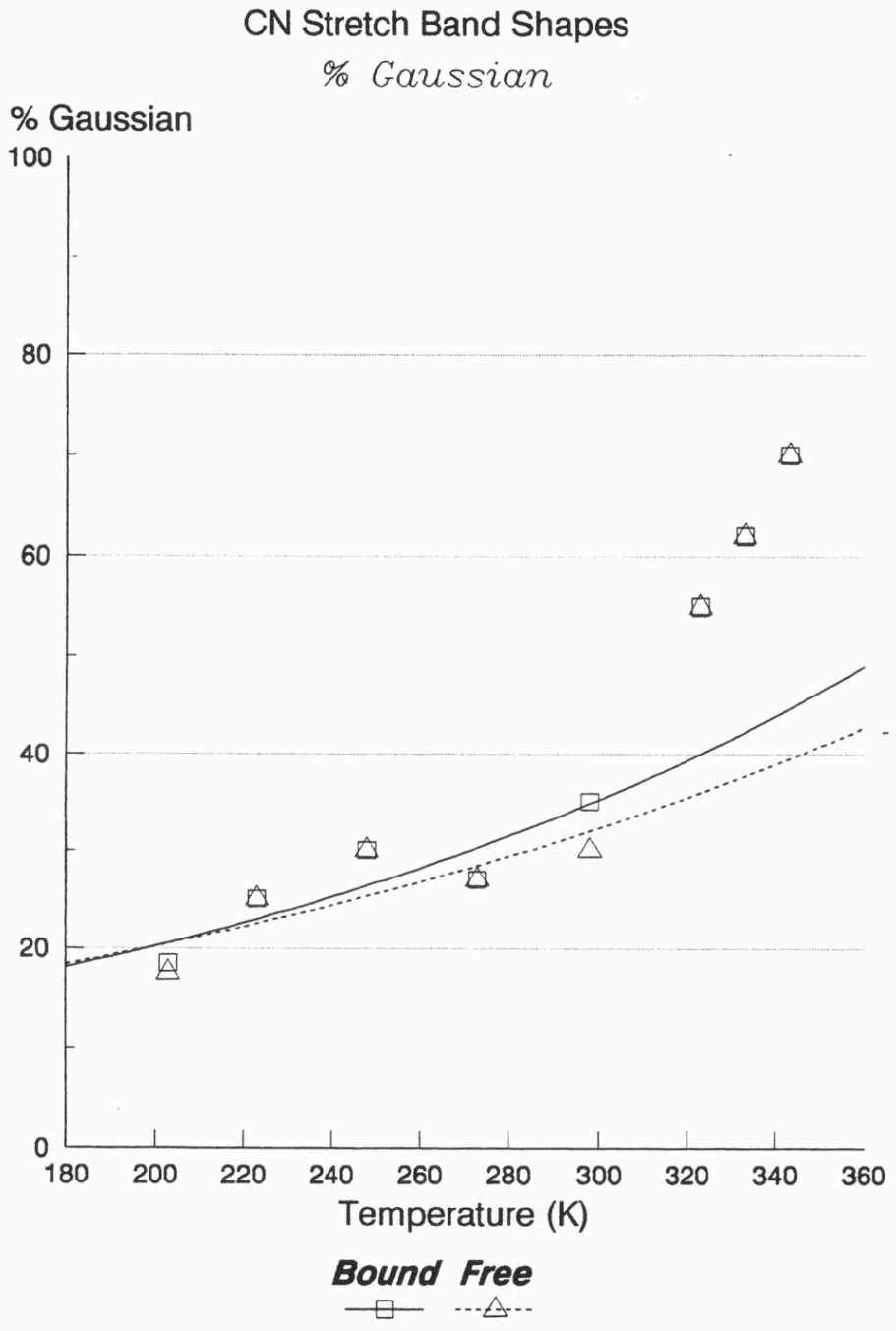

Figure 5.11 - CN stretch lineshapes of MeCN in Methanol

5.4.4. Band Position

The band positions are tabulated in Table 5.4 and plotted against temperature in Figure 5.13. Figure 5.14 is a plot of the separation between the two bands against temperature.

There is a clear moving together of bands with increasing temperature in these results. This last trend can be seen more clearly in Figure 5.13 where the separation between the two peaks (in wavenumbers) is plotted. The plot suggests that the separation between the peaks is a linear function of temperature. The only mechanism available for this phenomenon is the time-averaging mentioned in the introduction. Changing temperature could change the strength of the hydrogen bond of the cyanomethane/methanol dimer and hence the position of band 2. This would have no effect on band 1 assigned to the 'free' CN stretch.

Temperature (K)	Band Position (wavenumbers)	
	Free Band 1	Bound Band 2
203	2253.80	2263.73
223	2254.30	2263.60
248	2254.00	2262.30
273	2254.90	2262.10
298	2255.80	2262.30
323	2256.00	2261.25
333	2257.80	2261.25
343	2258.85	2261.70

Table 5.4 - CN Band Position

5.5. Conclusions

The lifetime of the hydrogen bonded methanol/cyanomethane dimer has been calculated from the linewidth of the infrared absorption band for the carbon-nitrogen triple bond. The lifetime shows a steady decrease with rising temperature. This suggests that the hydrogen bond breaks more readily in a hotter system, which would be expected.

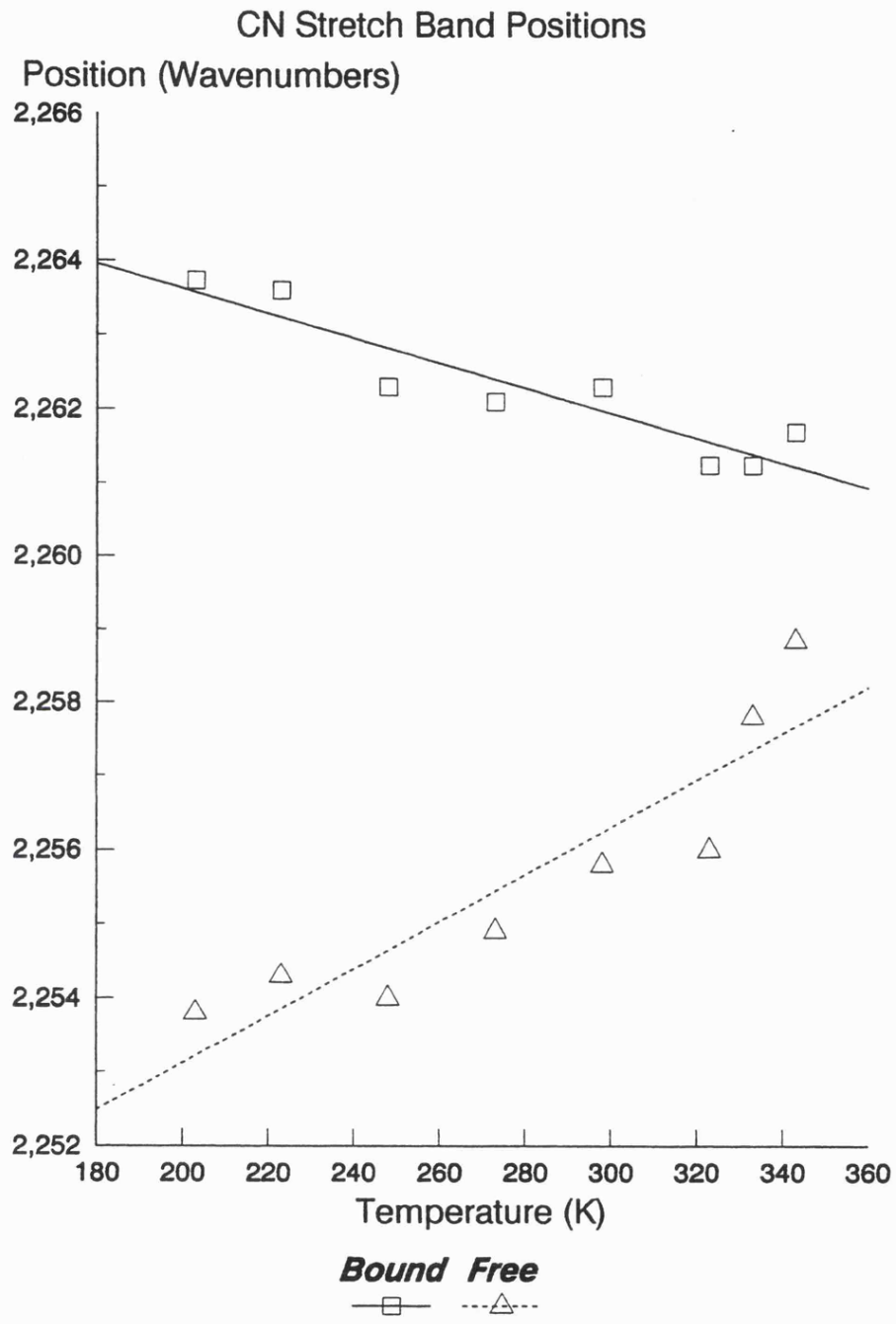

Figure 5.12 - CN stretch band positions of MeCN in Methanol

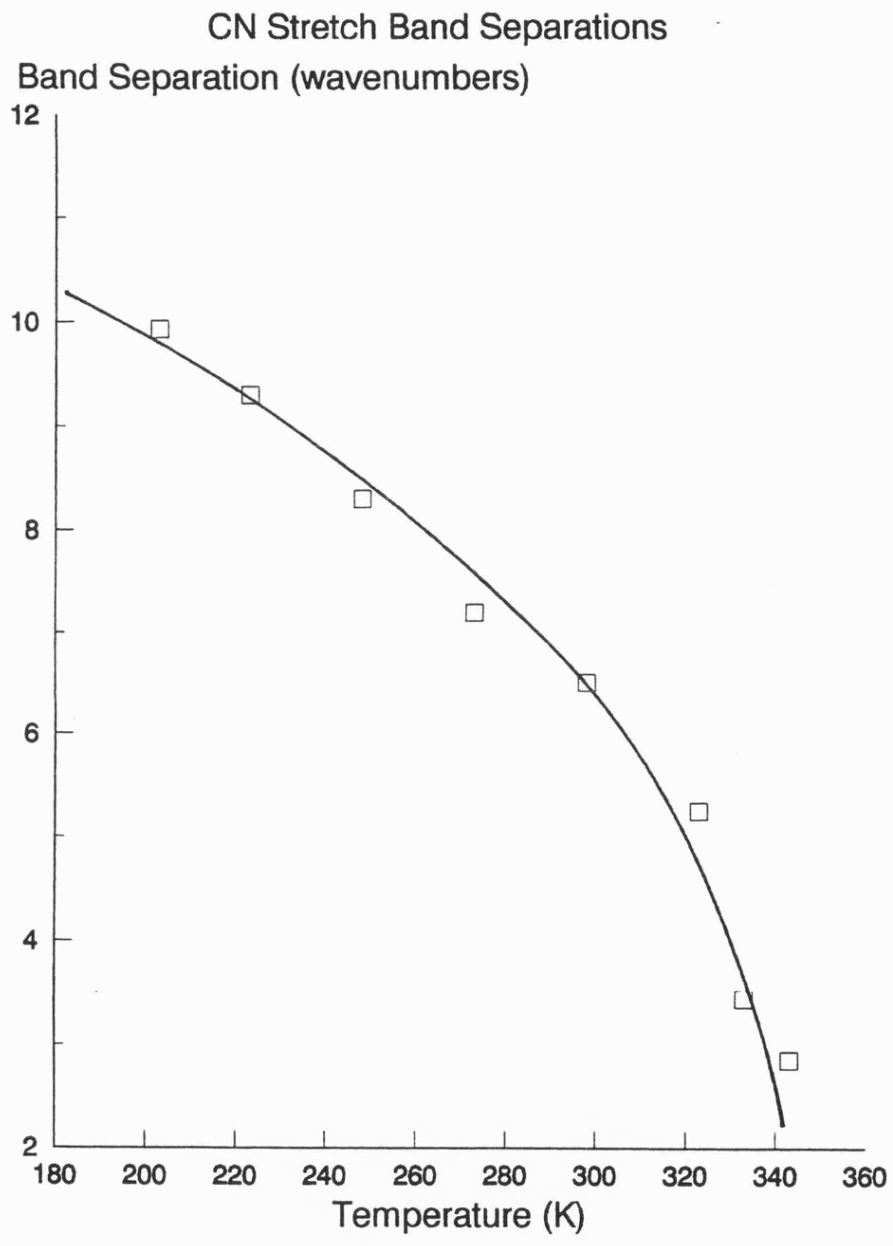

Figure 5.13 - Separation between CN stretch bands of Free and Bound MeCN in Methanol

The lifetime ranges from 1.3 x 10^{-12}s at 203K to 9 x 10^{-12}s at 343K. The molecular dynamics work[17] on cyanomethane in methanol studied the length of time that a solvent molecule remained bound to the cyanomethane. The result from that work gave a lifetime of 1 x 10^{-12}s at 298K. In view of the remarkably good agreement between experimental and theoretical results it seems that the lifetime of hydrogen bonded species can be investigated with infrared spectroscopy. This should prove to be of considerable use to those who study the structure and dynamics of hydrogen bonded systems. Many systems should exist which are suitable for study in this way. They are probably not recognised as such as variable temperature studies are not commonly undertaken.

5.6. Addendum

The approach outlined in the previous section is a simplistic one that relies upon a fundamental assumption about the behaviour of the observed IR bands; that exchange processes are the only possible cause of the observed changes in the spectra with temperature. This is not necessarily the case as the principal variables describing IR bands; position, intensity, width and shape function are all themselves functions of temperature.

Position	The mean oscillator frequency depends upon the nature of the surrounding dipoles, this will change with temperature
Intensity	The polarisability of the oscillators is a function of temperature

Width	Width is determined in part by both T_1 and T_2 relaxation processes, both of which will change with temperature.
Shape	The balance between T_1 and T_2 effects on relaxation will change with temperature, so altering the band shape function

The curve fitting is further complicated by another band[22], $\nu_2+\nu_8-\nu_8$, itself a potentially temperature sensitive feature, which lies close to the observed ν_2 band. Although this 'hot' band has a much lower intensity than the main free and bound ν_2 bands, so much so that there is no apparent third band in any of the experimental results reported in this work, it would contribute to the overall absorption profile.

Addition of a third band would not make a major quantitative change in the peak position parameters. In all but the two highest temperatures clearly defined peak positions can be seen in the experimental spectra. The other parameters derived from the curve analysis could be altered by adding the 'hot' band.

Using a three band curve analysis Besnard, Cabaco and Yarwood[23] have produced a series of fits to RAMAN spectra of the same system. These have been used to generate equilibrium constants for the equilibria between a series of solvated species. This treatment has required the invocation of a series of polymeric methanol species for which there is no supporting experimental

evidence. The justification offered for these species is that they provide a framework that fits a model for the deconvolution of the experimental RAMAN curves.

The experimental spectra of the system are clearly open to interpretation in different ways. The treatment presented in this Chapter assumes that only exchange processes can cause the apparent band positions to converge. As a result a simple relationship is assumed between lifetimes and line broadening. This is clearly an oversimplification since Besnard *et al*[23] have demonstrated a model that reproduces the experimental results without requiring exchange process to cause the observed line broadening. Further study of the system using a hybrid of exchange and non-exchange mechanisms may yet lead to a better interpretation of the observed data.

References

1 Dyke,Floyd,Sainsbury and Theobald, *Organic Spectroscopy :An Introduction*, Longman, 1978, p106.

2 *Proc. NATO ASI on Molecular Liquids - Dynamics and Interactions* (Eds. Barnes, Orville-Thomas and Yarwood), Reidel, 1984 and references therein.

3 Kreevoy, M.M. and Mead, C.A., *Diss. Faraday Soc.*,39, 166, (1965)

4 Lassegues, J.C. and Devaure J., *Protons and Ions in Fast Dynamics Phenomena*, (Ed. P. Laszlo) Elsevier, 1978, p.159

5 Covington, A.K., Freeman J.G. and Lilley T.H., *J. Phys. Chem.*, 74, 3773, (1970)

6 Chen, H. and Irish, D.E., *J. Phys. Chem.*, 75, 2672, (1971)

7 Strehlow, H., Wagner, I. and Hildebrandt, P., *Ber. Bunsenges. Phys. Chem*, 87, 516, (1983)

[8] Ackroyd, R., Robertson, G. and Yarwood, J., *Chem. Phys.*, **32**, 267, (1978)

[9] Cavagnat, D. and Lascombe, J., *J. Chem. Phys.*, **76**, 4336, (1982)

[10] Cohen, B. and Weiss, S., *J. Chem. Phys.*, **72**, 6804, (1980)

[11] MacPhail, R. and Strauss, H.L., *J. Chem. Phys.*, **87**, 6665, (1987)

[12] Voit, P., Tarjus, G. and Bratos, S., *J. Chem. Phys.*, **85**, 803, (1986); *J. Mol. Liq.*, **36**, 185, (1987)

[13] Pena-Nunez, A.S., Ph.D. Thesis, Leicester, 1984

[14] Pay, N.G.M., Ph.D. Thesis, Leicester, 1981

[15] Eaton G., Pena-Nunez A.S., Symons M.C.R., Ferrario M., and McDonald I.R, *Faraday Discuss. Chem. Soc.*, **85**, (1988)

[16] Atkins, P.W., *Physical Chemistry* (2nd Ed.) , Oxford University Press, 1982, p.570

[17] Personal communication from Dr. I.R McDonald to Prof. M.C.R. Symons

[18] Bratos, S., Rios, J. and Guissani, Y., *J. Chem. Phys.*, **52**, 439, (1970)

[19] Yarwood, J., *Spectroscopy and Structure of Molecular Complexes*, Plenum, 1973, p.191

[20] Kovacs, H., Kowalewski, J. and Maliniak, A., *Chem. Phys.Lett.*, **152**, (1988)

[21] Westlund, P-O. and Lynden-Bell, R.M., *Chem. Phys. Lett.*, **154**, (1989)

[22] Yarwood, J., *Adv. Mol. Relaxation Processes*, **5**, 375, (1973)

[23] Besnard, M, Cabaco, M.I., and Yarwood, J., *Chemical Physics Letters*, **198**, 207, (1992)
Besnard, M, Cabaco, M.I., and Yarwood, J., *Mol. Phys*, **75**, 139, (1992)

6. LIQUID PHASE WATER STRUCTURE

6.1. Introduction

In spite of the fact that water is of the greatest importance to man, easy to handle, abundant and inexpensive, there is still no general consensus as to its precise structure in the liquid phase. An examination of the water molecule shows that it is approximately tetrahedral in geometry with two lone pairs and two slightly acidic protons. These properties give water a bi-bifunctionality and hence it's ability to form a three dimensional hydrogen bonded structure, unlike alcohols which can only form chain-like hydrogen bonded structures[1].

In general two major classifications of water models have emerged; one (continuum models) in which water is described as being essentially completely hydrogen bonded with a broad range of bond energies and geometries, and another (mixture models) where a mixture of distinct types of water molecule environments are envisaged.

6.1.1. The Continuum Model

Pople[2] proposed a model for the structure of water based on a picture of ice melting. As ice melts the hydrogen bonding becomes more flexible. Changes in temperature would then cause hydrogen bonds to distort rather than break. The major consequence of this being that any regular structure water has can only extend a few molecular diameters from any given molecule.

6.1.2. The Mixture Models

Many models for the structure of water come under this classification. The idea that water may be described as a mixture of at least two molecular species dates from the nineteenth century and has appeared in many guises since.

As with the continuum model, the early mixture models were developed by examining, and then relaxing the structure of ice, so giving a structure for the liquid phase. Samilov[3] suggested that water can be thought of as a distorted version of ice in which the increased translational mobility of water causes water molecules to move from their 'ice-like' equilibrium positions and into interstitial spaces.

Pauling[4] proposed a model for water based upon water polyhedra similar to those observed in gas hydrates such as methane hydrate. It was envisaged that water consists of a mixture of two units, the pentagonal dodecahedron and the tetrakaidecohedron. These structures have cavities with diameters of 0.52nm and 0.59nm respectively, which would contain 'free' water molecules.

One concept which has gained widespread acceptance is the 'flickering clusters' model of Frank and Wen[5]. This describes water as consisting of groups of water molecules which are essentially fully hydrogen bonded, interspersed with monomeric water molecules. At the surface of these clusters water molecules have either one, two or three hydrogen bonds. These clusters are continuously, and cooperatively, being broken and reformed with a

timescale of ca. 10^{-11} s. The average size of the clusters, and the concentration of monomers, varies with temperature.

More recently Watterson[6,7] postulated a 'wave' model for water structure. The model suggests that the clusters of water molecules are formed in the condensed phase. These clusters, however, do not simply flicker on and off, rather they advance like a wave through the liquid. Watterson goes on to suggest that these clusters are cubic with edges about 3.3 nm long and contain approximately 1000 molecules. Watterson's view is that "... this basic domain size corresponds to that of the basic unit in water structure."

6.1.3. Arguments And Evidence

The very fact that this section is included implies that the debate over which model is most appropriate is a continuing one. The continuum model has been successfully used by various groups of workers to reproduce the observed properties of water such as dielectric constant[8], radial distribution functions and density changes[9].

Experimental support for the continuum model has come from Falk *et al*[10], who observed no asymmetry in the fundamental stretching bands of HOD and concluded that the results were incompatible with the idea of water molecules having different extents of hydrogen bonding. Another study of H_2O/D_2O[11] showed symmetrical stretching bands and that the OD stretch could be represented by

either a single Gaussian band or 10 to 15 Lorentzian bands, representing a continuous distribution of oscillator environments.

Using the same technique Senior and Verral[12] came to the opposite conclusion, that a mixture model was more appropriate. Their reasoning for this was based on the observation of temperature dependent asymmetry in the differentiated spectra, suggesting that relative populations of two species were changing.

The use of fundamental IR spectroscopy in trying to determine whether or not water bands are made up of more than one component suffers from the dependence of intensity on oscillator polarisation[1]. Polarisation of the O-H / O-D bonds increases when they form hydrogen bonds, so making them absorb more strongly. As a result, if hydrogen bonded species are present in large concentrations they will dominate the spectrum and make it very difficult to see any free (or weakly bound) oscillators.

In the overtone regions the relative intensity of bands is reversed[1] with free or weakly bound oscillators having greater extinction coefficients than those more strongly bound. The overtone region has another advantage over fundamental IR spectroscopy, the separation between bands is almost double that of the fundamental region. The use of the overtone region to study water is complicated by the possibility of combination tones contributing to the observed bands. This problem is almost entirely eliminated by the use of HOD in D_2O rather than H_2O.

The 2υ $\sigma\psi\mu\mu\varepsilon\tau\rho\iota\chi$ $\sigma\tau\rho\varepsilon\tau\chi\eta$ spectrum of HOD in D_2O shows a narrow feature at 7050 cm^{-1} which is the same energy seen for the 2υ OH stretch of monomer HOD in inert solvents. This feature has been assigned to the stretching of free OH oscillators (OH_{free})[13,14]. Raising the temperature increases the intensity of this feature. Some have suggested that this feature and its temperature dependency is proof of the existence of OH_{free} groups in water, others maintain that the feature is due to very weakly bound OH groups[15].

Sceats and Besley[16] showed that the observed temperature dependent changes could be simulated without any change in the band at 7050 cm^{-1}, they found that a decrease in intensity around 6800 cm^{-1} brought about the same observed effect.

Further evidence against the 'flickering cluster' model has come from molecular dynamics experiments performed by Rahman and Stillinger[17] who concluded that liquid water shows no marked tendency to organize the beginnings of ice structures.

Stevenson[18] estimated, using ultraviolet spectrophotometry, that at 25 °C water has, at most, a concentration of 0.15% monomer. As monomers form an integral part of the 'flickering cluster' model their presence in such small concentrations must be seen as an obstacle to the acceptance of that model. Other estimates of the concentration of monomers in water, derived from both experimental and computer simulation, suggest an upper limit of between 5% and 10%.

6.1.4. The Free Lone-Pair and OH Groups Concept

This concept was first proposed by Symons in 1972[1], although the idea of non-hydrogen bonded OH groups had been discussed earlier by Luck and Ditter[13]. Symons suggested that instead of observing the properties of liquid water and then developing models which reproduce them, it was better to examine the electronic structure of the monomer and its chemical properties, and then to develop a description based on those properties.

Water is bi-bifunctional and tends to form hydrogen bonds with approximately tetrahedral geometry. It will as a result attempt to form four hydrogen bonds resulting in a rigid polymeric structure. However hydrogen bonds are continually being broken and reformed at ambient temperatures and pressures. This leads to the observed fluidity in water. Whenever a hydrogen bond is broken two units will be formed, OH_{free} and LP_{free}. OH_{free} is an OH group where the proton is not participating in any hydrogen bonding to other molecules. A LP_{free} group is a lone pair on oxygen that is not participating in any hydrogen bonding. These two structures are illustrated in Figure 6.1.

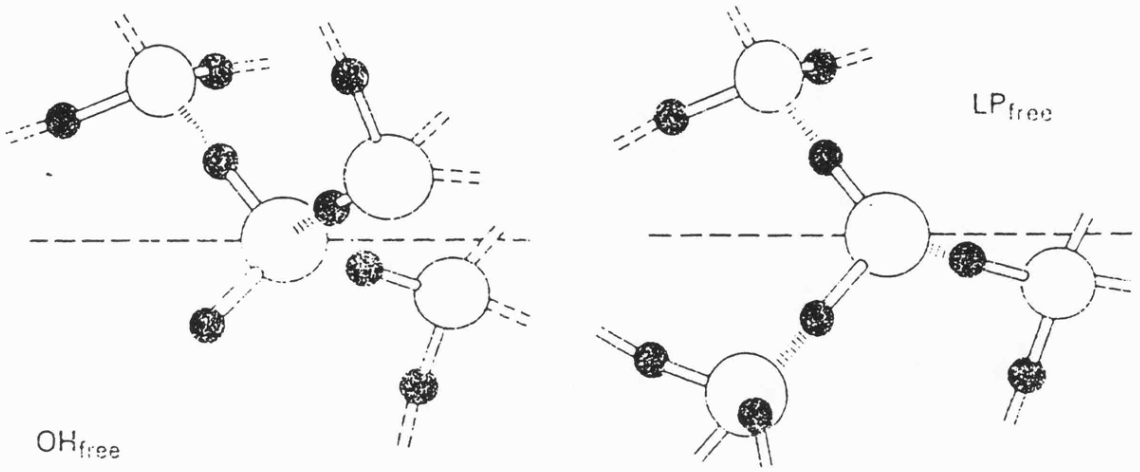

Figure 6.1 - Structure of OH_{free} and LP_{free} in water

The importance of these units comes from their unsatisfied hydrogen bonding capability, which make them relatively reactive compared to fully hydrogen bonded water molecules. The mobility of these groups is expected to be very high. They can be viewed as defects in the water lattice propagated through bifurcated intermediates in much the same way as hydroxyl and hydroxonium ions. Indeed, this mechanism for propagation of lattice defects has recently been proposed as an explanation for the high mobility of water molecules in the liquid phase[19]. Symons suggests that, since OH_{free} and LP_{free} must be far more abundant in water than hydroxyl or hydroxonium ions, they must be at least as significant in determining the properties of water.

Using this model the law of mass action successfully predicts the spectral changes observed in the overtone studies of the OH

stretch of HOD in D_2O. It also explains the initial downfield shift in the hydroxyl protons chemical shift seen when a base is added to water[20], but not when a base is added to methanol[21]. Methanol has an excess of LP_{free} and so very few OH_{free} are present. In water this is not the case and bases initially scavenge the OH_{free} groups present.

Criticism of this model has come from advocates of the continuum model who point out that studies show that the energy needed to break the hydrogen bond in the dimer (4-6 kcal mol^{-1}) is not available from thermal fluctuations. It is however debatable whether the situation which they envisage, that of molecules moving from equilibrium bonding positions to infinite separation, is relevant to the liquid phase.

6.2. Molecular Dynamics Studies

6.2.1. Introduction To Molecular Dynamics

Molecular dynamics (MD) studies are widely used to study the orientations of assemblages of molecules. The technique requires considerable computational power and as such developments in its use are restrained by the cost and availability of the most powerful computer hardware.

In molecular dynamics molecules are represented by potential models which consist of masses and charges fixed in their relative positions to one another. These masses and charges represent the atoms and charge distribution within the species modelled. The

interactions between the molecules are modelled by equations covering mass-mass interactions (usually modelled as Lennard-Jones type interactions) and electrostatic interactions. The resultant forces are used to determine the velocity vectors for each molecule. The motion of the molecules is integrated over successive time steps (typically around 10^{-15}s). The coordinates of all atoms can be recorded for later analysis.

The only representation of temperature in MD simulations is the total kinetic energy of all molecules present. Periodically the total kinetic energy in the system is calculated and velocities scaled up or down as required to re-establish the required total kinetic energy.

The density of the system is usually fixed by restraining the molecules to be within a specific sized 'box'. Restraining a relatively small number of molecules to remain within a volume causes problems with the interactions (or lack of them) between the molecules and the surrounding 'walls'. With no interactions beyond the 'walls' there would be a tendency for all molecules to clump together in the centre of the box, or else to spread themselves over the box walls. If there is no wall then the density of the system is uncontrolled and molecules can 'escape' the system. The boundary problems are overcome by applying periodic boundary conditions. This procedure surrounds the box with 26 images of the same assemblage of molecules (9 in a plane above, 9 in a plane below and 8 in a ring in the same plane as the primary box). A molecule near the edge of the box 'sees' images

of molecules at the far side of its box through the box wall. The molecule is free to leave the box, but as it does so it is replaced by an image of itself entering from the opposite side. To prevent a molecule from interacting with two (or more) images of the same molecule (or even itself) the maximum permitted range for interaction forces can be no more than half the length of a box side. This puts an upper limit on the range of interaction that can be studied, or conversely sets a minimum size on the box and the number of molecules required for the simulation. Periodic boundary conditions add to the computational complexity of the simulation but provide an environment without edges, which is a necessity for the study of any liquid phase structures.

6.2.2. Molecular Dynamics Simulations Of Water

Water is both extremely important and yet a relatively simple molecule. As a result it has been studied extensively by molecular dynamics simulations. The first molecular dynamics study of water was published by Rahman and Stillinger in 1971[17]. They used a potential previously developed by Ben-Naim and Stillinger[22], subsequently termed the BNS potential. The BNS potential was a perfect tetrahedron with four charges of 0.19562*e* at the apices of a tetrahedron. The charges (two positive and two negative) were placed 1Å from the oxygen atom. They took the unusual step of producing stereoscopic pairs of slides and used them to study three-dimensional images of the water assemblages. From these images they noted the following points about the structure of liquid water:

- Most molecules adopt approximately tetrahedral orientations.
- No large clusters of anomalous (low or high) density were observed.
- No polyhedral structures recognisable from studies of ices and clathrates were observed (these had been predicted by Pauling[4]).
- 'Dangling' OH bonds exist, which are not included in hydrogen bonds. These entities persist longer than water molecule vibrational periods.
- There is no obvious division of water molecules into 'network' and 'interstitial' sites.

The BNS potential was updated to the ST2 potential to yield a better agreement with thermodynamic data[23]. The ST2 potential had the magnitude of the charges increased to 0.2357*e* and the distance of the lone-pair charges from the oxygen reduced to 0.8Å.

A great number of potential models have since been used for water MD studies. These vary mostly on the magnitude of the charges and the geometry of the negative charge distribution. All have just one mass, at the oxygen and three or four charge centres. Two routes have been taken to represent the lone pair charges; four charge and three charge models. Earlier models, such as ST2, were four charge potentials which placed charges representing the lone

pairs above and below the plane of the molecule. Jorgensen *et al.*[24] reviewed a selection of potentials and compared the results with radial pair correlation functions derived from diffraction studies. They demonstrated that three charge potentials, with a single negative charge on the molecular plane on the bisector of the HOH angle, give results as good as the four charge models but with a reduced computational load.

Most recently simulations using the ST2 potential have been used[19] to investigate the translational and rotational freedoms of water molecules, so demonstrating that molecular dynamics can be used to study dynamic as well as static properties of water.

6.3. Hydrogen Bonds in TIP4P

6.3.1. Introduction

A great deal of research into the properties of liquid water is carried out by techniques such as molecular dynamics, as outlined in the previous section. Some study of the hydrogen bond network has been made using a purely energetic definition of hydrogen bonding. The existence of a hydrogen bond clearly depends on the definition used. If the combined coulombic and Lennard-Jones interaction between two molecules is the sole factor in determining the existence of a hydrogen bond then the geometry of the bond is not considered. If hydrogen bonds are considered to be characterised by molecular orbital overlap then geometry becomes very significant if directional orbitals are involved.

Since the molecular dynamics models use interaction energies to evaluate the interaction between two molecules, the data to define hydrogen bonds in energetic terms is already available. Hydrogen bond analysis has taken place and the mean number of bonds formed per molecule for different potentials has been summarised by Jorgensen *et al.*[24].

What follows is an analysis of data from a TIP4P molecular dynamics experiment using entirely geometric criteria for hydrogen bonding. If significant numbers of both OH_{free} and LP_{free} can be identified by their geometry alone then arguments that the 'free' groups are simply weakly bound will have been countered. If there is no accessible bonding partner present for a lone pair or hydrogen, strongly or weakly interacting, then there can be no bond, and the group must be 'free'.

6.3.2. The TIP4P Model

The TIP4P model for water was developed at Purdue University by Jorgensen *et al*[24] and was considered to be the better model from a series of potential models (TIPS2, TIP3P, SPC, BP, ST2). Although they found that SPC, ST2, TIPS2 and TIP4P all gave reasonable structural and thermodynamic descriptions of water, TIP4P, TIPS2 and SPC were significantly easier to use as they were computationally simpler than ST2.

The TIP4P water molecule is illustrated in Figure 6.2. The parameters used for the TIP4P potential are detailed below:

r(OH)	0.9572 Å
$\hat{HOH}$	104.52 deg
A	600000 kcal $Å^{12}$/mol
C	610 kcal $Å^{6}$/mol
q(O)	0.0 *e*
q(H)	0.52 *e*
q(M)	-1.04 *e*
r(OM)	0.15 Å

M is the point on the bisector of the HOH angle where the negative charge is placed. The interaction strength between two molecules a and b with O-O separation r is given by:

$$\varepsilon_{ab} = \sum_{i;j=1}^{3} \left[\frac{q_i q_j e^2}{r_{ij}} \right] + \frac{A}{r^{12}} - \frac{C}{r^6}$$

The geometric data used in this study was generated from a molecular dynamics simulation of TIP4P water. The data was provided by Dr. I.R. McDonald of Cambridge University, whose assistance is gratefully acknowledged. The simulation at Cambridge was run with the following parameters:

box length	15.6554 Å
Temperature	289.2 K
Time Step	0.0065 ps
Number of Molecules	128 (giving density of 0.9980 g cm^{-3})

The configuration of the system, in the form of the coordinates of the three atoms of each molecule, was provided for 2000 instances.

6.3.3. Bonding Criteria

The purpose of this study was to apply purely geometric criteria to hydrogen bonding in liquid water as modelled by the TIP4P potential. Three data items were used to control hydrogen bonds:

distance — A maximum separation (O-O) was set at 4.0 Å. This encompasses the entire first peak of the oxygen - oxygen radial distribution function as calculated from neutron scattering data[25].

θ — This angle is the allowed 'bend' on the hydrogen bond at the hydrogen. An entirely linear bond has $\theta = 0$. The maximum permitted value of θ in any analysis is θ_{max}.

ϕ — This angle is the allowed deviation from tetrahedral geometry at the lone pair donating oxygen. Since lone pair sites are not represented as specific sites in the TIP4P model the two angles between the intramolecular OH bonds and the potential hydrogen bond are calculated. If the angles were both 109.5° then the molecule would be perfectly tetrahedral. ϕ is taken as 109.5-$\hat{HOH_b}$, where H_b is the hydrogen bonding proton.

An alternative way to visualise ϕ is to consider an 'exclusion cone' aligned with each intramolecular OH bond in which hydrogen bonds may

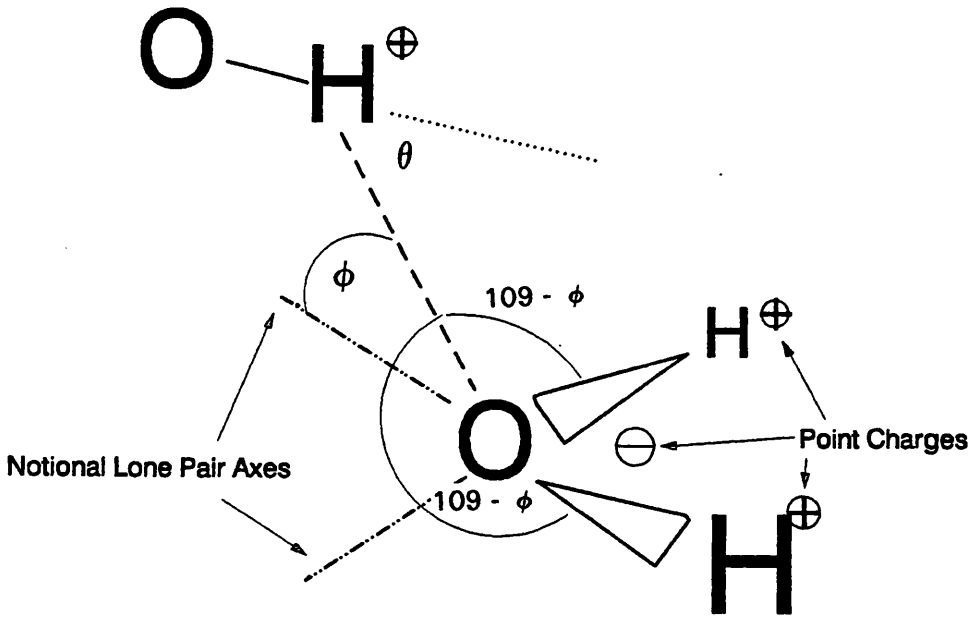

Figure 6.2 - Water Hydrogen Bonding Geometry

not form. The surfaces of such a cone form an angle of $109.5-\phi$ to the OH bond axis.

The maximum permitted value of ϕ in any analysis is ϕ_{max}.

6.3.4. Analytical Methods

A computer program was written in PASCAL running on Leicester University's VAX cluster to process the water configurations, henceforth termed 'frames'. The program was first developed to read the MD data files provided and to then check that the data had been read correctly by ensuring that OH separations were

consistent at 0.9572 Å. This was successfully achieved and the program was then extended to analyse the relative positions in space of the molecules. Analysis was undertaken frame by frame with statistics covering all data studied calculated at the end of the run. The results presented in this Chapter were produced using the same program modified to run on an IBM/AT compatible personal computer.

Insufficient storage space was available to keep all of the data available for processing. The data was divided into blocks of 250 frames. Early runs performed with these reduced data sets showed very little variation. In order to reduce computation time during development of the analysis programmes these 250 frame files were further reduced to 50 frames. The variation between the number of OH_{free} groups identified in any one file of data was found to be at most ±5%. The final analysis, presented below, was performed on a composite selection of 70 frames taken from four disjoint sections of the total time span covered by the available data. This data was selected as a reasonable compromise between the need to use independent data and the limited processing power available.

The programme uses the following outline algorithm for each combination of ϕ_{max} and θ_{max} required (the maximum allowed deviations from tetrahedral form and linearity respectively):

- The programme sorts a list of neighbouring molecules within the 4Å limit for each molecule in turn.

- It then evaluates possible bonds between the currently selected water molecule and each molecule in the list of near neighbours in turn, closest neighbours first. This process stops when the list of near neighbours has been traversed.

- Statistics on the number of bonds formed by oxygen and hydrogen atoms are updated.

- If when the list of neighbours within 4Å has been exhausted there is still unsatisfied bonding capabilities then the number of free groups found is increased. For a LP_{free} to exist then there must be only one proton accepting hydrogen bond formed by a molecule (if there are none then there are two LP_{free}). For an OH_{free} to exist then one of the molecule's two hydrogens must be unable to form a proton donating hydrogen bond, if this is true for both then two OH_{free} groups are present.

- As well as counting the total number of free groups identified a separate count is maintained of the number of molecules bearing one or more free groups. The distribution of the number of neighbours within 4Å is also recorded, as is the number of neighbours for each of the molecules bearing one or more free groups.

Number Of Neighbours	Frequency	Percentage
3	14	0.16
4	67	0.75
5	419	4.7
6	995	11
7	2073	23
8	2295	26
9	1687	19
10	1033	12
11	315	3.5
12	54	0.60
13	8	0.089

Table 6.1 : Distribution Of Number of Water Molecules Within 4Å

6.3.5. Neighbour Density

The number of neighbour molecules within 4Å of each water is tabulated in Table 6.1. Liquid water with a density of 1.0 g cm^{-3} would be expected to have 7.96 neighbours within 4Å. The mean number of neighbours from the data in Table 6.1 is 7.92 giving a density of 0.99 g cm^{-3}. The density of the system is therefore accurate which suggests that the programme is successfully evaluating the list of neighbours within 4Å.

Ice has a density of 0.9168 g cm^{-3} at 0°C, giving 6.30 neighbours within 4Å. It is significant that a little over 16% of TIP4P water from this study exists in an environment at or below the density of ice. This can not be reconciled with any model that views water as containing significant ice-like regions.

6.3.6. OH_{free} Population

The two angles θ_{max} and ϕ_{max}, defined in Section 6.3.3, were stepped through 10° intervals from 5° to 95°. The population of OH_{free} was evaluated for each combination of θ_{max} and ϕ_{max}. The results are presented in Table 6.2 and plotted in Figure 6.3.

θ_{max}	5°	15°	25°	35°	45°	ϕ_{max} 55	65°	75°	85°	95°
5°	98	97	96	96	96	96	96	96	95	95
15°	89	80	73	70	69	68	68	68	68	68
25°	79	62	48	71	38	38	38	38	38	38
35°	72	50	31	22	18	17	17	16	16	16
45°	69	44	23	12	7.6	6.4	6.0	6.0	5.9	5.9
55°	67	40	19	7.1	3.3	2.3	2.1	2.1	2.1	2.1
65°	64	36	14	4.3	1.3	0.82	0.78	0.75	0.74	0.74
75°	61	32	11	2.5	0.59	0.32	0.31	0.27	0.26	0.26
85°	58	29	8.7	1.6	0.30	0.15	0.15	0.14	0.13	0.13
95°	56	26	7.3	1.2	0.21	0.12	0.11	0.11	0.10	0.10

Table 6.2 - Percentage OH_{free} For Different Hydrogen Bond Criteria

The most interesting feature of the above results can be seen with the effect of loosening the ϕ restraint. The number of free groups rapidly falls away until $\phi_{max} \approx 35°$, at which point the population becomes almost insensitive to ϕ_{max}. Changing θ_{max}, in contrast, produces a smooth and continuous fall in the OH_{free} population.

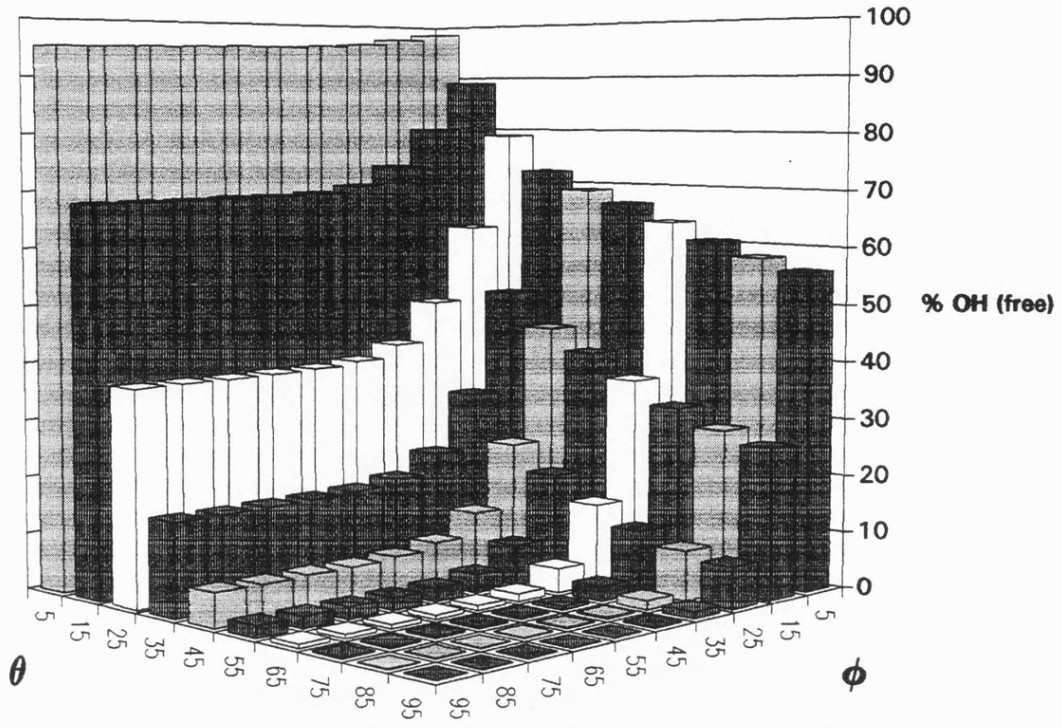

Figure 6.3 - Percentage OH_{free} For Different Hydrogen Bond Criteria

In order to extract a population level for OH_{free} from the data presented in Figure 6.3 it is necessary to make some assumptions about θ_{max} and ϕ_{max}. It has been noted that ϕ_{max} has little effect above $\approx 35°$. It is proposed that this marks the boundary between 'real' hydrogen bonds in water and those bonds that are model artifacts caused by setting too lenient a constraint on ϕ. The ϕ limit for a hydrogen bond in water will therefore be taken to be 35°.

Other studies of TIP4P at 298K, using energetic bonding criteria, have produced values for the mean number of bonds formed by water molecules in the region of 3.57[26] to 3.59[24]. This gives around

10.5% of bonds missing, so the predicted population of OH_{free} should be around 10-11%.

Using the assumed limit of ϕ_{max} = 35° and the requirement to have an OH_{free} population around 10-11% it is possible to find a value for θ_{max} in Table 6.2. This value is 45° (11.7% OH_{free}); given the assumptions made about ϕ_{max} and the limited extent of the data set it is not justifiable to claim any more accuracy. The values used here, 10.5%-11.7%, agree with the predictions made by Symons for the OH_{free} concentration[27] made from overtone spectra of HOD of approximately 10% under ambient conditions.

It has been shown that it can be argued that the hydrogen bonds in liquid water have a limit of 35° deviation from a tetrahedral structure about oxygen, alternatively that hydrogen bonds never form within ~74° of an intramolecular OH bond (109°-35°). This limit on behaviour prevents hydrogen bonds forming in the space between the intramolecular OH bonds, proton-proton repulsion over-riding the attraction of the negative charge (which, it must be remembered, is not centred on oxygen - see Figure 6.2). This restriction is not sufficiently severe to prevent three coordinate structures with three hydrogens in a plane about oxygen. If this structure were favoured a large number of hydrogen/lone pair/lone pair three centre bonds would occur. This structure would be recorded as a LP_{free} group if the lone pairs had no alternative bonding partners.

6.3.7. LP_{free} Population

It should be re-stated that these results come from the same programme as the OH_{free} population, running with the same data. The only difference is that it is checking possible hydrogen bonds from the perspective of the oxygen atoms, rather than from that of the hydrogen atoms. The data is presented in Table 6.3 and plotted in Figure 6.4.

θ_{max}	5°	15°	25°	35°	45°	ϕ_{max} 55°	65°	75°	85°	95°
5°	98	97	96	96	95	95	95	95	95	95
15°	89	80	73	69	68	68	68	68	68	68
25°	79	61	48	41	39	39	38	38	38	38
35°	72	50	32	23	20	20	20	20	19	19
45°	69	44	24	14	11	11	11	10	10	10
55°	66	39	19	8.9	6.3	5.5	5.1	4.9	4.8	4.7
65°	63	34	14	4.9	2.7	1.9	1.7	1.4	1.3	1.3
75°	59	29	9.3	2.2	0.73	0.41	0.27	0.21	0.19	0.19
85°	56	26	7.2	1.2	0.30	0.13	0.08	0.08	0.07	0.07
95°	54	23	5.9	0.75	0.13	0.07	0.06	0.05	0.03	0.03

Table 6.3 - Percentage LP_{free} For Different Hydrogen Bond Criteria

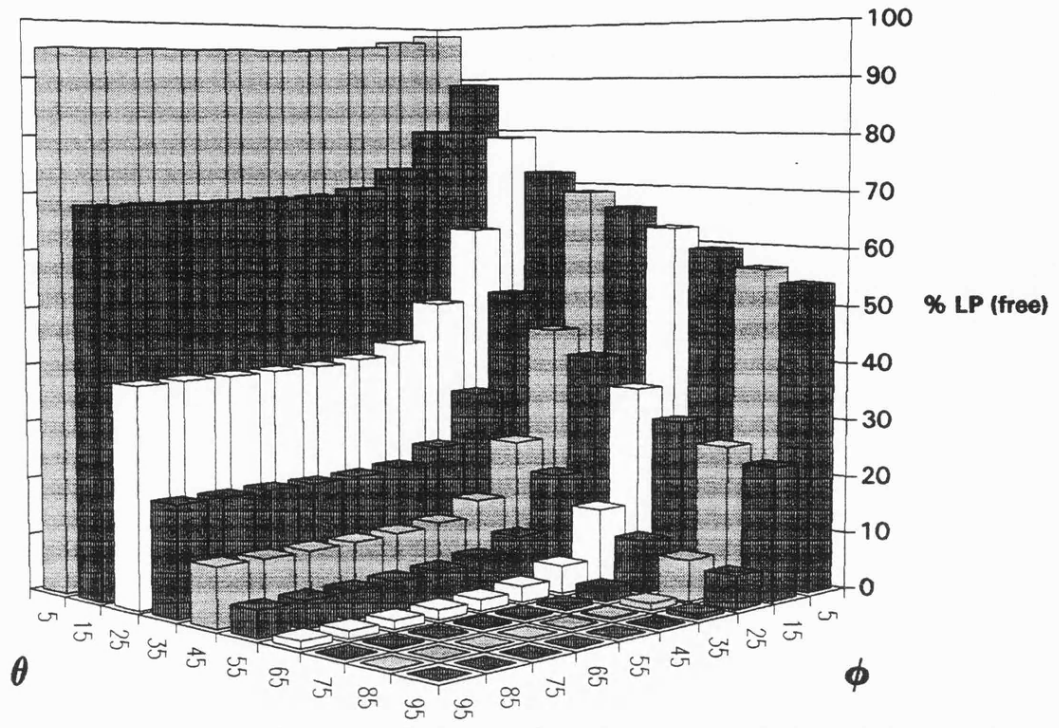

Figure 6.4 - Percentage LP_{free} For Different Hydrogen Bond Criteria

It is clear that the results for the LP_{free} population follow much the same pattern as those for the OH_{free} population.

In the previous section the combination of ϕ_{max} = 35° and θ_{max} = 45° was taken as representing a case where the proportion of OH_{free} groups equalled the proportion of missing bonds calculated by energetic bonding criteria. If this case is examined for LP_{free} then a population of 14.1% is recorded, 2.4% higher than the OH_{free} population.

This anomaly can be explained by considering the possibility that some OH_{free} groups are being scavenged by oxygen atoms forming three, or more, hydrogen bonds. This would result in an OH_{free}

population lower than the LP_{free} population. While the free groups must be created in pairs there is no requirement that their populations remain exactly equal. The total number of bonds being formed by each atom is addressed in the following section.

6.3.8. Number Of Bonds Formed

As already mentioned the analytical programme used to study TIP4P water evaluates the possibility of hydrogen bonds forming between each water molecule and all neighbouring molecules within 4Å. The total number of hydrogen bonds formed within the geometrical constraints applied is recorded for each combination of ϕ_{max} and θ_{max} studied. In the previous sections it has been established that the criteria ϕ = 35° and θ = 45° give a hydrogen bond structure with similar characteristics to those calculated on energetic criteria. The distributions of bonds formed for this case are presented in Table 6.3

Number Of Bonds	Hydrogens (%)	Oxygens (%)
0	11.7	1.1
1	86.3	25.9
2	2.0	63.7
3	0.02	8.9
4	0	0.35
5	0	0

Table 6.3 - Number Of Hydrogen Bonds Formed Per Atom

The majority of atoms form the expected number of hydrogen bonds, two for oxygen and one for hydrogen. The LP_{free} population is

almost entirely based on oxygens forming just one hydrogen bond. 25.9% of oxygens have one LP_{free} whilst 1.1% have two LP_{free} (ie. form no hydrogen bonds through lone pairs).

Just over 9% of oxygen atoms form three or more hydrogen bonds while only 2% of hydrogens form more than one. This effectively means that oxygen atoms are scavenging OH_{free} more effectively than hydrogens are scavenging LP_{free}. This is reflected in the mean number of bonds formed per molecule by lone pairs (1.814) and hydrogens (1.807). The presence of lone pairs bonding to two hydrogens in a three centre bond, effectively removing OH_{free} groups from the system, and of hydrogens forming bonds to two lone pairs, effectively removing LP_{free} from the system, allow the discrepancy to be explained.

8.9% of oxygens have lone pairs that are behaving in this way, whilst 2% of hydrogens form the equivalent bonds to two lone pairs. Allowing for the fact that twice as many hydrogens are present as oxygens an excess of 8.9% - 4% = 4.9% of oxygens remains forming one extra bond. 4.9% of the oxygens behaving in this way would account for a further 2.45% of hydrogens being bonded, almost exactly the difference between the observed OH_{free} and LP_{free} populations (14.1% to 11.7%).

6.3.9. Correlation Between Free Groups and Density

Another statistic that is calculated by the programme is the number of neighbour molecules within 4Å of each molecule bearing a

LP_{free} group. Once again confining attention to the ϕ_{max} = 35° and θ_{max} = 45° case the data in Table 6.4 is obtained.

Number Of Neighbours (4Å)	Frequency (%)	Molecules Bearing LP_{free} (%)
3	0.2	43.9
4	0.8	23.9
5	4.7	12.2
6	11.1	23.1
7	23.1	25.5
8	25.6	26.5
9	18.8	26.3
10	11.5	31.5
11	3.5	40.6
12	0.6	33.3
13	0.1	0

Table 6.4 - Distribution of LP_{free} With Water Density

The data in Table 6.4 initially appears to suggest far too many LP_{free} groups, but it must be stressed that these values are the proportions of molecules possessing a LP_{free} group. It has already been shown that the vast majority of such molecules have only one LP_{free} group, and so most of the molecules counted in Table 6.4 are also forming a hydrogen bond through a second lone pair.

The results show a marked increase in the likelihood of a LP_{free} group being located on a molecule that is in an area of high local density. The average number of neighbours within 4Å in liquid water is around eight, so the areas in which free groups are over concentrated are roughly 25% more dense than water in the expected

tetrahedral arrangement. This could be accounted for by the insertion of an extra water molecule into the first coordination shell. In a study using ST2 water Stanley *et al*[19]. found that water molecules possessing a fifth water in their first coordination shell possessed enhanced translational and rotational mobility. Their argument was that by forming bifurcated hydrogen bonds the move from one tetrahedral configuration to another was catalysed. The presence of increased numbers of 'free' groups in areas of high density may represent the 'wreckage' of former bonds disrupted by the translational and rotational movements of water molecules adjusting to new bonding configurations.

6.4. Conclusion

These results demonstrate that it is plausible to look at hydrogen bonding in water in terms of geometric criteria. The bonding behaviour of water hydrogens calculated on purely energetic criteria can be reproduced by a geometrical argument; that hydrogen bonds are within 45° of linear and do not form an angle of less than 74.5° to an intramolecular OH bond. These two values are arbitrary constants that allow the same number of bonds to be present as have been predicted elsewhere[26]. The use of interaction energies calculated for various geometries of dimer may allow these values to be refined.

The trends revealed in Figures 6.3 and 6.4 certainly suggest that the value of ϕ_{max} = 35° has some significance. Higher values have almost no effect on the number of hydrogen bonds present. It

would seem reasonable to conclude that in TIP4P water hydrogen bonds do indeed form within 35° of tetrahedral configurations. The value of θ_{max} is much more of an arbitrary value, increasing values produce more bonds but the effect is smooth over the range of angles considered.

It is also clear that it is impossible to deny the existence of non-bonding lone pairs in water if the concept of the non-bonding proton is accepted. The two entities go hand in hand as can be seen by the very great similarities between Figures 6.3 and 6.4. Any discrepancies between the two population levels can be accounted for by the presence of small percentages of atoms that form more than their notional number of hydrogen bonds. The data studied suggests that lone pairs are slightly better scavengers of OH_{free} than hydrogens are of LP_{free}.

The values produced by this work can only be considered as approximate as the number of configurations studied is only 70. The smooth shape of the plots in Figures 6.3 and 6.4 does suggest that the trends identified are real and not experimental noise. Further studies using the same techniques in conjunction with a larger data set should be capable of producing results with a very much higher level of confidence.

The most important conclusion from this work is that the 'free' groups predicted to be present in water by Symons[1] can be identified in a TIP4P molecular dynamics simulation. It is particularly significant because the OH_{free} / LP_{free} concept

contains no energetic criteria and molecular dynamics simulations contain no geometric definitions of bonds. That a geometric argument for bonding can be applied to molecular dynamics data and produce such good results should be taken as vindicating both the OH_{free} / LP_{free} hypothesis and the TIP4P potential model.

References

1 Symons, M.C.R., *Nature*, **239**, 257, (1972)

2 Pople, J.A., *Proc. Roy. Soc.*, **A205**, 163, (1951)

3 Samilov, O.Y., *Disc Fara Soc*, **24**, 216, (1957)

4 Pauling, L., in *Hydrogen Bonding* (eds Hadzi and Thompson), Pergamon, London (1959)

5 Frank, H.S. and Wen, W.Y., *Disc. Fara. Soc.* **24**, 133, (1957)

6 Waterson, J.G., *Phys. Chem. Liq.*, **16**, 313, (1987)

7 Waterson, J.G., *Phys. Chem. Liq.*, **16**, 317, (1987)

8 Harris, F.E. and Alder, B.J., *J. Chem. Phys.*, **21**, 1031, (1953)

9 Kavanau, J.L., *Water and Solute-Water Interactions*, pp 8-20, Holden-Day, San Fransisco, (1964)

10 Falk, M., and Ford, T.A., *Can. J. Chem.*, **44**, 1699, (1966)

11 Yellin, W. and Courchene, W.L., *Nature*, **219**, 852, (1968)

12 Senior, W.A., and Verrall, R.E., *J, Phys. Chem.*, **73**, 4242, (1969)

13 Luck, W.A.P. and Ditter,W., *J. Mol. Struct*, **1**, 339, (1967-8)

14 Symons, M.C.R., in *Water and Aqueous Solutions - Colston Papers No. 37*, (Nielson, G.W., and Enderby, J.E. eds), Adam Hilger, Bristol, (1986)

15 Efimov, Y.Y. and Naberuhkin, Y.I., *Mol. Phys.*, **36**, 973, (1978)

16 Sceats, M.G., and Besley, K., *Mol. Phys.*, **40**, 1389, (1980)

17 Rahman, A and Stillinger, F.H, *J. Chem. Phys.*, **55**, 3336, (1971)

18 Stevenson, D.P., *J. Phys. Chem.*, **69**, 2145, (1965)

[19] Sciortino, F., Geiger, A. and Stanley, H.E., *Nature*, **354**, 218, (1991)

[20] Symons, M.C.R., Harvey, J.M. and Jackson, S.E., *J. Chem. Soc. Fara. Trans. I*, **76**, 256, (1980)

[21] Symons, M.C.R., Fletcher, N.J. and Thompson, V.K., *J. Chem. Soc. Fara. Trans. I*, **77**, 1899, (1981)

[22] Stillinger, F.H. and Ben-Naim, A., *J. Chem. Phys.*, **47**, 4431, (1967)

[23] Stillinger, F.H. and Rahman, A., *J. Chem. Phys.*, **60**, 1545, (1974)

[24] Jorgensen, W.L., Chandrasekhar, J., Madura, J.D., Impey, R.W, and Klein, M., *J. Chem. Phys.*, **79**, 926, (1983)

[25] Thiessen, W.E. and Narten, A.H., *J. Chem. Phys.*, **77**, 2656, (1982)

[26] Jorgensen, W.L. and Madura, J.D., *Molecular Physics*, **56**, 1381, (1985)

[27] Symons, M.C.R, personal communication